DSE - Water Bomber

Towards a Next Generation of Water Bombers

E.V.M. van Baaren	1506641	W.F.S. van Lingen	4001796
S.A.W. van den Broek	4009185	H.A. Mulder	1507435
D.A. Eisses	4010094	L.A. van der Schaft	4090128
L.H. Geijselaers	4081978	G. Stolwijk	4095413
F. Heddes	4081595	M.C.G. van der Werf	4083768

Final Report

Design Synthesis Excercise

TU Delft Delft University of Technology

Aerospace Engineering

January 22, 2014

Preface

This report, the Final Report, is the final of three reports of the Group 6 Design Synthesis Exercise. The goal of this exercise is to design a next generation of aerial firefighting aircraft. Over the course of ten weeks, a team of ten TU Delft Aerospace Engineering students will work closely together in several areas, including design, application of knowledge, communication, sustainable development and teamwork in order to fulfil this challenge. The team consists of the following ten members:

E.V.M. (Edzard) van Baaren

S.A.W. (Stefan) van den Broek

D.A. (Dagmar) Eisses

L.H. (Liset) Geijselaers

F. (Frank) Heddes

W.F.S. (Wouter) van Lingen

H.A. (Halbe) Mulder

L.A. (Luuk) van der Schaft

G. (Joris) Stolwijk

M.C.G. (Martijn) van der Werf

The team would like to express their gratitude towards its tutor Ir. P.C. Roling, its client Prof. dr.ir. J.A.A.M. Stoop (Chairman of the Stichting Behoud Erfgoed De Vries Robbé), its coaches G. Tescione and Q. Guan for their dedication, support and time.

Contents

List of Figures

List of Tables

List of Symbols and Abbreviations

Abbreviations

AGL	Above Ground Level
APU	Auxiliary Power Unit
ATGS	Air Tactical Group Supervisor
CADAS	Computer Augmented Detection and Aiming System
CFD	Communication Flow Diagram
CFD	Computational Fluid Dynamics
c.g.	Center Of Gravity
EASA	European Aviation Safety Agency
FB	Functional Breakdown
FCC	Firefighting Coordination Center
FFD	Functional Flow Diagram
FOB	Forward Operating Base
FR	Final Report
HLD	High Lift Device
ISA	International Standard Atmosphere
MTOW	Maximum Take-Off Weight
MTR	Mid-Term Report
NICC	National Interagency Coordination Center
OEI	One Engine Inoperative
OEW	Operative Empty Weight
RTB	Return To Base
STOL	Short Take-Off and Landing
TOP	Takeoff Parameter
UAV	Unmanned Aerial Vehicle
ZPLW	Zero Payload Weight

Definitions

Client	The launch customer (Red Cross)

Greek Symbols

α_{δ_f}	Angle of attack of deflected flap	rad^{-1}
α_{panel}	Angle of the panel with respect to the incoming flow	rad

α_{stall}	Stall angle of attack	rad
C_{Δ_0}	Initial load coefficient	$-$
δ_0	Initial load on the water	N
δ_{f_L}	Deflection angle of flaps	rad
η_P	Engine shaft to propeller efficiency	$-$
η_s	Shock absorber efficiency	$-$
η_t	Tire absorption efficiency	$-$
γ	Climb angle	rad
Γ_w	Wing dihedral angle	$^\circ$
λ_w	Wing taper ratio	$-$
$\Lambda_{c/4}$	Wing quarter chord sweep angle	$^\circ$
μ	Dynamic viscosity	$\frac{kg}{m \cdot s}$
ν	Poisson's ratio	$-$
ρ	Density	$\frac{kg}{m^3}$
ρ_{panel}	Density of the panel material	$\frac{kg}{m^3}$
$\rho_{stringer}$	Density of the stringer material	$\frac{kg}{m^3}$
ρ_{water}	Density of water	$\frac{kg}{m^3}$
σ_{crit}	Critical normal stress	N/m^2
σ_z	Normal Stress	$\frac{N}{m^2}$
τ	Shear Stress	Pa
θ	Roll angle required to completely submerge a float	$^\circ$
Roman Symbols		
A	Aspect ratio	$-$
b	Width at the main step	m
b	Wing span	m
$B.M.$	Distance between buoyancy center and metacenter	m
B	Boom area	m^2
C	Rate of climb	$\frac{m}{s}$
C_D	Drag coefficient	$-$
C_{D_0}	Zero-lift drag coefficient	$-$
C_f	Skin friction coefficient	$-$
$\frac{c_f}{c}$	Wing chord to flap chord ratio	$-$
$C_{L,x}$	3D lift coefficient in wing configuration x	$-$
C_{l_α}	Section liftcurve slope	rad^{-1}

$C_{l_{\alpha_f}}$	Section liftcurve slope with flaps down	rad^{-1}
$C_{L_{clean}}$	Clean 3D lift coefficient	–
$C_{L_{deS}}$	Design 3D lift coefficient	–
$C_{L_{land}}$	Landing 3D lift coefficient	–
$C_{L_{max}}$	Maximum 3D lift coefficient	–
C_l	2D lift coefficient	–
$C_{l_{\max}}$	Landing 2D lift coefficient	–
C_m	Moment coefficient	–
c	Chord length	m
c'	Landing configuration chord length	m
D_P	Propeller diameter	m
E	Young's modulus	Pa
e	Oswald factor	–
f	Equivalent parasite area	m^2
F_{engine}	Shear force caused by engine weight	N
F_{fuel}	Shear force caused by fuel weight	N
$F_{structure}$	Shear force caused by structure weight	N
$F_{tipfloat}$	Shear force caused by tip float weight	N
G	Shear modulus	Pa
g	Gravitational constant	$\frac{ft}{s^2}$
γ_w	Specific weight of water	N/m^3
h	Negative metacentric height of hull in upright condition	m
$h_{stringer}$	Height of the stringer web	m
I	Moment of inertia of hull load water plane	m^4
$I_{required}$	Required moment of inertia	m^4
i_w	Wing incidence angle	$^\circ$
I_{xx}	Moment of inertia	m^4
K	Single slotted flaps correction factor	–
K_Λ	Sweep factor	–
L	Lift	N
l	Length	m
l_{ab}	Afterbody length	m
l_{wet}	Wetted length of the hull	m
l_{fb}	Forebody length	m

l_{panel}	Length of a panel	m
$l_{stringer}$	Length of the stringer	m
M_{crit}	Critical Mach number	$-$
m_{panel}	Mass of the panel	kg
$m_{stringer}$	Mass of the stringer	kg
M_x	Moment around x axis	Nm
n_{bl}	Number of propeller blades	$-$
N_g	Landing gear load factor	$-$
n_s	Number of struts	$-$
P	Power	W
p	Magnitude of the distributed load	$\frac{N}{m}$
P_{bl}	Propeller blade loading	$\frac{N}{m^2}$
$P_{dynamic}$	Dynamic pressure	Pa
P_{req}	Required power	W
P_{shaft}	Shaft power	W
P_{static}	Static pressure	Pa
P_{tot}	Total pressure	Pa
q	Dynamic pressure	Pa
q	Shear flow	$\frac{N}{m}$
q_{s0}	Inner shear flow	$\frac{N}{m}$
R	Propeller radius	m
Re	Reynolds number	$-$
$R.M.$	The righting moment	Nm
S	Wing surface area	m^2
S_{wf}	Flapped wing surface area	m^2
S_{ref}	Reference wing surface area	m^2
S_{wet}	Wetted area	m^2
s_t	Maximum allowable tire deflection	m
s_{tofl}	Takeoff field length	m
s_{lfl}	Landing field length	m
T	Thrust	N
t_D	Skin thickness	m
t_{panel}	Panel thickness	m
$t_{stringer}$	Stringer web and flange thickness	m

V	Submerged hull volume	m^3
V	Velocity	$\frac{m}{s}$
V_A	Approach speed	$\frac{m}{s}$
V_{ftw}	Volume fuel tank in the wing	m^3
V_{rotate}	Rotation speed	$\frac{m}{s}$
$V_{s,x}$	Stall speed in configuration x	$\frac{m}{s}$
$V_{section}$	Shear force per section	N
V	Shear Force	N
W	Total aircraft weight	N
w_{max}	Maximum deflection	m
w_{panel}	Width of a panel	m
$w_{stringer}$	Width of the stringer flanges	m
x_p	Propeller position in x direction	m
Y	Yield stress	Pa
y	Y-distance to boom location	m
y_p	Propeller position in y direction	m
y_{rts}	Root to section distance	N
z	Submerged depth	m
z_{fh}	Flap hinge vertical dispositioning	m
z_p	Propeller position in z direction	m

Abstract

The Red Cross expressed the need for the development of an aerial vehicle that can extinguish wildfires in a more cost-efficient and time-efficient manner. Since the impact and frequency of wildfires are increasing, the threat imposed to communities living near large forested areas is growing. This report describes the development of the next generation aerial firefighting aircraft from concept as described in the Mid-Term Report [67], to the point that the main dimensions of the aircraft are known, the first design iterations are performed and the vital systems are sized.

This design process resulted in an amphibious aircraft with a weight of 54,243 kilograms and an estimated cost price of USD 118.9 million with an expected lifespan of thirty to forty years. The design has a T-tail with a high wing configuration. The total fuselage length is 34.72 meters with a wingspan of 39.25 meters. For the loading of water the aircraft is designed such that it is able to perform scooping operations but also land and take off from both land and water. Therefore, the bottom of the fuselage is designed to be a two step V-shape hull design with a maximum width of 3.3 m. As this design is a next generation it is equipped with innovative features like control canards, weight reducing inflatable floaters and hydrofoils for better take-off performance in water. Furthermore, a new real-time information system is initiated which enables improved mapping of the fire and more accurate drops.

At the end of this design process, the planning for the later design processes up to actual production has been made. As the design is not yet finished at this point in time, many iterations have to be performed, parts and systems to be designed and detailed analysis are to be made. For now it is forecasted that the aircraft is certified by July 2021 and actual production of this effective aerial firefighting aircraft can start.

Chapter 1

Introduction

Wildfires pose a significant threat to communities living near large, forested areas. Due to biomass growth and climate change, wildfires are an increasingly common phenomenon [23]. Common solutions to combat wildfires from the air include the use of water bombers, such as the Bombardier CL-415 and the Beriev Be-200. However, as the intensity and impact of wildfires are increasing, the need for the development of an aerial vehicle that can extinguish wildfires in a more cost-efficient and time-efficient manner has grown over the years. To meet this need, the team has been given the task to design a next generation water bomber.

From the Baseline Report (BR) and the Mid-Term Report (MTR), it was decided that a fixed-wing amphibious aircraft is the best concept to meet the project requirements [66, 67]. The purpose of the Final Report (FR) is to create a preliminary design of the fixed-wing amphibious aircraft, which involves the design and integration of main subsystems.

The approach of this design phase starts with a weight estimation, followed by the power and wing loading. From this, the the main sizing can commence on the hull, tail, wings and structure. After that the subsystems will be sized, which include the sizing of the engines, high-lift devices, fuel system, landing gear, and the intake/release system. The integration of all systems will be an iterative process requiring continuous updating. As this project is a preliminary design project, only a conceptual design will be delivered. The major design decisions have been made, yet further detail is left for the detailed design phase. The report is split into five parts, consisting of *Mission Analysis*, *Main Sizing*, *System Sizing*, *Design Performance Analysis* and *Recommendations for Future Design Phases*.

Part I of the FR start with a market analysis, a study on the current aerial firefighter market and its current demands. Chapter 2 concerns the firefighting mission analysis, in which certain mission requirements are set. Chapter 3 and 4 relate to the aircraft functions, from which in Chapter 5 the operations and logistics concept has been established. Chapter 6 and 7 concerns with the communication flow and safety, respectively. Finally, Chapter 8 discusses with the multifunctionality of the aircraft

Part II discusses the sizing of the main components of the aircraft. The wing and power loading is determined in Chapter 1, which forms the basis for further main- and subsystem sizing. In Chapter 2 an airfoil is selected, while the wing is sized in Chapter 3. The internal structured of the wing is determined in Chapter 4. Chapter 5 and 6 discusses the tail- and hull sizing, respectively. This part concludes with Chapter 7 in which the iterative and optimization process is discussed.

Part III is about the (sub-)system sizing. First, the control surfaces and high-lift devices are sized. Chapter 2 and 3 entail the sizing and positioning of the engines, respectively. The landing gear is discussed in Chapter 4 while Chapter 5 deals with innovative hydrofoils. Chapter 6 discusses the fuel system of the aircraft. The wing tip floats, required during on-water operations, are sized in Chapter 7. The type of retardant is discussed in Chapter 8, whereas the retardant intake- and release system are discussed in Chapters 9 and 10. The interaction between all electrical systems on board the aircraft, is discussed in Chapter 11.

Part IV relates to the performance of the design, not only in terms of flight performance, but also in terms of verification and validation procedures and compliance to requirements. Chapter 1 and 2 discuss the stability and control, as well as the flight performance of the aircraft, respectively. A risk analysis has been performed in Chapter 3. A sensitivity analysis and verification and validation procedures are performed in Chapter 4 and 5, respectively. This part concludes with Chapter 6 in which a check of compliance to the requirements imposed by the client, is performed.

Part V discusses recommendations for further design. Chapter 1 is on the project design and development logic whereas Chapter 2 explains further design phases on a time-wise scale by means of a Gantt Chart. The production of the aircraft is discussed in Chapter 3. Chapter 4 is devoted to sustainable development whereas Chapter 5 provides an overview of development- and production costs. In Chapter 6 a marketing strategy is introduced. Finally, Chapter 7 provides a list of innovations that are, or may be, included in the final design.

Part I

Mission Analysis

Chapter 1

Market Analysis

In the following chapter, an analysis of the market conditions for aerial fire fighting aircraft will be presented. The US Forest Service expenditures related to wildfire-fighting activities averaged at $1 billion in the 1990s, but this figure has increased to more than $3 billion per year since 2002. On top of that, $1-$2 billion is spent each year on wildfire-fighting by states themselves [23]. Aerial firefighting activities have been playing a major role in fighting large wildfires for several decades, and many kinds of solutions have been developed for this purpose. With wildfire threats and firefighting expenses evidently rising, it is only logical to seek for improvements. These should result in more cost-effective and time-effective ways of extinguishing wildfires. After all, the safety of civilians and their properties is at stake. In this chapter, the most significant solutions that exist today are identified and analyzed. Then, market possibilities for a new solution are discussed, as well as the costs that would be involved with a possible new project.

1.1 Current Solutions - Fixed-wing

A number of significantly used fixed-wing firefighting aircraft with a capacity of over 4,000 liters are listed in Table 1-1. The water bomber to be designed should be capable of dropping at least 15,000 liters of fire retardant. As can be seen from Table 1-1, there currently are only a few fixed-wing water bombers that can hold at least this amount of fire retardant capacity, but these water bombers' capacities actually exceed the 15,000 requirement by a large margin and are therefore also outside the design range for the new solution.

Many smaller fixed-wing water bombers are outdated World War II aircraft or other commercial aircraft from a similar era which have been refitted to accommodate water tanks. The fire retardant capacity of these water bombers typically ranges from 4,000 liters (PBY Catalina) to 11,000 liters (Lockheed L-188 Electra). These aircraft however are in general old and expensive to maintain, as most of these aircraft are no longer in production and spare parts are scarce [9].

Table 1-1: List of Comparable Fixed-Wing Water Bombers [9, 20, 45]

Aircraft Type	Fire Retardant Capacity [Liters]	Number of Aircraft in Service
Bombardier 415	6,140	80
Beriev Be-200	12,010	7
Evergreen 747 Supertanker	78,000	1
Douglas DC-10	45,000	1
Martin Mars	27,000	2
Iliyushin Il-76P/MDP/TDP	43,230	Unknown
BAe 146	11,000	6

As seen in Table 1-1, the Bombardier 415, which has a fire retardant capacity of 6,140 liters, can be considered to be a commercial success selling over 80 aircraft in the last 20 years. Together with its predecessor, the CL-215, it is the most used purpose-built firefighting aircraft with a capacity of over 4,000 liters. On the other hand, Beriev delivered only 7 Be-200 thus far since 2003, with 15 orders pending. According to Jane's All The World's Aircraft, the break-even point for this fixed-wing water bomber will be reached at 48 orders [9]. Therefore, a joint market analysis has been conducted by Irkut and EADS in 2002 for a Rolls-Royce BR715 powered variant of the Be-200 which would be introduced

to the western market. This analysis was completed in March 2003 and revealed a potential market of 320 Rolls-Royce powered Be-200 over 20 years [27]. However a study in late 2004 study concluded that the market for the Rolls-Royce version would not cover the development costs and the program was canceled [9]. Still, the regular version of the Be-200 has been certified for the European market in 2010, and an undisclosed number of aircraft has been ordered by the Greece Government in 2007. It is unknown whether this order has been canceled or not [69].

The other fixed-wing water bombers which have a fire retardant capacity in excess of 15,000 liters are custom built in only very small numbers. Furthermore, these large fixed-wing water bombers are generally considered to be cost inefficient. The Martin Mars for example was grounded after 53 years of service. This aircraft was not awarded an aerial firefighting contract in 2013. According to Canadian Forest Minister Steve Thomson this aircraft no longer makes economic sense as there are more cost-effective, efficient options available due to advances in airplane technology [37]. Other high capacity water bomber conversion projects such as the 747 Supertanker and the DC-10 have only been completed on one aircraft of either type, and neither of these aircraft are used frequently. Evergreen, the owner and operator of the 747 Supertanker, announced on November 8, 2013 that it would cease all of its operations by November 30, 2013 [41]. The Iliyushin Il-76 allows for temporary installation of water bombing equipment, and several models have been permanently converted for this purpose [48].

More recent fixed-wing water bombers are the Beriev Be-200 and Bombardier 415, which are specifically designed and built for aerial firefighting. Both of these aircraft have the capability of scooping water from a lake or river.

1.2 Current Solutions - Rotorcraft

Currently, not only fixed-wing aircraft are being employed for aerial firefighting but rotary-wing aircraft such as the Sikorsky S-61 and Boeing CH-47 "Chinook" are widely used to fight wildfires as well. In general these are helicopters on which a water bucket will be attached. The fire retardant capacity of such rotary-wing aircraft is in general smaller than fixed-wing aircraft. However, there are some helicopters that should be considered during this market analysis as their fire retardant capacity is comparable to large current fixed-wing water bombers. Some of these large rotary-wing aircraft are listed in Table 1-2.

Table 1-2: List of Rotary-Wing Aircraft with Firefighting Capabilities [45, 9]

Aircraft Type	Fire Retardant Capacity [Liters]	Number of Aircraft Built
Sikorsky S-64 Skycrane	10,031	110
Eurocopter AS332L Super Puma	7570	780 (2011)
Boeing CH-47 Chinook	7570	1,179
Mil Mi-26	15,000	322 (2010)

An important remark with respect to the rotary-wing aircraft listed in Table 1-2 is that the majority of these helicopters (except Sikorsky S-64 Skycrane) are being used as military heavy-lift transport helicopters. Only a small number of these helicopters will specifically be employed as aerial firefighting vehicle during the wildfire-seasons.

1.3 Market Volume and Price

In this stage of the design process, it is not possible to accurately estimate a potential market price. Therefore, the market price will be solely based on current list prices of reference aircraft. An extrapolation of market prices of reference aircraft, as can be seen in Figure 1-1, revealed a potential market price of 67.6 million US$ in the year 2013.

In order to estimate the potential market volume, an analysis of air attack against wildfires conducted by the RAND Corporation will be used [19]. A model was used to perform this analysis and revealed that the overall cost-minimizing solution required eight 11,000 liter water bombers and forty-eight 6,000

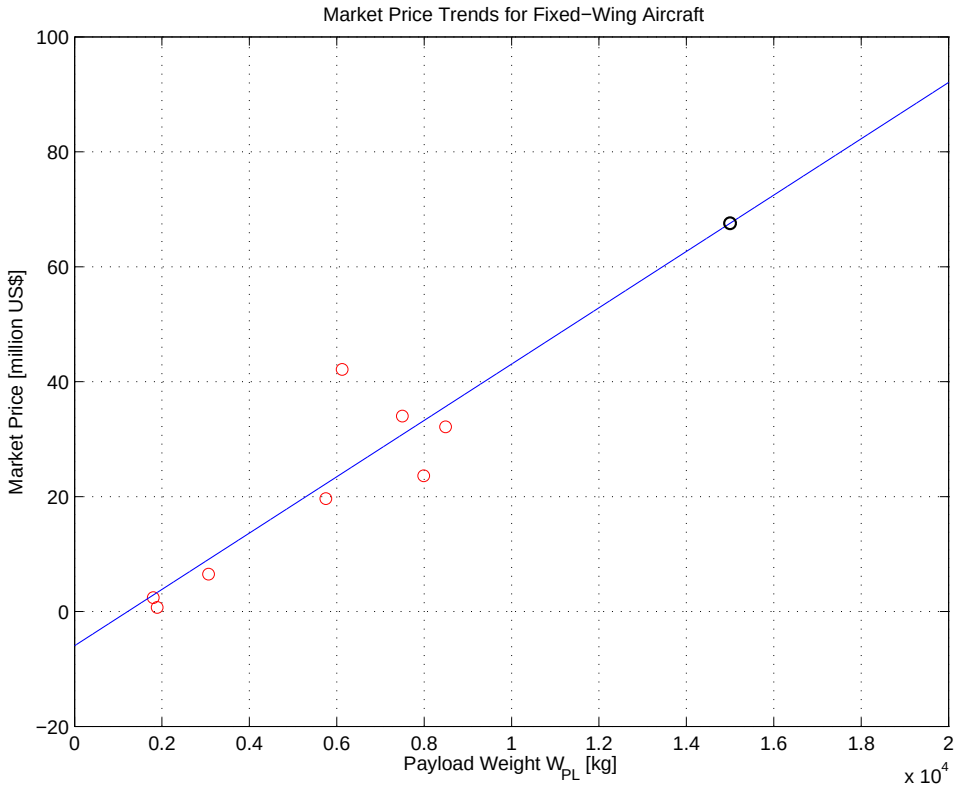

Figure 1-1: Extrapolation of Market Prices of Reference Aircraft

liter scoopers. It should be noted that this only applies to the US and not all 11,000 liter water bombers need replacement. Based on the results of this model, it is estimated that the market volume for the next generation water bomber is approximately 40 aircraft over the next 30 years. As the next generation water bomber will be a revolutionary aerial firefighting aircraft with a significantly larger payload capacity compared to current water bombers, it would face little competition in its market segment. However, if the entire aerial firefighting market is considered, there is a large variety of aerial firefighting vehicles, ranging from small agricultural aircraft, to helicopters and a converted Boeing 747 or Douglas DC-10. Therefore, it is estimated by the design team that a market share of 10% is be achievable.

1.4 Market Possibilities

It can be concluded from previous projects that large water bombing aircraft have not proven to be successful commercially. However, this does not mean that there is no demand for such aircraft. Apart from the and Beriev Be-200, there have not been any purpose-built solutions meant for large scale production, and the Be-200 project can therefore be considered to play a pioneering role in this industry. So far, high operational costs and a lack of worldwide availability have been major obstacle for wide usage of these aircraft. Also, the Be-200 has been found unsuitable as a scooping aircraft in many countries, since it needs large lakes or rivers for scooping which are often not present. If a high capacity aerial firefighting solution can be developed which does not suffer as much from these obstacles, it can be a direct competitor to the Bombardier 415 and therefore it could have the potential for a similar sales figure. Given that the Bombardier 415 can be seen as the market leader in this industry, it can be worthwhile to design a new aircraft that can succeed the Bombardier 415 and therefore can gain interest of organizations looking to renew their aging CL-215 and Bombardier 415 fleet. At the same time, it is very important that a newly designed aircraft offers a substantial improvement over existing solutions in many aspects, such as a higher tank capacity, quicker turnaround times and higher usage flexibility.

Chapter 2

Firefighting Mission Analysis

In this chapter, an analysis is performed to investigate to what extent the given specific requirements define the mission, after which the optimal general firefighting mission is presented. Finally, the firefighting mission possibilities and limitations is assessed and its implications on the design are discussed.

2.1 Assessment of Client Imposed System Requirements

The client imposed requirements already define the scope of the firefighting mission to a certain extent. This section presents an analysis of these requirements and assesses their feasibility.

- The requirement that the load capacity must be at least 15 m^3 of water directly implies that the designed aircraft will be more suited to fighting relatively large fires, and that the retardant loading method will have to be optimal to prevent excessive turnaround times. In 2005, the US Forest Service conducted a study on the aerial application of wildland fire management, which concluded that airtankers with a retardant capacity of over 3,000 US gallons (11.4 m^3) are justified as an integral component of the initial attack resources for land management agencies [35]. Also, it was concluded that these airtankers continue to show significantly greater economic benefit over smaller capacity platforms [35]. Based on these statements, the development of an aerial firefighting solution with this range of retardant capacity is justified.
- The range requirement of at least 500 nm (926 km) fully loaded also has consequences for the mission design. For example, the airbase from which the aircraft will operate must not be located too far from the fire, since it must be able to travel to the fire, drop and refill retardant, and return to the base within this flight range.
- The requirement that the retardant must be reloaded both on land and on water results in the incorporation of these loading techniques into the mission design. According to [19], at least two-third of the historical fires in the U.S. were within 10 miles (16 km) of a scooper-accessible body of water, while about 80 percent have been within five miles (8 km) of a helicopter-accessible body of water. Since the U.S. market will be one of the main targets for the project, these findings justify the use of such reloading techniques.
- The requirement that the design must be versatile enough to carry other loads implies that these activities will also be part of the mission design.

Other stated requirements, such as climb rate, take-off field length and maneuvering envelope, all affect the mission in the sense that they define a range of environments in which the aircraft must be able to operate. Maximizing this range is clearly beneficial to the viability of the mission design, and therefore it is justified to attempt to fulfill these requirements completely.

2.2 Determination of Optimal Firefighting Mission

Based on the given assessment of the given specific requirements, the market analysis performed in the Baseline Report and the mission characteristics of current solutions, the mission characteristics that have been defined to be the most favorable are as follows:

- Operations are to be carried out from any suitable airbase. Depending on the design, the maximum required runway field length may be up to 1,000 meters, and the airbase should be located within an hour of flying from the wildfire. The base could also be a suitably sized water body, thus the

ablility to take off and land on water would add a lot of possibilities for setting up a mission basis. Basic equipment for setting up the base must be carried on board. Retardant tanks can be filled at the base before take-off.

- The aircraft flies to the fire location in cruise configuration.
- (Re-)loading of retardant is performed by using available water bodies. The retardant consists of water retrieved from a water body, optionally mixed with foam additives or other additives.
- The firefighting method that is pursued is to perform initial attack extinguishing methods with high capacity retardant drops. If a fire has already expanded to a large area, the mission is aimed at controlling the fireline by covering the area around the fire with retardant. Both methods support ground forces in accessing the fire.
- Dropping of the retardant is to be performed at a speed lower than 100 knots (185.2 km/h) at the lowest possible height. Maneuvering capabilities are of importance especially in mountainous areas. Accuracy, dosage and control over the location where the retardant hits the ground must be sufficiently high to assure that usage efficiency of the retardant is as high as possible.
- It must be possible to repeat loading and dropping procedures multiple times before refueling is necessary.
- The aircraft should be versatile enough to perform other tasks such as surveillance, Search and Rescue (SAR), smoke jumper drop-offs, transport of other loads etc.

2.3 Mission Assessment

Based on the analysis of a firefighting mission, its implications on the design of the next generation water bomber can be established:

- Fixed-wing aircraft need an airbase that can provide all the required facilities for the firefighting mission. Therefore, the mission duration and effectiveness depends on the availability of such an airbase within a reasonable vicinity of the wildfire. Generally, the available runway length is the critical factor which decides whether an airbase can facilitate the aircraft. Several design measures are taken to increase the possibilities for the aircraft to operate from within a reasonable vicinity of the wildfire. Firstly, the design will be optimized for short landing and take-off distances by using special high-lift devices, a larger wing area or by making a lighter design. Another measure is to design the aircraft such that it can land on water; in that case a temporary airbase can be set up next to any suitable water body such as a lake or a river.
- Fixed-wing aircraft can reach a relatively high cruise speed, which brings the advantage of being able to cover and reach a larger area with the same flying time compared to rotorcraft. For this reason, less aircraft will be needed to cover the same area of land.
- Regarding the loading and reloading techniques, several methods are considered. Scooping can be done within half a minute depending on the tank capacity, while pumping the retardant into the tanks on the ground can require several hours. For scooping a water area longer than 800 meters is required within the vicinity of the fire. According to an air tactical group supervisor from Kern County [19], at least two-third of the historical fires in the U.S. were within 10 miles (16 km) of a scooper-accessible body of water. From these findings it can be concluded that incorporating scooping capabilities into the fixed-wing mission design is beneficial to the overall performance of the mission.
- There are various options for the retardant dropping technique. Most smaller fixed-wing aircraft use gravity-assisted retardant delivery methods. This method is simple and and quick, but it does not provide a lot of control on the dosage of the dropped retardant: the entire tank content is dropped at once and it is not aimed. In order to optimize the retardant delivery, the fixed-wing airtanker to be designed will have a computer controlled retardant dispersal system capable of both

precise incremental drops and long trailing drops. Retardant flow rates must also be controllable to vary the retardant coverage level dispersed as required by the intensity of the fire behavior and vegetative fuel type. Finally, to improve the accuracy of the dropping operation, it can be considered to use water capsules. The capsules keep the water together during the fall, which increases the degree of controllability on the dropping operation.

- Another consideration is that fixed-wing aircraft need to maintain a minimum airspeed at all times while airborne, which adds complexity to the retardant delivery procedures. Generally, retardant drops are performed at airspeed ranges of 125 to 150 knots (230-280 km/h) from a height of 150 to 200 feet (45-60 m) [5]. However, as mentioned in section 2.2, a dropping speed of 100 knots (185 km/h) or less is considered more optimal. Optimizing the design to allow for lower airspeeds and heights will greatly enhance the effectiveness of the mission.
- To make the aircraft versatile enough for multi-purpose use, the aircraft design will need to have a fuselage with an interior that can be easily modified to suit a variety of missions.

2.4 Conclusion

The system requirements imposed by the client have been assessed and deemed realistic. Following these requirements, a set of mission characteristics has been defined which describes how the aircraft will be used to fight fires. For the design concept, the mission characteristics have been assessed and design recommendations were made to fulfill these characteristics as much as possible. Now it is possible to assess the other operational and logistical parts of the concept design.

Chapter 3

Functional Flow Diagram

The next generation water bomber should be able to perform several functions. In order to clearly describe what these functions are and in what sequence they should be performed, a Functional Flow Diagram (FFD) has been set up. A FFD consists of various blocks describing these functions which are interconnected by arrows that indicate the dependence of various functions on one another. The Functional Flow Diagram that has been established for the next generation water bomber is depicted in Figure 3-1. In the following sections, these blocks and the different types of missions that have been considered for this design will be discussed.

3.1 Main Block Diagram

The main starting point of the mission is depicted in the upper left part of the diagram (figure 3-1). A distinction has been made between take-off on water and take-off from land. This distinction has been made as after a water take-off, the tip wing floats need to be retracted into the wings instead of the landing gear, which makes for a slightly different functional flow. After take-off, the functional flow for both take-off types is the same again. Once the gear or floats have been stowed, the actual mission can be performed. For a sequential description on the mission, please refer to Section 3.2. Once the mission has been performed, the aircraft is ready to return to base (see upper right part of Figure 3-1). For the subsequent steps, a distinction between a water landing or a landing on land has been made again because of the difference in either deploying the gear or the floats. A more detailed description of the mission can be found in Chapter 5 in which the operations of the water bomber will be discussed.

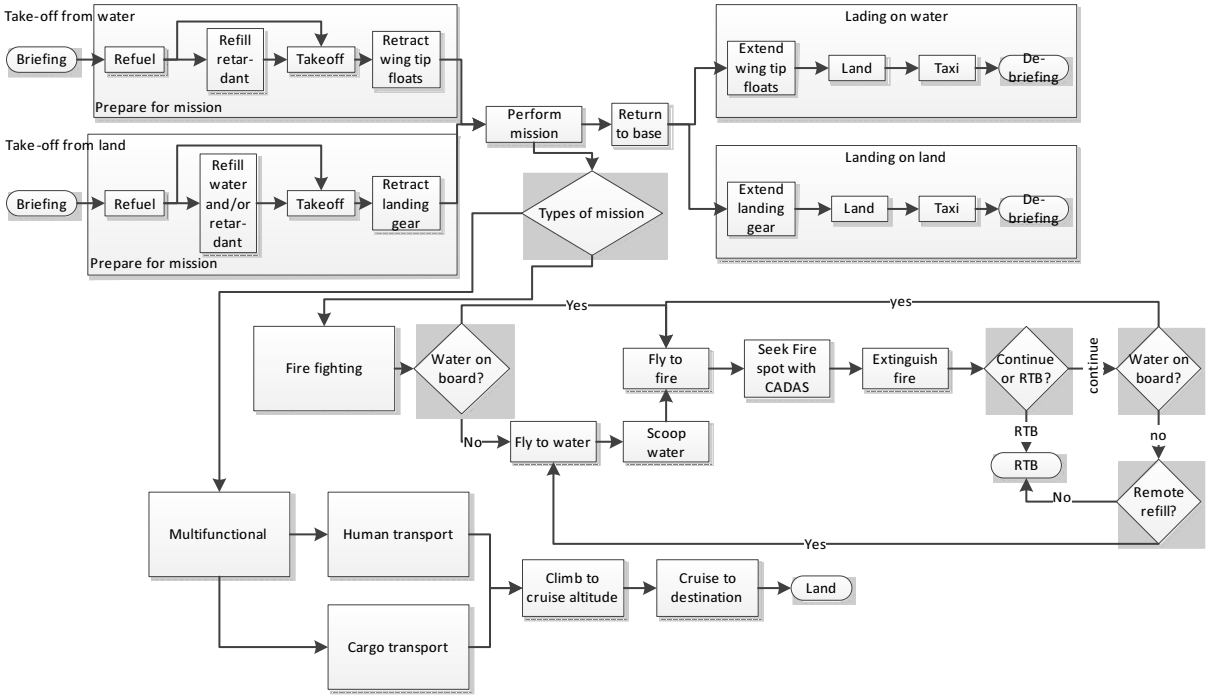

Figure 3-1: Functional Flow Diagram for Proposed Design

3.2 Type of Missions

As described in Chapter 2, the aircraft should be able to perform multiple missions. As wildfires will not occur during the entire year, the aircraft has been designed with the ability to perform multiple missions in mind so that it does not have to be grounded several periods a year, which would be a waste of (monetary) resources. Hence, two other missions next to firefighting are considered, namely emergency relief and cargo transport missions. A more detailed description of the mission can be found in Chapter 5, in which the operations of the water bomber will be further discussed.

The firefighting missions starts after take-off. The first step that follows depends on whether the aircraft already has water on board or not. If it does not, it first needs to scoop water to fill its retardant tanks. After that, or if the water was already loaded on the ground, the aircraft can fly in the general direction of the fire, after which Computer Augmented Detection and Aiming System (CADAS) will be engaged to accurately locate the fire. When the plane flies above the fire, the retardant will be released to extinguish the fire. If there is still retardant left in the tank, the aircraft can make a loop and drop the remainder of the load. After that, the aircraft can fly back to the water body to refill its tanks or return to base.

In case the aircraft will not perform a firefighting mission, it can be used for cargo or human transport. In that case, the step of refilling the retardant will be omitted, however the aircraft will be loaded with other payload. The aircraft will then take off, climb to cruise altitude, cruise to its destination and land, either on water on land. After each mission ends, a new mission can be performed or the same mission can be repeated again.

Chapter 4

Functional Breakdown

In this section all functions the aircraft will be able to perform are listed in a Functional Breakdown Structure (FBS) as depicted in Figure 4-1. It is structured in different levels in which the functions and subsystems of the aircraft during different phases are described. This FB is a more detailed version of the one that was set up in the Baseline Report, providing a more extensive overview of all functions [66].

4.1 First & Second Level of the Diagram

The first and second level are similar to the one presented the Baseline Report and encompass the mission of a 3rd generation water bomber, as well as all main mission phases listed below:

- Ground-Operations
- Operations at Water
- Deployment
- Take-Off
- Landing
- Cruise

4.2 Third Level of the Diagram

The third level of the diagram provides a more detailed overview of the functions the aircraft will be able to perform during each mission phase. Specific systems, such as scooping and data traffic, are listed as subfunctions of a mission phase. Several design features have been incorporated in the FBS. These features include flaps and slats that are installed on the aircraft's wing and the operation of (cargo) doors. Furthermore, incorporated features such as innovative inflatable wing tip floats and a sophisticated mapping system (CADAS) are included as well.

The FBS also provides a great tool to identify the functions that are considered most critical. For this aircraft, they are the deployment of flaps, inflation and deflation of tip floats, opening and closing of (cargo) doors, deploying and retraction of the scoops and mapping the location of the fire(s). It also enables the identification of tasks that the aircraft will need to be able to perform during the entire flight, such as maneuvering and establishing contact with the ground station.

4.3 Fourth level of the Diagram

The fourth level of the FBS only consists the sub-functions of *Maneuver* which are:

- Pitch control
- Roll control
- Yaw control

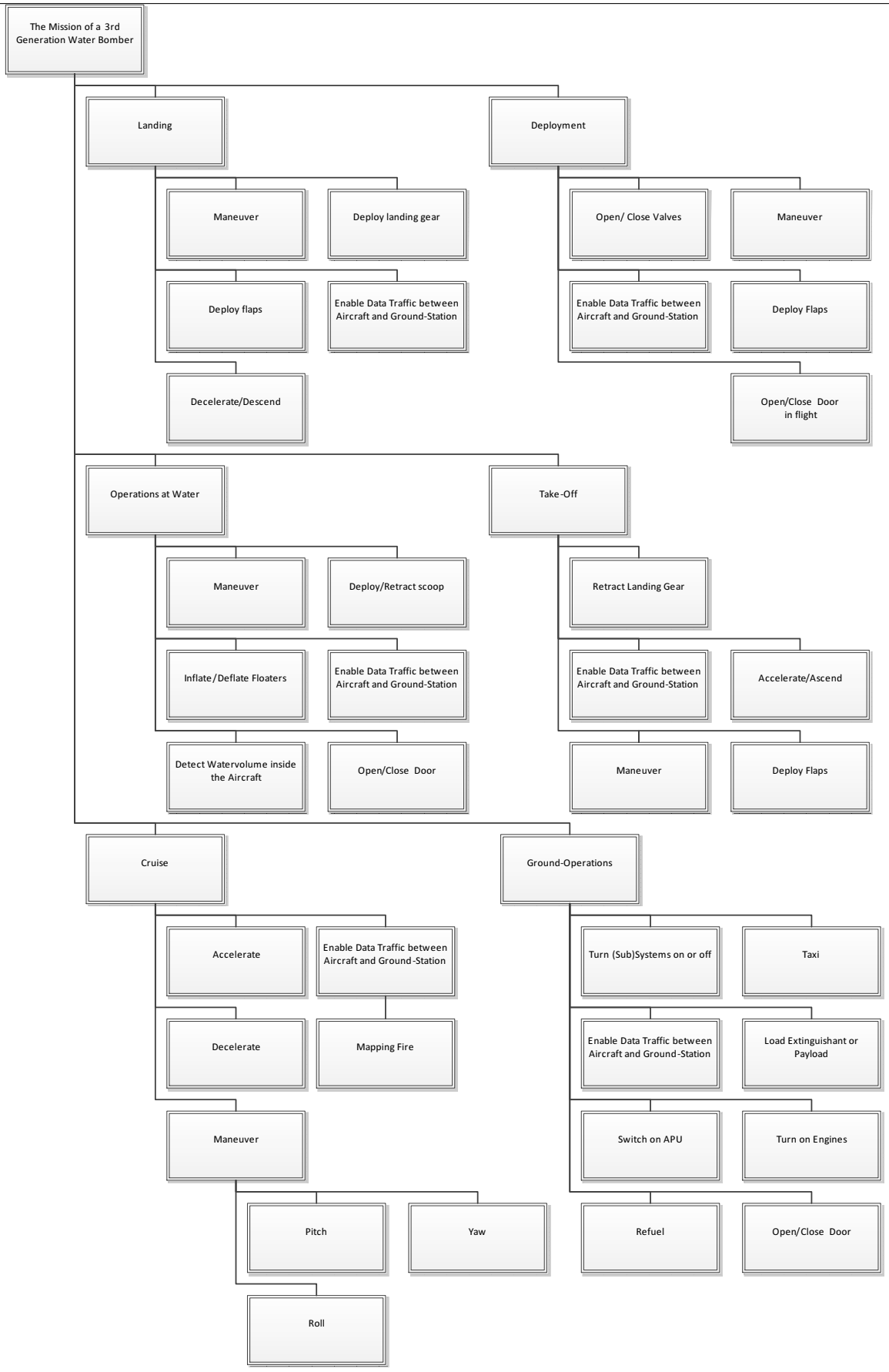

Figure 4-1: The Functional Breakdown of Proposed Design

Chapter 5

Operations & Logistics Concept Description

Next to the purely structural parts of the design, a concept for *Operations & Logistics* is also required in order to be able to deliver a satisfactory product. It is important to create this concept early on in the design phase and keep it updated throughout the design process, as this means the design can be adjusted to optimally fullfill its role, and it can be determined what is needed in terms of personnel and (ground) support equipment.

Section 5.1 will deal with the projected operations of the aircraft, while the associated logistics will be dealt with in Section 5.2.

5.1 Operations

The operation of a waterbomber is less straight-forward than it may seem. There is not only the fire-fighting mission to consider, but also ferry flights and alternate missions like emergency relief, transport and reconnaissance. All of these missions can be split up into seperate flight phases, which in turn can be seperated into actions.

In this section, functional flow diagrams (FFD's) are presented to determine which actions the aircraft needs to perform, so this information can be incorporated in the design process. Where already known, specific values or suggested operating procedures are given for each action.

5.1.1 Generic Flight Phases and Actions

Some flight phases return for every flight, regardless of which type of mission is flown. This includes basic operations like take-off and landing, but also "flight" phases like start-up, loading and refuelling. An FFD showing a generic mission is given in Figure 5-1.

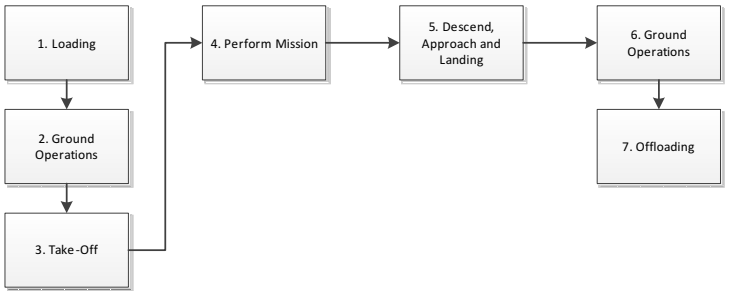

Figure 5-1: The Generic Mission Functional Flow Diagram [67]

The flight phases shown in Figure 5-1 are split up into seperate actions, for which seperate FFD's have been created. This is also done for the firefighting mission, as this is the most non-standard and demanding mission expected.

5.1.2 Mission Independent Flight Phases

Loading

For every mission, the aircraft needs to be loaded, for which the actions are shown in Figure 5-2. This not only covers payload, but also fuel and crew loading.

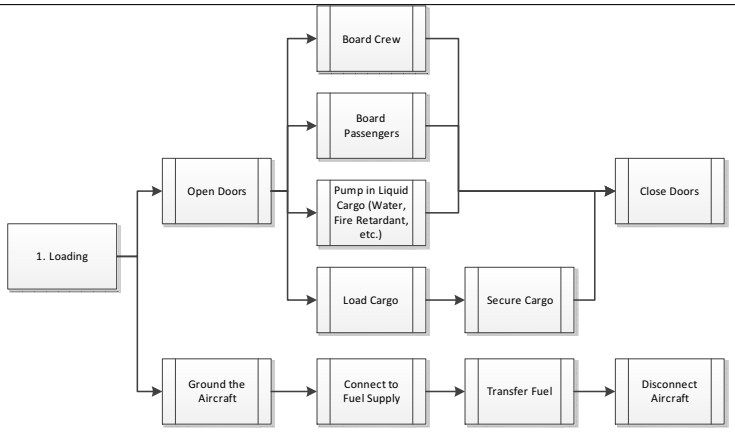

Figure 5-2: Loading Functional Flow Diagram

In order to refuel the aircraft, the aircraft first needs to be grounded (electrically connected to the fueling system). This is a standard required procedure to avoid fires caused by static discharges during fueling. Provisions for this should be present, but a bare piece of metal can already suffice for this. As this can usually be found somewhere on for example the landing gear, this is not expected to give any issues further on in the design. Next the aircraft fuel tanks need to be connected to the fuel supply, implying the fuel tanks should have provisions like fuel caps, which must be relatively easily accessible. After fueling, everything should be disconnected safely.

In order to load cargo, passengers and crew, doors of sufficient size are needed. In case of liquid cargo like retardant, or any other liquids stored in the tanks, this requires provisions for pumping it in. In the case of solid cargo, provisions are required within the cabin to secure it during flight. In case of passengers or stretchers, provisions for allocating and securing these should also be available or installable.

Ground Operations at Originating Airport

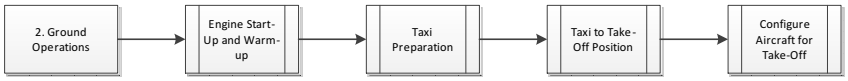

Figure 5-3: Ground Operations at Originating Airport Functional Flow Diagram [67]

The ground operations at the originating airport are shown in Figure 5-3. These include engine start-up and warm-up, systems start-up, preparation for taxi, taxi to take-off location and configuring the aircraft for take-off. The last step includes actions like setting the flaps for take-off, turning off taxi lights et cetera. Although the exact execution of these steps differ slightly for water runways with respect to conventional runways, it does not pose non-obvious restrictions on the design.

Take-Off

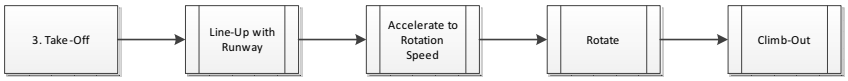

Figure 5-4: Take-Off Functional Flow Diagram [67]

The take-off procedure again does not differ significantly between land and water operations. It starts with lining up the aircraft with the runway (or the most favourable direction on the body of water), then accelerate to V_{rotate} (expected to lie around 105 knots), at which point the stick will be pulled back and the craft will become airborne. During the climb-out, the aircraft should be configured for flight, which means retracting the flaps as well as the landing gear or tip floats in case of a land or water take-off, respectively.

Descent, Approach and Landing

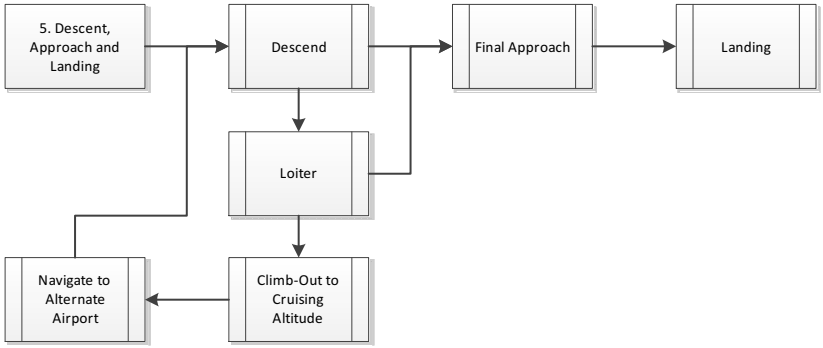

Figure 5-5: Descent Functional Flow Diagram [67]

The descent, approach and landing can be summarised as shown in Figure 5-5. When near the projected landing location, the aircraft will descend. During this descent, it will also slow down to approach speed (currently projected at 105 knots for a landing at MTOW), set the flaps incrementally to the landing setting and deploy the landing gear or tip floats, whichever is applicable. The aircraft should then turn to line up with the runway for its final approach, descend to runway level and stall out there, touching the aircraft down gently on the runway.

In case of a blocked or unusable runway, the aircraft should enter a loiter, for which sufficient fuel reserves should be present. If the runway is not foreseen to be usable within the maximum loiter time, the aircraft should climb to cruise altitude and navigate to an alternate landing site, where the whole procedure starts over again. Again, the aircraft should have enough fuel reserves for this.

Ground Operations at Destination Airport

Figure 5-6: Ground Operations at Destination Airport Functional Flow Diagram [67]

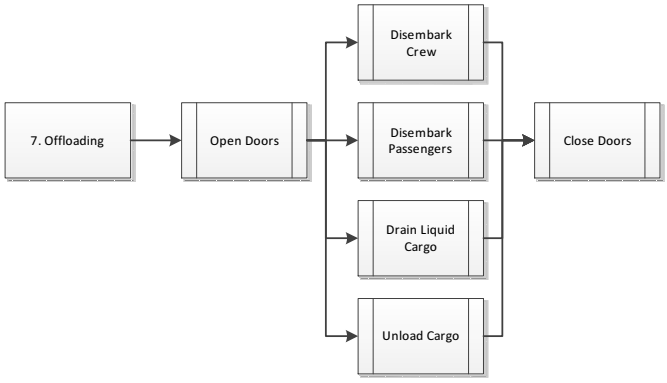

Figure 5-7: Offloading Functional Flow Diagram

After the aircraft has touched down, it has to perform some ground operations again (shown in Figure 5-6. This mainly involves leaving the runway and taxi to the ramp or parking, where the engines and other systems should be shut down. Here, also the aircraft should be fixed in place, on land by means of parking brakes, wheel chocks and tie-downs or on water by means of mooring and/or an anchor. This implies provisions for tying down the aircraft or mooring it should be present, as well as the items needed for this should be taken along.

After engine shutdown (usually), the aircraft should be unloaded, as depicted in Figure 5-7. The exact steps depend on what was loaded, but usually consist of opening the doors, disembarking passengers and crew, unloading the normal cargo and draining liquid cargo from the tanks. This implies also an extra draining provision should be present there.

5.1.3 Mission Dependent Flight Phase: Sequence of Actions for a Firefighting Mission

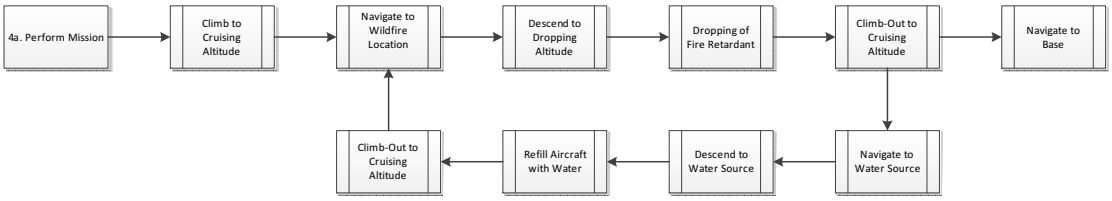

Figure 5-8: Firefighting Mission Functional Flow Diagram [67]

Performing a firefighting mission is a very specific mission phase. As the water cannon in its current form has been deemed impractical, only the used of the water bombing system will be discussed here. After take-off, the aircraft first will cruise to the location of the wildfire (assuming it has taken off with filled tanks, which is not the case when taking off from water). There, it will descend to dropping altitude, if the surrounding area permits it. If it is the first drop in this location and there is no leadplane available, the pilots may elect to do a reconnaisance run over the target area first, in order to find the best drop path, location(s) and patterns. The drop run itself commences with establishing take-off configuration, in order to facilitate slow flight combined with good climb characteristics. Next, the aircraft will fly over the target and drop the load before reaching the target. The optimum drop height varies between 30 and 60 meters AGL depending on the conditions and desired drop pattern. After dropping, the aircraft will start a climb due to the sudden abundance of lift, but this will also induce a much lower angle of attack which needs compensation by the pilots, who should also steer the aircraft clear of terrain obstacles and the fire hazard area, bringing it back to cruising altitude.

If this was the last drop of the flight, the aircraft can RTB, but otherwise, if there is a suitable water body nearby, it will refill its tanks there. Upon reaching the location of the water body, the pilots will descend to a low level flight. If this is the first approach to the scooping location or it is a particularly busy body of water, again a reconnaissance run is advised. The actual scooping run will consist of the pilots establishing take-off configuration and approach speed appropriate for the zero payload weight, then setting the aircraft down lightly on the water surface on only the first step, adding power to compensate for the upcoming increase in weight and drag during the scooping, after which the scoops are extended into the water. This will fill the tanks and, as the tanks are filled up, the scoops will be retracted and the aircraft lifted out of the water, after which the aircraft should be brought back to cruising altitude and headed to the dropping location once more.

A typical firefighting mission will see the aircraft carry its full payload weight around half of the time. This results in a realistic mission time of slightly under 3 hours before refueling is required. Using the typical distance to a scoopable water body of 16 km (which goes for two-thirds of the US historic fires as mentioned in the previous report [67]), a cruise speed of 111 m/s and some leaway for lining up, scooping, maneuvering and dropping, this results in a turn-around time of around 10 minutes. Taking into account that the tanks can make four seperate 3750 liter drops per scoop, this amounts to 24 drops per flight. As the distance to the water source increases, this decreases the amount of drops per flight. Assuming a turn-around time for refuelling and other resupplies of half an hour, this results in around 4 flights a day or a total of 360 tons of water delivered to the fire each day.

5.2 Logistics

Next to the immediate operations of the aircraft, some logistics are needed to allow these operations and also the neccessary maintenance for the aircraft and its systems. The resulting requirements set to bases

and aircraft systems will be discussed in this section.

5.2.1 Ground Support

Refueling Facilities
As the aircraft requires fuel to operate, a fuel supply should be present or provided at the base. In case of a water base, the aircraft should carry all equipment to get the fuel from the shore-based fuel supply into the aircraft tanks. This includes all the hoses and pumps required for this task.

Retardant Supply
In case of a land base, the water should be pumped into the aircraft, and be provided at the base. As pumps cannot be assumed present on-site, these will be carried within the aircraft. The pumps also need to be able to pump in retardant and additive chemicals, the last into seperate tanks for in-flight mixing when scooping. This is independent of whether the aircraft is based on land or water. Upon deployment to a field base, a 2-day supply of the additive chemicals also needs to be able to be taken along, in order to ensure fast deployment.

Maintenance Facilities
The nature of the aircraft mission and the typical government requirements involved implies that the aircraft may be used very intensively, with barely any time available for (scheduled) maintenance or full repairs. Also, being confined to field bases means that only the bare minimum of resources is available for this. This means that only consumables (fluids, gaskets, nuts and bolts) for a small amount of days should be taken along, as well as a maintenance technician, untill more resources can be brought in through supply lines. In the off-season, enough time should be reserved for the major repairs and overhauls that cannot be done during deployment.

Communication Facilities
In the absence of an actual airfield, the aircraft should carry enough communication equipment (radio's, antenna's, tracking equipment et cetera) to set up a rudimentary forward operating base (FOB), which can run a skeleton operation for enough days to set up proper supply lines and establish a more complete field base.

Loading Facilities
For performing cargo missions, the originating and receiving airports should both provide the neccesary cargo handling equipment, like forklifts et cetera.

Power
In case of a skeleton FOB, the aircraft APU should be available for charging the batteries of the base equipment if necessary. Bringing in indepent generators or other means of power supply should be a priority when upgrading the FOB through other supply lines.

5.2.2 On-board Items

Next to the items required for deployment, there are also items which have to be take along mandatorily. For operations over water (very likely in case of an amphibian) this includes for example a dinghy or life raft, while firefighting operations require portable fire shelters. Other standard items include first-aid kits, all tie-downs, remove-before-flight-covers, dock-lines, an anchor et cetera, as well as hydraulic fluids and engine oil.

5.3 Conclusion

From all the above, it can be concluded that, even to establish only a skeleton FOB, there is still a lot of equipment and personell to take along on an initial deployment. Even so, it is critical that proper supply lines are established as soon as possible to support the FOB and upgrade it into something which can do more than support the aircraft and its crew in only its barest needs. Also, there are some things that have to be on-site even for a skeleton FOB, like fuel.

Chapter 6

Communication Flow Diagram

A Communication Flow Diagram (CFD) illustrates the flow of information during a mission to and from the aircraft with respect to its environment. A CFD gives an overview of all people and systems involved and the influence they have on the aircraft. As described in Chapter 8, the aircraft will be multifunctional which imposes different flight scenarios on each potential communication flow. However, the Communication Flow Diagram that will be described in this chapter and shown in Figure 6-1, has been based on a traditional firefighting scenario which requires aerial assistance.

6.1 Organizational Structure

The number of firefighting units active in fighting a particular wildfire, and whether aerial support is required, mainly depends on the size, the complexity and the location of the wildfire. The number of people and systems that are present in the environment of the aircraft therefore heavily depends on the type of fire. In the CFD, the most common personnel and systems are illustrated. The elements that may vary in size depending on the wildfire are grouped together as much as possible. As aerial firefighting is primarily performed in order to support the firefighting activities on the ground, the number of airplanes and rotorcraft that are deployed for fighting a specific wildfire heavily depends on the ground activities and the support they require.

The entire firefighting operation is coordinated from the Firefighting Coordination Center (FCC). The FCC is an organization or group of people which is concerned with general coordination of the firefighting activities. In the USA, the National Interagency Coordination Center (NICC) is responsible for the mobilization of units, crew dispatching and aircraft dispatching when it concerns large fires. For relatively small fires, the firefighters are most likely to be the coordinator. The size and type of organization that is responsible for the coordination of wildfires, depends mainly on the type of operation [12].

The FCC receives information from multiple sources, as indicated in the CFD. Information from satellite images, aerial surveillance and reports from the ground troops are used to determine the most effective way of fighting the wildfire. The FCC subsequently informs the Air Tactical Group Supervisor (ATGS) what the locations are where aerial support is needed. The ATGS, usually airborne, is primarily responsible for the coordination of the aircraft operations. However, for small fires, this group may be excluded and the FCC is in direct contact with the flight crew [14].

When the aerial firefighting operation becomes very complex due to the number of aircraft involved, the ATGS may choose to identify an airplane as the leadplane. The leadplane pilot maintains an overview of the locations of the airplanes and rotorcraft involved and the release location of the fire retardant from the ATGS. The leadplane coordinates and directs multiple aircraft and the rotorcraft to the assigned fire retardant release location. This increases the safety and firefighting effectiveness for complex aerial firefighting missions.

Depending on the size of the fire and the complexity of the operations, the flight crew receives information about the release location from either the lead plane, ATGS or directly from the FCC. The flight crew of the design consists of four persons, two pilots and two flight engineers. It should be noted however, that the number of on-board flight engineers may be reduced in a later stage of the design.

The flight crew is responsible for the flight trajectory of the aircraft, the aircraft itself and its payload. For its operation the crew uses the received information, data from the avionics and the specially designed *Computer Augmented Detection and Aiming System (CADAS)*. The flight crew, in turn, provides the FCC with valuable information about the fire. Likewise, the flight crew communicates with the ground crew about payload and flight data as well as system information. The maintenance crew needs to be informed what parts of the aircraft need repairing, whilst the operational team needs to know when the aircraft is landing and how much fuel it requires.

As can be seen in the CFD, the operation of fighting a fire is a complex operation with many people and systems that affect the aircraft. As complexity of the operation increases with the size of the fire, a large variety of communication flows could be identified. However, to maintain a clear overview in the CFD, depicted in Figure 6-1, only the most important communication flows are depicted.

6.2 Computer Augmented Detection and Aiming System (CADAS)

As shown in the CFD, the aircraft will be equipped with a specially designed Computer Augmented Detection and Aiming System (CADAS). The purpose of this system is to provide real-time information about the fire and the surrounding environment to optimize the firefighting operation. In a complex mission like fighting wildfires, where risks are high and a large number of uncertainties are present, real-time information offers valuable insight in the development of the fire. The development of the CADAS is initiated with this in mind in the post-DSE design phases and will give valuable data about drop locations, optimal flight routes, wind speeds, fire intensity but also about the conditions of the surrounding forests.

At this point in the design process a preliminary study is performed from which it is determined that this system will be a design in which among others infra-red sensors, cameras, computer algorithms and the avionics of the aircraft form an integrated system. For instance, combining GPS, video cameras, image analyzing software and infra-red sensors enable the production of a real-time map of the fire with respect to its intensity and the direction in which it is propagating. This map in turn enables the FCC and the ATGS to alter the firefighting strategy, determine drop locations or determine where fire lines must be made. Furthermore, it might be possible, using this system, to optimize the exact location of the drop and then determine the shortest flying route to water and back, as well as an optimal drop approach trajectory suggestion.

At this stage of the design process, the advantage of such a system is identified yet the detailed configuration of this integral system, the potential advantages and the effects on the firefighting mission must be investigated and analyzed during the detailed design phase.

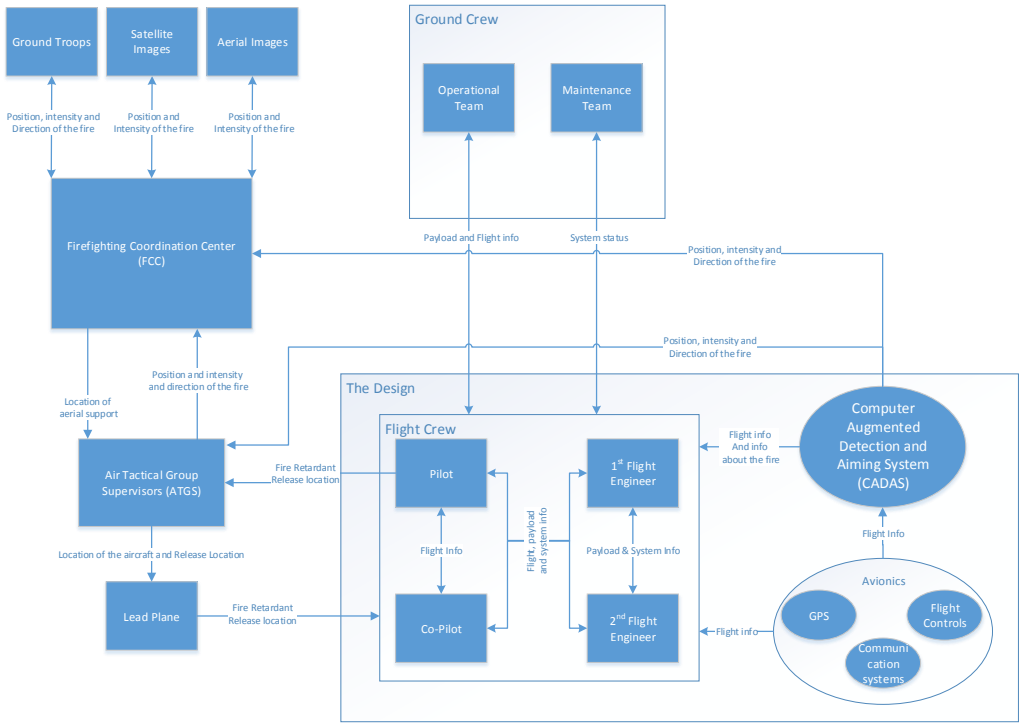

Figure 6-1: Communication Flow Diagram

Chapter 7

Safety Aspects

As the main mission of this firefighting aircraft is a rather hazardous one, safety is an important aspect in the design. In aircraft design however, increasing safety usually has the nasty side-effect of increasing weight and decreasing performance, so this makes for an interesting trade-off.

In this chapter, the safety aspects and philosophies for this firefighting aircraft will be discussed. The first section covers redundancy in safety systems, exploring and explaining the possibilities and possible usefulness of (automated) emergency systems. Next, in Section 7.2, the safety issues regarding human factors will be covered. This includes desired level of automation, required pilot experience, control complexity and other related issues. Of course, risks not only need to be countered, but the solutions also need to be tested. Examples of crash tests will be given in Section 7.3. Finally, Section 7.4 covers a set-up for possible training programs to reduce those human factors risks.

7.1 Redundancy in Safety Systems

Modern day subsonic aircraft are typically controlled using ailerons, an elevator, a rudder and a propulsive element with the help of flight computers and communication channels. Recent aviation crashes, such as that of Air France flight 447 have shown that in case of a drop-out or damage to one of these systems, extreme weather conditions or disturbed flying conditions, the plane may become poorly controllable, which in extreme cases may lead to total loss of control of the aircraft [17, 16]. This may happen when, for example, the plane stalls after which the control surfaces and propulsive elements end up in turbulent flow, which then renders these controlling elements ineffective. This can lead to the plane to become uncontrollable as the pilot is unable to or does not have the time to recover which in the most catastrophic case may lead to a crash.

For the designed aircraft, due to the challenging operating conditions, the risk of such a situation occuring is higher than for regular commercial aircraft. This stems from the fact that the aircraft will fly at low altitudes and speeds when dropping the retardant . The risk of a stall occuring in these conditions is high while the available recovery time is extremely limited due to the low altitude. Also, because of this low altitude flying, the chances of the aircraft colliding with a foreign object which may damage a control surface or propulsive element are considerably higher than for regular aircraft. Therefore, in order to guarantee the safety of the mission, an extra dimension of redundancy in safety will be added to the final design. This extra layer consists of a patented design by J.L de Kroes [16]. The intention of the design is to provide an extra, improved, subsonic adjustable control surface which is still controllable should a stall or drop-out or damage to one of the other control elements occur. Located near the cockpit, it can be regarded as a canard for control purposes only. This design enables the aircraft to quickly recover from a stall and it guarantees controllability should other control surfaces fail (either due to them being in turbulent wake due to stall or due to damage). In the neutral position, the surfaces are stowed, hardly influencing the aircraft's aerodynamics but when in working position, the canards will be deployed and controlled by a separate computerized flight control system (the system computer).

When the aircraft is in flight and the pilot senses loss of control of the aircraft, the system will be activated by pressing an emergency button in the cockpit, after which the canards will be deployed and the system computer will engage. The computer will then adjust the pitch of the canards in order to restore controllability. By including this system, an extra layer of safety will be added to the overall aircraft, further ensuring safe operations for all involved.

7.2 Human Factors

Human factors are some of the most vital aspects with respect to safety. Just as in Section 7.1, the crash of Air France flight 447 has exposed the inability of pilots to properly deal with sudden and unexpected situations in the cockpit in a high workload environment [17]. This phenomenon, which is commonly referred to as the startle effect, may have serious consequences for the safety of the mission and may, in the most catastrophic cases, lead to a crash. It was found that the startle effect leads to loss of cognitive control of the situation which subsequently leads to loss of physical control of the aircraft. Therefore, this effect should be avoided at all costs. As the mission profile of the designed aircraft is more challenging than that of a regular commercial aircraft, the risk of startling the pilots with multiple inputs increases. This is because the plane will have to manoeuver at low altitudes in order to properly drop its load, which will result in a high workload for the pilots as they constantly have to monitor their position, speed and altitude while flying the plane. Therefore, the cockpit controls should be kept as simple and intuitive in order to keep the workload as low as possible, mitigating the chances of the startle effect occurring. Also, by keeping the controls as intuitive as possible, should the pilot find himself in an unexpected situation, his initial reflexes will be more effective in recovering the aircraft due to the simplicity of the design which reduces the time needed for the plane to respond to pilot inputs. In order to guarantee maximum operational safety, the pilots need to be properly trained. This will be elaborated on in Section 7.4. Other, more basic methods to ensure safe operations will include standardization with respect to operating procedures and maintenance (for example on ground operations, retardant intake, visual flight through smoke plumes) across all operators as set by the manufacturer.

7.3 Crash Testing

To prove the aircraft is able to survive several likely danger scenario's, and to determine in which state the aircraft will be afterwards, it is proposed to do some extra testing of the scenario's mentioned below. This is most practically done as the final stages of the test program on the dedicated test aircraft.

As the aircraft operates on the water surface and thus should be able to stay afloat, it should be able to cope with a leak under the waterline. As the aircraft has a compartmentized hull, this should not form a serious problem, but to demonstrate this, the compartments should be filled individually with water while the aircraft is afloat. If the aircraft does not sink, the test is passed.

Propable cause for the abovementioned leaks can be rocks or large floating objects missed during reconnaisance overflights before landing or take-off. A proposed test is to taxi into a floating log at high speed on purpose under controlled enviroments. Serious but repairable hull damage is allowed but, more importantly, the occupants should not be harmed in any way. This means no significant cockpit compartment deformation is allowed, nor any entry of debris in cockpit or passenger areas.

Also, since the aircraft can perform both land and water landings, there is a certain risk of confusing a gear-up or gear-down landing scenario. In order to prove no critical systems are damaged in this case, two tests are proposed. The first test is a wheels-down waterlanding under controlled circumstances with a flat sea state. In order to be able to perform this test safely, first some high-speed taxi tests on the water should be performed with the gear down to evaluate the aircraft response. The test is passed if no uncompensatable moments occur and the aircraft can make a safe landing. The second test is a gear-up landing on a tarmac runway under controlled circumstances. The test is passed if no critical systems are damaged, no fuel tanks or fuel lines are punctured and the hull damage is not beyond repair.

7.4 Training Program Set-up

In order to keep the crews experienced throughout the year, it is important to have a training program covering the specific challenges of flying this aircraft. This can be divided up into several aspects, namely low-level flight (including dropping and manoeuvring), water operations (including manoeuvring and scooping) and associated emergency scenarios.

Low-level flight differs from normal flying for a pilot in that there is the possibility of obstacles in or very near the flight path. Also, the usual vertical room for recovery and manoeuvring does not exist in low-level flight, requiring a lot of pilot skill to avoid these errors. For example, slight altitude loss

in a turn might not be critical during normal flight, but in these flight conditions, it might mean a tree clipping a wing. What also needs to be considered is the higher-stress environment which might affect pilot behaviour and decision-making. Training a lot under these flight conditions should be aimed at reducing this stress-level, keeping the pilots clear-headed in the field. Practising dropping retardant under different wind and terrain conditions is important to improve pilot decision-making regarding the best approach to a drop. As there will not always be a leadplane available to show the best approach and drop points, it is a very necessary skill for crews to master. In this part of training, also coordination with ground crews should be covered, in the sense that the crew should be able to drop in a certain spot only with the guidance from ground crews.

Water operations, especially take-offs, approaches and landings, require slightly different speeds, angles and checks, as well as overall gentleness in touching down. Getting used to these, as well as the specific handling characteristics of this aircraft on the water, is the first objective of water training flights. The other is training the scooping operation under different sea state and approach conditions, paying special attention to manouevering during scooping and scooping only partial loads.

The emergency scenarios should cover at least losing an engine during all critical mission parts, particularly in high-workload situations, such as drop approach, scooping and the other standard situations like take-off. Also situations like non-opening drop doors, non-functioning scoops, aborted scoop attempt due to water traffic should be covered, as well as the standard losing of flap or gear control or electrical or hydraulic power.

Chapter 8

Multifunctionality

One of the main advantages of the designed aircraft compared to other firefighting aircraft are its multi-functional capabilities. The aircrafts capability of landing on both land and water makes it an extremely versatile platform. Due to the strategic location of the water tanks, the airplane can be reconfigured in under an hour, as the main water tanks are located under the fuselage floor whereas the parts extending above the floor will be removable. Also, the total volume of the water tanks is considerably lower than the total volume of the aircraft (less than 10%), so even when the tanks remain installed, the aircraft can be used for other purposes. This versatility creates unique opportunities for operators of the aircraft, as current firefighting aircraft suffer from low utilization rates due to their limited usability. For this aircraft, utilization can be improved in two ways. Firstly, it can be used for extinguishing other fires than wildfires, supplementing or replacing regular fire department operations. Secondly, the aircraft can be used for other purposes during times when the aircraft will not be used to fight wildfires. Both applications will be elaborated on below.

8.1 Firefighting

One of the main intended purposes of the aircraft is the ability to combat wildfires. The aircraft, however, is capable of fighting more types of fires. The aircraft can be used to extinguish fires in remote places that are hard to access or far away from ground-based fire departments. One of these applications is road vehicle fires. In Canada, aerial firefighting is currently employed to extinguish vehicle fires on remote stretches of highways [59], as driving a fire truck up to the fire would take too long. An other innovative application is extinguishing fires on oil rigs. Oil rigs are typically located far from the coastline, so it can take long for firefighting and evacuation ships to arrive from the harbor where they are stationed. With this design however, the aircraft can fly up to the rig where it can extinguish the fire after which it can land on water to evacuate workers on the rig (or the other way around). This presents great efficiency and safety gains, as only one aircraft can perform the task of firefighter and evacuation vessel faster and simultaneously instead of needing multiple vessels.

In order to look for (potential) fire hazards and more accurately dropping the retardant load, the aircraft will be fitted with a Computer Augmented Detection and Aiming System (CADAS). This system, which is to be developed further as part of the post-DSE design phase, provides the pilots with environmental information (more information on CADAS can be found in Section 6.2). Together with CADAS, the pilots will be able to better detect (potential) fires, increasing the accuracy of the drops. Coupled with the large capacity, this creates further efficiency gains compared to current aircraft.

8.2 Other uses

As the aircraft is able to land on water and has STOL capability, it can reach remote or hard-to-access areas that other aircraft of this size cannot reach. Due to the large allowable payload, the aircraft can be used for cargo, mail or passenger transport flights when it is not needed for firefighting missions. Possible uses include passenger, mail and/or cargo transport in the Amazon or between Greek islands without an airport, making optimum use of the water landing capability. Also, it can be used for, for example, relief missions by delivering large amounts of cargo or evacuating people through water landings in disaster-struck locations where the local airport is damaged. Making use of the two large doors, troops or relief aid can also be airdropped in hard-to-access areas.

Part II

Main Sizing

Chapter 1

Assessment of Wing and Power Loading Diagrams

In order to start sizing the design, the customer requirements must be translated into technical requirements. The sizing of the design is done through determining a required wing and power loading. In the Mid-Term Report (MTR), such a sizing procedure has alereadly been performed [67]. Each step, each covering a requirement, was carefully calculated, guided by Roskam [54, 53], and documented. As Roskam uses imperial units, all metric inputs were converted to imperial inputs and the imperial outputs were converted back to metric units to prevent errors in the equations.

1.1 Initial Assumptions

Several assumptions were made in advance of sizing the design. All flight requirements are set at sea level, as opposed to the 1,400 meters altitude suggested in the MTR. This is due to homologation of flight characteristics; flight characteristics are usually given at ISA sea level. Also, several C_L values were assumed by Roskam and are summarized in Table 1-1.

1.2 Sizing for Different Requirements

Several performance related requirements have been imposed by the client. These include a stall requirement, take-off and landing requirement and a climb gradient. The following section will discuss these requirements and their individual influence on the required wing and power loading.

1.2.1 Sizing to Stall Speed Requirement

According to the requirements, the stall speed must be a maximum of 100 knots, or 51.5 $\frac{m}{s}$, at MTOW. However, it has not been specified in what wing configuration this stall speed requirement has to be met. For completeness, the stall requirement was considered for all three configurations. Rewriting Eq. 1-1 using the accompanying assumption yields an expression for $\frac{W}{S}$ as shown in Eq. 1-2.

$$L = \frac{1}{2} C_L \rho V^2 S \tag{1-1}$$

As for steady flight $L = W$

$$\left(\frac{W}{S}\right)_s = \frac{V_s^2 \rho C_L}{2} \tag{1-2}$$

Table 1-1: C_L Values for Different Configurations [54]

Wing Configuration	C_L value
Clean	1.5
Takeoff	1.9
Landing	2.6

1.2.2 Sizing to Take-off Distance Requirement

The take-off distance requirement is set at 1,000 meters which, after consulting the client is referred to as the take-off field length. However, it is not stated whether this should be at Zero Payload Weight (ZPLW) or Maximum Take-Off Weight (MTOW). Roskam provides a relation of field length, wing loading $\frac{W}{S}$ and thrust loading $\frac{T}{W}$, as stated in Eq. 1-3.

$$s_{tofl} \propto \left(\frac{W}{S}\right) \frac{1}{\sigma C_{L,TO}} \left(\frac{W}{T}\right)_{TO} = TOP \tag{1-3}$$

In Eq. 1-3, the wing loading is the input whereas the thrust loading is the output, whilst the Take-Off Parameter (TOP) remains the unknown. Furthermore, the constant σ is the density ratio which at sea level equals 1. The TOP of this design was calculated through the Bombardier 415, of which a wing loading, power loading and take-off field length were retrieved from Jane's [9]. As both the Bombardier 415 and this design feature propeller propulsion units, Roskam was consulted for converting the thrust loading $\frac{T}{W}$ to power loading $\frac{W}{P}$ [54]. For further design research, it is required to calculate the takeoff distance from actual specifications instead of using statistical data to make a guesstimate.

The calculated TOP can subsequently be used in Eq. 1-4 which relates the wing loading to power loading. As the client has not specified a weight at which the take-off requirement of 1,000 meters had to be met, it initially has been assumed that the take-off will be performed at MTOW. However, if the takeoff field length requirement turns out to be critical, the required wing surface area S and required installed power P_{req} may be matched to the second-critical requirement by performing a ZPLW take-off and scooping afterwards.

$$\left(\frac{W}{P}\right)_{TO} = \frac{TOP \cdot C_{L,TO}}{0.005} \left(\frac{W}{S}\right)^{-1} \tag{1-4}$$

1.2.3 Sizing to Landing Requirement

Although a landing requirement has not been imposed by the client, it has been decided that the aircraft should be able to land on the same length as which it takes off from. In Roskam, landing field length and approach speed are related through Eq. 1-5, in imperial units.

$$s_{lfl} = 0.3V_A^2 \tag{1-5}$$

Substituting in the required landing field length of $s_{lfl} = 1000m$ yields a maximum approach speed of $V_A \approx 54\ \frac{m}{s}$. As the approach speed is defined as $V_A = 1.3V_{s,land}$, $V_{s,land} \leq 41.5\ \frac{m}{s}$. Using this stall speed for Eq. 1-1 yields a certain $\frac{W}{S}$ value. Using the maximum landing weight, which is assumed equal to the ZPLW, a wing area S can be determined.

1.2.4 Sizing to Climb Gradient Requirement

According to the requirements imposed by the client, the climb gradient should be 15 degrees at MTOW. CS-25 certifications also specify a climb gradient for a One-Engine-Inoperative (OEI) scenario which is 0.9 degrees for four-engined aircraft. In case of an engine failure, the retardant should be dumped as soon as possible to relieve weight. However, the design will be multi-purpose and sometimes carry non-disposable loads. Hence, the CS-25 OEI climb gradient requirement must be met at MTOW. As climb-out usually occurs after takeoff and at relatively low speeds, the takeoff wing configuration will be used to assess the climb performance of the aircraft.

The formula used to determine $\frac{W}{P}$ from $\frac{W}{S}$ is given in Eq. 1-6. In this formula, $\frac{C}{V} = \sin\gamma$, as illustrated in Figure 1-1. Also note that in Eq. 1-6, a C_D term is used. As this is still an unknown, the drag coefficient first need to be estimated. Although based on statistical data, Roskam provides a method to estimate the drag coefficient.

$$\left(\frac{W}{P}\right) = \frac{\eta_p}{\sqrt{\frac{W}{S}}\left(\frac{C}{V} + \frac{C_D}{C_L}\right)\sqrt{\frac{2}{\rho C_{L,TO}}}} \tag{1-6}$$

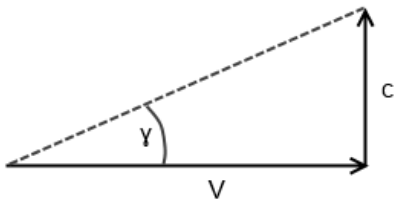

Figure 1-1: Conversion of $\frac{C}{V}$ to $\sin\gamma$

Several constants have to be determined in order to calculate the drag coefficient C_D. C_D is determined through Eq. 1-7. In this equation, $C_{D,0}$ depends on several variables, being the equivalent parasite area f and the wing reference area S_{ref}. The latter is determined through the initial Class I weight estimation and the Bombardier 415 wing loading, whereas the former is calculated through Eq. 1-8, obtained from Roskam.

$$C_D = C_{D,0} + \Delta C_{D,0} + \frac{C_L^2}{\pi A e} \tag{1-7}$$

$$C_{D,0} = \frac{f}{Swet}$$

$$\log f = a + b \log S_{wet} \tag{1-8}$$

The wetted area S_{wet} is determined through reference aircraft, using Figure 3.22d in Roskam [54]. The values a and b are determined through Table 3.4 in Roskam. For this, a skin friction coefficient was required. This skin friction was selected to be $C_f = 0.045$, resulting in values of $a = -2.355$ and $b = 1$. Using these values, a equivalent parasite area of $f = 5.57\ m^2$. However, f can also be determined graphically using Figure 3.21b in Roskam. Using this method, an entirely different value for f is obtained, namely $f = 12.1\ m^2$. To be on the safe side for now, the larger of the two values will be used in calculating $C_{D,0}$. This yields $C_{D,0} = 0.043$.

In order to calculate the induced drag, both the aspect ratio A and Oswald factor e had to be assumed. Also, $C_{D,0}$ increases with increasing C_L due to the flap setting. Based on reference aircraft, these values are taken as in Table 1-2.

Table 1-2: Assumptions for Calculating Drag Coefficient

Configuration:	**Clean**	**Take-Off**	**Landing**
Aspect Ratio A	8	8	8
Oswald Factor e	0.85	0.80	0.75
Drag Coefficient Increase $\Delta C_{D,0}$	0	0.015	0.06
Drag Coefficient C_D	0.1408	0.2372	0.4613

Using the method explained in Roskam, values of C_D are found and summarized in Table 1-2. Using these values, the climb gradient power loading can be determined as function of a wing loading.

1.3 Determining Wing and Power Loading

Having established the required $\frac{W}{S}$-$\frac{W}{P}$ relations and wing loading requirements for different requirements, it is possible to determine a wing and power loading. The relations have been plotted in the graph as shown in Figure 1-2. Furtermore, the intersections have tabulated in Table 1-3. In Table 1-3, the subsequent wing area and power requirements have also been listed. The respective weights are calculated and listed in Chapter 7.

In order to optimize the design, both $\frac{W}{S}$ and $\frac{W}{P}$ must be maximized, giving priority to $\frac{W}{S}$. Also, the requirements are only met when the design point lies on or beneath and to the left of the lines. This

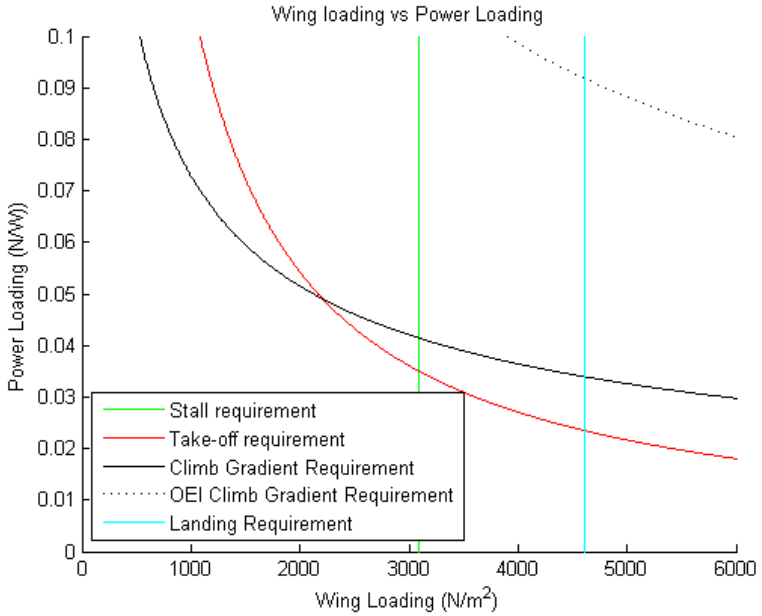

Figure 1-2: Wing- and Power Loading Diagram

Table 1-3: Wing- and Power Loading Intersections

Requirement 1	**Requirement 2**	**Associated Weight**	$\frac{W}{S}$ $[\frac{N}{m^2}]$	$\frac{W}{P}$ $[\frac{N}{W}]$	**Required Wing Area m^2**	**Required Power MW**
Stall	-	MTOW	3087	-	178	-
Stall	Takeoff	MTOW	3087	0.0351	178	15.7
Stall	Takeoff	ZPLW	3087	0.0351	130	11.5
Stall	Climb Gradient	MTOW	3087	0.0415	178	13.2
Stall	OEI Climb Gradient	MTOW	3087	0.1123	178	4.9
Landing	-	MTOW	4091	-	134	-
Landing	Takeoff	MTOW	4091	0.0235	134	23.4
Landing	Takeoff	ZPLW	4091	0.0235	98	17.1
Landing	Climb Gradient	MTOW	4091	0.0340	134	16.2
Landing	OEI Climb Gradient	MTOW	4091	0.0919	134	6.0

implies the stall speed requirement is considered critical in determining the wing loading. Based on the related wing loading, a wing area requirement of 178 m^2 subsequently follows.

Determining the required power is a little more complex as the takeoff requirement can be met at different weights, as also explained in Section 1.2.2. An installed power of 15.7 MW is required in order to comply with the MTOW takeoff. If a ZPLW takeoff is considered, 11.5 MW are needed to successfully take off within the required 1000m. The climb gradient requirement requires an installed power value of 13.2 MW. The excess power difference between the climb gradient and ZPLW requirement allows to carry more payload weight on takeoff. In Chapter 2, the required takeoff field length is plotted for various takeoff weights.

1.3.1 Tuning

In Section 1.2.3, it was stated that $V_{s,land} \leq 41.5\frac{m}{s}$. Using a wing area of $178m^2$ results in a $V_{s,land} = 44\frac{m}{s}$. Fine-tuning the C_L at which the stall requirement of $100kts$ is met, decreases the stall speed wing loading. A decrease in the wing loading in turn results in a decrease in the stall speed, according to Eq. 1-1. It turns out a C_L of 1.7 allows a $V_{s,land}$ of 41.5 $\frac{m}{s}$, which is exactly what the maximum is for landing performance, as calculated earlier. As the airfoil already has a high lift coefficient, the value of 1.7 is to be met by changing $C_{L,TO}$. However, a decrease in $C_{L,TO}$ causes an increase in $\frac{W}{P}$ for the climb gradient requirement, as the climb is performed at take-off settings. This issue is solved by taking two different flap settings to create a TO1 and TO2 configuration, providing the best of both flap configurations.

1.4 Updated Wing Area and Power Requirement

Having set an updated value for C_L, a new wing loading and power loading can be calculated. In Figure 1-3, the relevant limiting requirements are sketched. In Table 1-4 the new wing loading and power loading ratios have been tabulated.

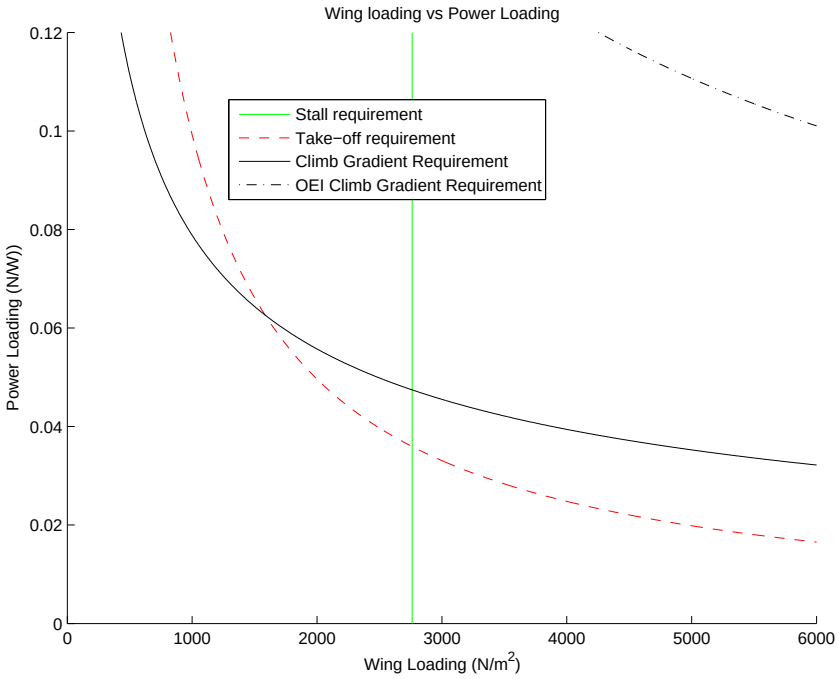

Figure 1-3: Updated Wing-Power Loading Diagram

Table 1-4: Wing loading and power loading intersections.

Requirement 1	Requirement 2	Associated Weight	$\frac{W}{S}$ $[\frac{N}{m^2}]$	$\frac{W}{P}$ $[\frac{N}{W}]$	Required Wing Area m^2	Required Power MW
Stall	-	MTOW	2762	-	199	-
Stall	Takeoff	MTOW	2762	0.0428	199	12.8
Stall	Takeoff	ZPLW	2762	0.0428	146	9.4
Stall	Climb Gradient	MTOW	2762	0.0462	199	11.9
Stall	OEI Climb Gradient	MTOW	2762	0.1369	199	4.0

From Table 1-4, it becomes clear the required wing loading equals $\frac{W}{S} = 2762 \frac{N}{m^2}$. The requirement is set as the wing loading instead of the wing area as the design weight is bound to change.

The power loading requirement is set to be $\left(\frac{W}{P}\right)_{req} = 0.0462$. The maximum required power is the result of the takeoff requirement at MTOW. As stated before, no weight requirement was set on the takeoff. The aircraft's main mission must not be forgotten; that is to takeoff within $1000m$, scoop retardant, extinguish fires and land. This requirement does not state that the aircraft must already carry $15m^3$ of retardant when taking off. A ZPLW takeoff only requires $9.4MW$, which is lower than the climb gradient P_{req}. Load values are used instead of an absolute power requirement because the aircraft weights are subject to change throughout the design phase. When a final weight estimation has been performed, an absolute P_req can be set.

Chapter 2

Airfoil Selection

The wing profile has a large influence on the lift generated by the wing and also has a large impact on the stability of the aircraft. Based on reference aircraft, a first estimation of the lift coefficient could already be made. Before the airfoil parameters can be established, more insight with respect to design parameters such drag coefficient, lift coefficient, moment coefficient, critical mach number and Reynolds number had to be obtained. Based on these parameters, an appropriate airfoil was chosen.

Several airfoil parameters are of importance, being the thickness, camber and the location of the camber and thickness. The effects of changing these design parameters will be discussed in Section 2.2. With the knowledge of the design and airfoil parameters, an airfoil with the required characteristics can be selected using a numerical model, JavaFoil [25].

2.1 Design Parameters

The design parameters are the parameters that influence the design of the airfoil. As mentioned, the parameters consist of the lift coefficient, drag coefficient, moment coefficient, critical mach number and moment coefficient

2.1.1 Lift Coefficient

As the water bomber has to carry a large payload and perform short take-offs and landings, it is important what the lift coefficient will be for different angles of attack and at what angle of attack the airfoil will stall. First, the design lift coefficient is determined through Eq. 2-1, taken from the TU Delft AE3201 course [50].

$$C_{L_{des}} = 1.1\frac{1}{q}\left\{\frac{1}{2}\left[\left(\frac{W}{S}\right)_{start\_mission} + \left(\frac{W}{S}\right)_{end\_mission}\right]\right\} \tag{2-1}$$

As the water bomber flies multiple times in cruise conditions during a single mission and no intermediate wing loading values are available, the wing loading at the start and the end of the mission have been selected to be used in Eq. 2-1. A first estimate of the required wing area, MTOW and OEW have already been determined in the Mid-Term Report (MTR) and can readily be inserted in Eq. 2-1. This equation yields an estimation of the design lift coefficient in cruise conditions $C_{L_{des}}$ of 0.37.

During a retardant drop over a wildfire, the water bomber flies with a large angle of attack at approach speed to release it retardant. Due to thermal currents above wildfires, the angle of attack may suddenly change as the aircraft overflies the wildfire location. This change in angle of attack should not lead to a stall. Therefore, the airfoil should have a large stall angle of attack α_{stall}. Furthermore, the airfoil stall should start at the trailing edge *(trailing edge stall)*, as this way the lift force will not suddenly drop but slowly decrease.

2.1.2 Drag Coefficient

As a lower drag coefficient results in a lower drag, the drag coefficient should be minimized for a specific lift coefficient. Furthermore, the range of angle of attack of 2 to 7 degrees should be considered, since this is the range the aircraft will operate in, while designing for the drag coefficient. In this range of angle of attack, a low drag coefficient is preferred. Therefore this range of angle of attack should fall in the laminar bucket, the part in the lift, drag polar where the C_D is low and barely increasing due to laminar flow.

2.1.3 Moment Coefficient

The moment coefficient of the airfoil influences the moment acting in the aerodynamic center of the wing. A large negative pitching moment will result in a larger tail size, as the counteracting moment produced by the tail must be larger. Furthermore, a negative $\frac{dC_m}{d\alpha}$ preferable for stability reasons.

2.1.4 Critical Mach Number

The water bomber has a cruise speed of $111\frac{m}{s}$ and a maximum speed of $120\ \frac{m}{s}$ at an altitude of 4,000 meters. In these conditions, the Mach number at cruise altitude is 0.370. Therefore, the airfoil must feature a minimum critical Mach number greater than 0.370 in order to avoid supersonic flow over the wings whilst operating within the design flight envelope.

2.1.5 Reynolds Number

The Reynolds number is the ratio between the inertia forces and viscous forces. At a higher Reynolds numbers the flow stays better attached to the wing profile, causing the airfoil to stall at higher angles of attack. On the other hand, the drag coefficient increases significantly while the lift coefficient decreases. The Reynolds number can be calculated using Eq. 2-2.

$$\mathrm{Re} = \frac{\rho \cdot V \cdot l}{\mu} \tag{2-2}$$

From Eq. 2-2, it can be deducted that the Reynolds number depends on the type of fluid considered, velocity and the chord length. Hence, as μ and ρ depend on altitude, ISA conditions are used to determine these parameters. In cruise the aircraft has a velocity of $111\,\frac{m}{s}$ and an altitude of 4,000 meters, resulting in a Reynolds number of $29.5 \cdot 10^6$. In the approach phase at sea level, the velocity is $54.8\ \frac{m}{s}$, thus the Reynolds number is $18.1 \cdot 10^6$.

2.2 Airfoil Characteristics

First, the type of airfoil for the next generation water bomber should be selected. Based on the reference aircraft, the design choice airfoil must be one of the NACA 4 digit-series airfoil. However, the parameters of this airfoil series still need to be determined, which are:

- Thickness t/c
- Camber f/c
- Camber location along the chord, xf/c

2.2.1 Thickness of the Airfoil

As the aircraft should have good stall characteristics, a thickness of at least $t/c \geq 14\%$ should be selected. At a thickness of 14 or more, the stall initiates at the trailing edge causing the lift coefficient and the pitching moment to change slowly.

Secondly, a large lift coefficient is beneficial. It allows for smaller required C_L increments for the different high-lift device (HLD) configurations, in turn lowering the required area of these HLDs. Also, the HLDs won't be as complex, improving the reliability and maintainability of the aircraft.

Although a thicker airfoil causes an increase in lift force, it increases the drag coefficient as well. A trial and error method has been used to determine an optimal airfoil thickness. Using this method, a thickness of 17% is selected as this provides a high lift coefficient and a relatively low drag coefficient.

A thickness of 17% is a also beneficial for structural reasons as it allows a smaller overall wing weight. Due to a larger possible cross-sectional area,a larger wingbox can be fitted. This in turn increases the bending and torsional stiffness. Furthermore, the larger cross-sectional area allows for a larger fuel volume.

2.2.2 Camber Size of the Airfoil

A increase in camber results in a shift of the C_L-α-curve to the left, increasing the wing lift coefficient for an angle of attack of zero degrees. A higher camber value also yields a larger $C_{L_{\max}}$ and a larger laminar bucket. On the other hand, the moment coefficient decreases and therefore the required area of the tailplane has to increase accordingly.

The camber is selected to be 4% of the chord length, which is the optimal configuration for the water bomber mission, as the moment coefficient still suffices the required stability while providing an increased lift coefficient at an angle of attack of 7 degrees. Hence, less complex the High-Lift Devices can be selected to provide a sufficient lift coefficient increase for landing and take-off. Furthermore, the plots generated by JavaFoil suggested that the laminar flow bucket in case of a 4% camber airfoil extends to an angle of attack of 8 degrees.

2.2.3 Camber Position of the Airfoil

The position of the camber is important as bringing the camber forward will increase the maximum lift coefficient, yet it introduces less favorable stall characteristics. Investigating this effect of changing the location of the camber resulted in locating the camber position at 30% of the chord length. This position increased the $C_{L_{\max}}$ sufficiently while significantly comprising the stall characteristics of the aircraft which is especially important during the unloading of the extinguishant.

2.3 Selected Airfoil

Using the knowledge explained in Section 2.2, the NACA4317 airfoil has been selected for the design. It features the airfoil characteristics summarized in Table 2-1 and Figure 2-1.

Table 2-1: Characteristics of the NACA4317 Airfoil

Airfoil Characteristics	Values
$\frac{t}{c}$	17 %
$\frac{f}{c}$	4 %
$\frac{x \cdot f}{c}$	30 %
$C_{l_{\max}}$	2.067[-]
C_{d_0}	0.00476[-]
α_{stall}	17 [degrees]
$C_{l_{\alpha=0}}$	0.507 [-]
C_{l_α}	6.9 $[\frac{1}{rad}]$

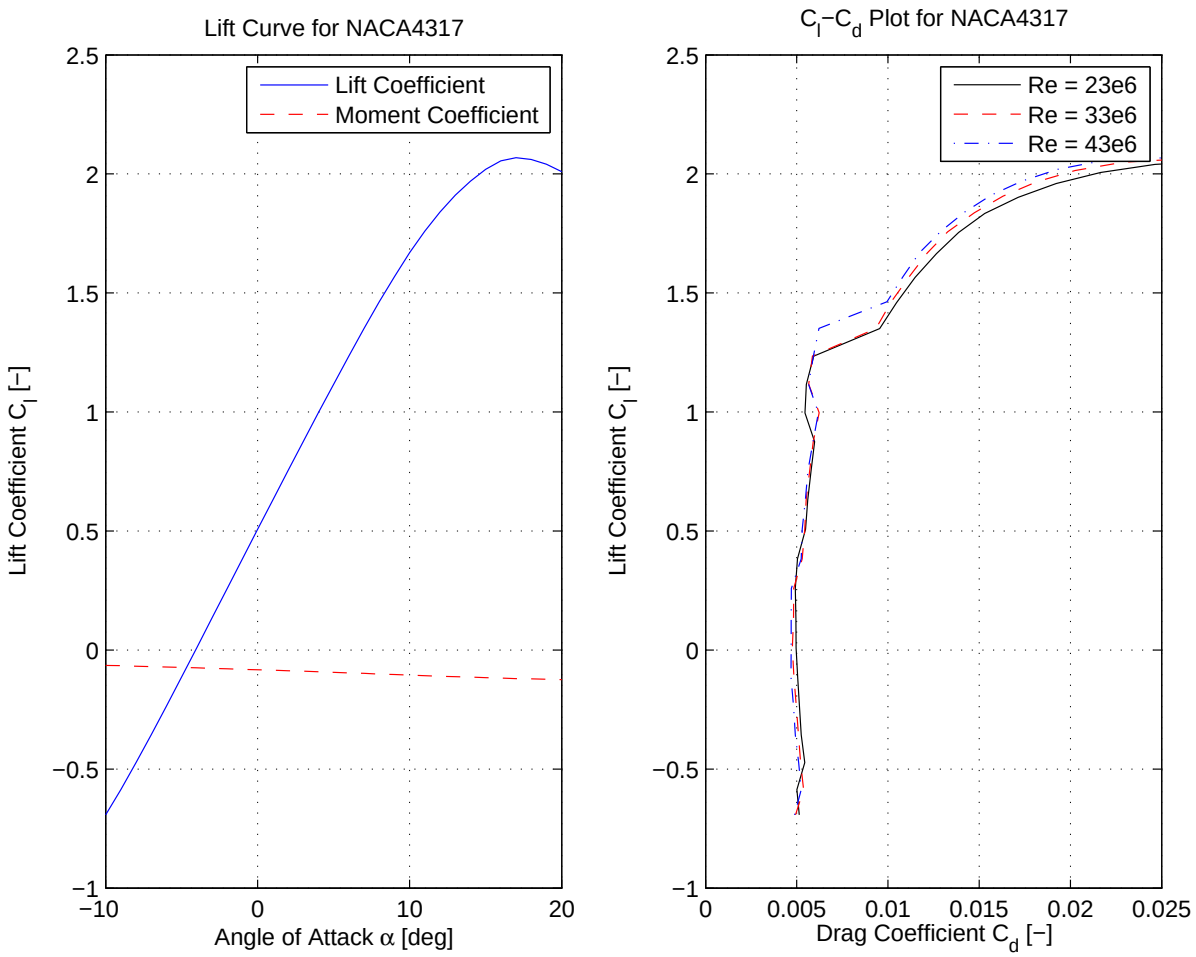

Figure 2-1: Aerodynamic Characteristics of NACA4317

Chapter 3

Wing Sizing

From the initial wing sizing, it has been established that $\frac{W}{S} = 2762 \frac{N}{m^2}$ is required in order to conform to the stall requirement. This requirement is considered to be most critical, as these requirements require the largest wing surface area S and required power P. Based on the $\frac{W}{S}$-$\frac{W}{P}$ diagram, a wing surface area of 199 m^2 will be required for the Class I weight estimate.

3.1 Wing Positioning

During the water takeoffs and landings, the design introduces a lot of spray which can be ingested by the engines and subsequently stall them. In order to provide sufficient clearance between the water line and the engines, the wing will be mounted in a high-wing configuration, on top of the fuselage.

3.1.1 Wing Sweep Angle

The main reason for introducing a quarter chord wing sweep angle $\Lambda_{c/4}$ is to increase the critical Mach cumber M_{crit} which is the Mach number at which the airfoil will experience supersonic flow conditions for the first time. Furthermore, in case a wing sweep angle is applied, thicker airfoils can be used to achieve the same M_{crit}. Using thicker airfoils will result in lighter wings and a larger fuel capacity. Finally, the use of wing sweep can be useful to affect the longitudinal position of the aircraft center of gravity.

On the other hand, due to wing sweep, the lifting capabilities of the wing are diminished. In order the generate the same amount of lift as a unswept wing, the swept wing should be larger which brings along an increase in weight.

As the water bomber will fly a low speeds, the M_{crit} is allowed to be relatively low. Therefore, the design will feature no quarter chord wing sweep angle ($\Lambda_{c/4} = 0°$).

3.2 Wing Aspect Ratio

The aspect ratio A_w has a large influence of the induced drag. High aspect ratio wings tend to have lower induced drag compared to low aspect ratio wings, as per Equation 3-1. Hence, a large aspect ratio will improve aerodynamic efficiency of the design. On the other hand, a high required aspect ratio will result in large wing spans which can pose operational issues such as accessibility on airports and maneuverability on water. Furthermore, high aspect ratio wings are in general heavier than low aspect ratio wings.

$$C_{D,i} = \frac{C_L}{/piAe} \tag{3-1}$$

According to Roskam, reference aircraft should be used in order to determine a proper value of A_w. Based on the data found in Table 3-1, the aspect ratio was set at $A_w = 8$. This is equal to the aspect ratio assumed in Chapter 1.

Table 3-1: Wing Aspect Ratio of Reference Aircraft [9]

Aircraft Type	Wing Aspect Ratio
Bombardier 415	8.2
ShinMaywa US-2	8.1
Beriev Be-200	9.1

3.3 Wing Taper Ratio

As the lift distribution near the wing tips tends to zero, the area near the wingtip is not very effective. Introducing a small taper ratio to the wing, will decrease the 'wasted' area near the wingtip and thereby reducing the overall weight of the wing.

However, a small taper ratio will result in small tip chords. This implies smaller Reynold's numbers and therefore lower maximum lift coefficients at the wing tip. As a result, the wing tips will stall sooner compared the rest of the wing (tip stall) which is not desirable as the wing control surfaces are usually located near the tip of the wing. As a result, the aircraft may become uncontrollable in case of a stall. Furthermore, wings with small taper ratios are more expensive to produce compared to straight, untapered wings. Straight, untapered wings allow for common wing ribs are therefore tend to have lower manufacturing costs. Finally, large taper ratio will result in a larger fuel volume, as statd by Roskam [53].

Table 3-2: Wing Taper Ratio of Reference Aircraft

Aircraft Type	Wing Taper Ratio
Bombardier 415	1
ShinMaywa US-2	0.478
Beriev Be-200	0.308

According to Raymer, the induced drag for an unswept wing is smallest for a wing taper ratio of about 0.4 [47]. Based on this and on data from reference aircraft listed in Table 3-1, the wing taper ratio has been set to $\lambda_w = 0.4$.

3.4 Wing Dihedral Angle

The wing dihedral Γ_w has a large influence on the Dutch roll effect and spiral stability, as well as on the ground clearance. Positive dihedral angles will result in better spiral stability and worse Dutch roll stability, yet will ensure a larger ground clearance.

According to Roskam, aircraft with high wing configurations feature a "dihedral effect" which makes the aircraft laterally more stable compared to low wing configurations. However, a negative dihedral angle (anhedral) is often used in order to increase the controlability of the aircraft at the expense of stability. Therefore, the design dihedral angle is chosen at $\Gamma_w = -1°$.

3.5 Wing Incidence Angle

The wing incidence angle i_w is the pitch angle of the wing with respect to the fuselage. A wing incidence angle can be introduced in case high C_L values are required during landing and take-off. In such cases, the wing will experience an already increased angle of attack and therefore the lift coefficient will become larger. Furthermore, a positive wing incidence angle will allow the aircraft to approach the airport at a lower pitch angle, enhancing visibility from the cockpit.

On the other hand, in case of a positive wing incidence angle, the aircraft will "cruise" in a nose down position and therefore will experience an increased cruise drag. In order to reach a higher lift coefficient during landing, it is decided that the wing incidence angle is set to $i_w = 2°$.

Chapter 4

Structural Wing Design

Based on loads the wing has to endure, a first approximation of the wing structure is made. The wing structure is sized for loads from -2 to 5g, for filled- and empty fuel tanks and maximum- and zero lift generation. The wing structure is built up from a wing box that consist of a front and rear spar and an upper and lower panel. The spars are placed at 0.15 to 0.75c such that the wing box will cover the largest possible volume of the wing without interfering with the location of the slats and flaps, as determined in Chapter 1.

4.1 Assumptions

The wing box is sized for lift forces, the weight of the tip floats, engine weight, weight of the structure and for several scenarios for the weight of the fuel. The loads on the wings during the release of the retardant have been considered, however, these loads did not exceed the 5g load case. The assumptions which have been made for the first approximation of the wing box structure are;

- The structure is thin-walled.
- The skin only resists loading in shear in the z-direction.
- Lift forces act on a quarter chord length.
- The wing box has an axis of symmetry on the x axis.
- The engine is assumed as a point load applied at quarter chord length.
- The tip float is assumed as a point load applied at quarter chord length.
- The wing box does not deform.
- The wing box is idealized with booms.
- The upper- and lower booms are sized to be mirrored, such that the horizontal axis of symmetry will remain.
- The normal force which the booms resist is taken in spanwise direction, the angle caused by taper is not taken into account .

4.2 Loads on Wing Box

The loads that have been evaluated to size the wing box are the maximum lift force, fuel weight, engine weight, tip float weight and weight of the structure. The wing box is sized for three critical load cases:

1. Zero fuel weight, maximum lift generation at 5g
2. Maximum fuel weight, zero lift
3. Maximum fuel weight, negative lift generation at -2g

These loads on the wing box are evaluated in a MATLAB simulation model [18], which computes the shear forces, bending moment, normal stress distribution, shear flow distribution and yield stress distribution on the wing box. From the yield stress distribution, the boom area is determined which is transformed into skin thickness of the wing box. A safety factor of 1.5 has been taken into account for the wing box sizing.

First the shear force distribution is computed through Eq. 4-1 and is shown in Figure 4-1a, 4-1b and 4-1c for loading cases 1, 2 and 3 starting at the tip to the root.

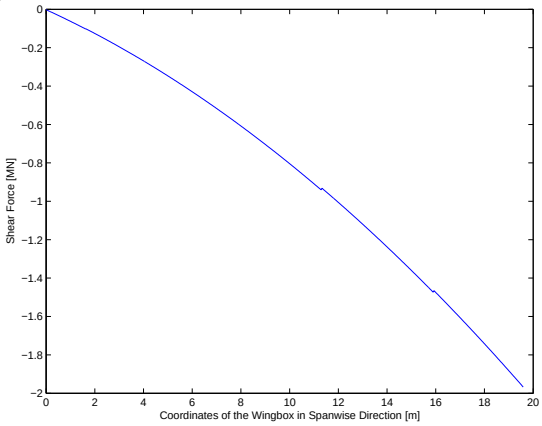

(a) Shear Forces on Wing Box at Zero Fuel Weight, Maximum Lift Generation at 5g

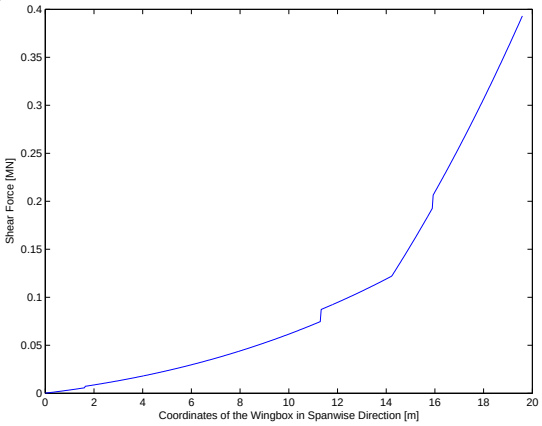

(b) Shear Forces on Wing Box at Maximum Fuel Weight, Zero Lift

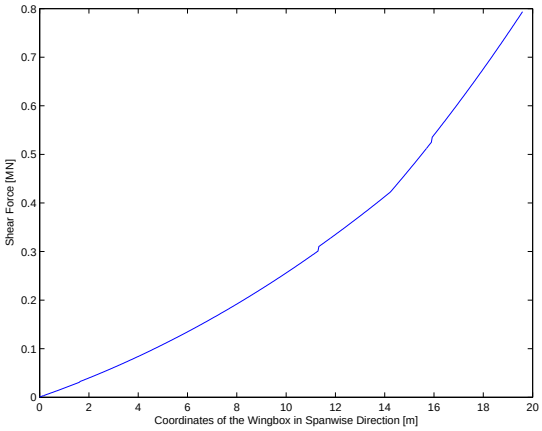

(c) Shear Forces on Wing Box at Maximum Fuel Weight, Negative Lift Generation at -2g.

Figure 4-1: Shear Force Distribution for the three loading cases

$$V = F_{lift} - F_{engine} - F_{tipfloat} - F_{fuel} - F_{structure} \tag{4-1}$$

From the shear forces, the wing bending moment is computed through Eq. 4-2. The shear forces that are generated are multiplied with the moment arm that acts from the location on the wing where the force acts to the root of the wing.

$$M_x = V_{section} \cdot y_{rts} \tag{4-2}$$

The wing box is idealized by adding booms while the skin only resists loading in shear. The normal stresses in the booms are computed through Eq. 4-3. The shear flow in the wing box is computed with Eq. 4-4 whereas the inner shear flow is determined with Eq. 4-5. The boom areas are subsequently converted to the thickness the spars and panels would require in a non-idealized case, according to Eq. 4-6 [38]. From the shear flows in the wing box, the shear stresses were be computed using Eq. 4-7. [38]

$$\sigma_z = \frac{M_x \cdot y}{I_{xx}} \tag{4-3}$$

$$q = -\frac{S_y}{I_{xx}} \left(\int t_D y ds + \sum B y_r \right) + q_{s,0} \tag{4-4}$$

$$q_{s,0} = \frac{\int \frac{q}{Gt} ds}{\int \frac{1}{Gt_D} ds} \tag{4-5}$$

$$t = \frac{\frac{B_1 6}{b}}{2 + \frac{y_2}{y_1}} \tag{4-6}$$

$$\tau = \frac{q}{t_D} \tag{4-7}$$

Next, the yield stress can be computed from the shear stress and normal stress. The yield stress is computed according to Eq. 4-8 [38]; its distribution over the wing box is shown in Figures 4-2a, 4-2b and 4-2c, again for the different load cases.

$$Y = \sqrt{(\sigma_z^2 + 3\tau^2)} \tag{4-8}$$

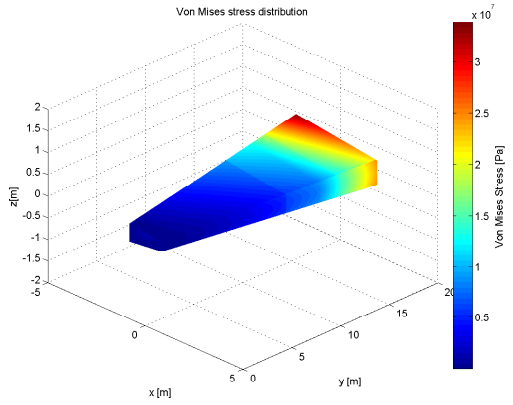

(a) 3D Yield Stress on Wing Box at Zero Fuel Weight, Maximum Lift Generation at 5g

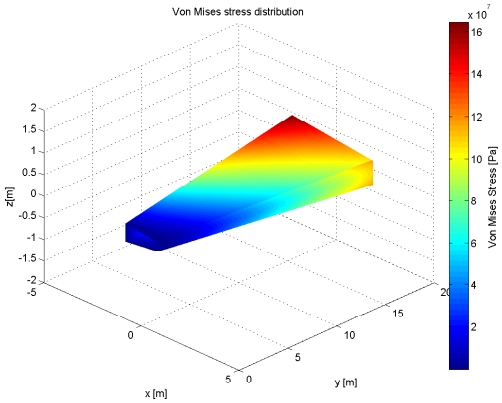

(b) 3D Yield Stress on Wing Box at Maximum Fuel Weight, Zero Lift

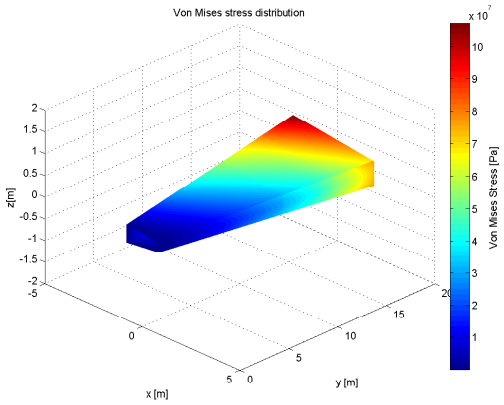

(c) 3D Yield Stress on Wing Box at Maximum Fuel Weight, Negative Lift Generation at -2g.

Figure 4-2: 3D Yield Stress Distribution for the three loading cases

Several material characterics have been used to select a material to construct the wing box of. Based on its fatigue performance and yield strength, the aluminium alloy 2024 has been selected. The aluminium alloy 7xxx series has been investigated as well. However, these series have less favorable fatigue characteristics and will create a heavier structure. The chosen allow AL2024 has a density ρ of 2780 $\frac{\text{kg}}{\text{m}^3}$ and a yield strength Y of $= 276$ MPa, the Youngs modulus E of the material is 73.1 GPa and the Poisson's ratio ν of 0.33 [39].

4.3 Fatigue

The water bomber will be used for 30 to 40 years for extinguishing missions, as stated in Section 4.3 of Chapter 4. During this lifetime, the number of fatigue cycles will be very high during the months in which the aircraft is operative. The aircraft is expected to take in and drop retardant, meaning multiple fatigue cycles and excessive vibration loads occur multiple times per mission. Also, during scooping and dropping, rapid changes of aircraft weight impose loads on the wing structure. To prevent failure caused by fatigue, a material has been selected for the wing box which has good fatigue handling properties. For further design stages, it is recommended to strengthen and redesign areas such as sharp corners, cut-outs and rivet holes to prevent fatigue failure [38].

4.4 Final size selection

For the preliminary sizing, the boom areas have been solely converted into skin thicknesses. However, the booms can also be represented as a stringers or flanges. For the more detailed design stage it is recommended to add stringers and decrease the thickness of the skin in order to decrease the overall weight of the wing box while still be able to handle the loads imposed on the wing.

According to the MATLAB model, the most critical loading case is 1, in which a zero fuel weight and maximum lift generation of 5g is considered, as this loading case induces the highest yield in the top of the leading edge spar, around the root chord. The required thickness of the spars and panels for this loading case, are expressed as a function of the chord. As the chord decreases in span wise direction, the thickness of the spars and panels decrease accordingly. The yield stress is highest at the root and therefore the thicker spars and panels are required compared with the tip.

The thicknesses are defined as follows:

$$t_{forwardspar} = 0.0068c$$

$$t_{aftspar} = 0.006c$$

$$t_{top} = t_{bottom} = 0.0068c$$

With the thicknesses as stated, above the maximum attained yield stress is 272 MPa, including a safety factor of 1.5, whilst the allowable yield stress equals 276 MPa.

$$\sigma_{crit} = \frac{\pi^2 E}{\left(\frac{l}{r}\right)^2} \tag{4-9}$$

In the more detailed design phase the locations of the ribs also need be determined. The ribs will be placed according to the critical buckling stresses in the wing box, which are be determined with Eq. 4-9. The number and locations of ribs can only be determined as soon as the number, size, locations and shape of the stringers have been determined.

Chapter 5

Tail Sizing

In order to provide lateral and longitudinal stability as well as controllability, the tail sizing is a trade-off between tail size and distance to the main wing. As this the design of the water bomber is still in the preliminary phase, the dimensioning of the tail is solely based on the data from reference aircraft.

5.1 Horizontal and Vertical Tail Area

In this preliminary phase, data of reference flying boats and amphibians are used in Eq. 5-1 and 5-2 to calculate the horizontal tail area and vertical tail area respectively.

$$S_h = \frac{\overline{V_h} \cdot S \cdot \bar{c}}{x_h} \tag{5-1}$$

$$S_v = \frac{\overline{V_v} \cdot S \cdot b}{x_v} \tag{5-2}$$

V_h and V_v are volume ratios of the respective airfoil surfaces, calculated from reference flying boats and amphibians. As the Bombardier 415 is an aircraft performing similar missions as the next generation water bomber, its ratios are used in Eq. 5-1 and 5-2, being $V_h = 0.7635$ and $V_v = 0.06$.

As stated earlier, a trade-off has to be made between the tail surface size and the distance to the main wing, referred to as *tail length*. If the tail length is too small, a large tail is required which significantly increased the aircraft's weight. On the other hand, if the tail is too small, a large tail length is required which adds to the fuselage weight and subsequently to the aircraft's overall weight.

5.2 Characteristics of the Vertical Tail and Horizontal Tail

In this preliminary phase of the design, characteristics of the vertical tail and horizontal tail are determined using data of reference aircraft. Three comparable aircraft have been selected, being the Canadair CL-215, the Beriev Be-200 and the ShinMaywa US-2. The characteristics of these aircraft are summarized in Table 5-1 and 5-2. Based on the data provided in these tables, a first estimate of the characteristics of the tail design is made. This estimation is tabulated in Table 5-3.

5.3 Airfoil

During flight, the horizontal tail generates negative lift to counteract the moment created by the wings. Furthermore, as the next generation water bomber is a scooper, a larger counteracting moment is required

Table 5-1: Characteristics of the Horizontal Tail

	Canadair CL-215	**Beriev Be-200**	**ShinMaywa US-2**
Aspect Ratio [-]	4.16	4.1377	4.69
Sweep Angle [°]	0	28	0
Taper Ratio [-]	1	0.61	0.48
Incidence Angle [°]	0	0	0
Dihedral Angle [°]	0	0	0

Table 5-2: Characteristics of the Vertical Tail

	Canadair CL-215	Beriev Be-200	ShinMaywa US-2
Aspect Ratio [-]	2	1.09	1.13
Taper Ratio [-]	0.38	1	0.73
Sweep Angle [°]	29	34	26

Table 5-3: Design Characteristics of the Tail Surfaces

Horizontal Tail	
Aspect Ratio [-]	4.33
Sweep Angle [degrees]	0
Taper Ratio [-]	0.40
Incidence Angle [degrees]	0
Dihedral Angle [degrees]	0
Vertical Tail	
Aspect Ratio [-]	1.0
Taper Ratio [-]	0.4
Sweep Angle [degrees]	30

to cope with these scooping forces. Secondly, the stall angle of the tail should be higher so the aircraft will still be controllable during stall of the wing.

In general symmetric airfoils are used for the tail to minimize the drag. Furthermore, the airfoil should preferably be symmetrical as to minimize drag forces. Typical airfoils used for tailplanes are the NACA0009, NACA0012 and NACA0018 [53, 63].

As the stall angle of the NACA0009 profile is at a lower angle of attack than the wing profile, this wingprofile is discarded for the next generation waterbomber. The NACA0018 profile, on the other hand, has a approximate stall angle of 19 degrees. Furthermore, the NACA0018 has a higher lift coefficient, reducing the required tail area. For these reasons, the NACA0018 profile has been selected for the tailplane of the design.

5.4 Control Surfaces

The dimensioning of the tail control surfaces such as the elevator and rudder are based on data of reference aircraft. Extensive data of the Canadair CL-215 is provided in the second book of Roskam [53]. Besides this data, also data of its successor, the Bombardier 415 is used [9]. The tail control surface reference data is used in designing the next-gen waterbomber. The values that have been selected for this design are summarized in Table 5-4.

Table 5-4: Characteristics of the Control Surfaces

Elevator	
Elevator Width [% of the chord]	40
Elevator Area [% of the horizontal tail area]	28
Rudder	
Rudder Width at the Root [% of the chord length]	41
Rudder Width at the Tip [% of the chord length]	57
Rudder Area [% of the vertical tail area]	35

Although this method is sufficient for the preliminary phase of the design, a more detailed look has to be taken in future phases of the design. Most importantly, tt has to be verified whether the control surfaces are able to generate sufficient control forces to pitch and yaw the aircraft such that the maneuverability requirements are met using wind tunnel testing.

5.5 Empennage Configuration

The empennage consists of the vertical and horizontal tail where the horizontal tail placed is on top of the vertical tail, better known as a T-tail configuration. This configuration will provide the largest possible c.g. range of the aircraft, at the expense of weight. This weight increase is caused by the fact that the structure of the vertical tail should be heavier compared to a conventional empennage configuration in order to support the horizontal tail. Furthermore, the T-tail may suffer from the occurrence of deep-stall.

As especially low wing configurations in combination with a T-tail suffer from this phenomenon and the fact that wing of this design is high mounted, the question remains whether deep stall will occur. However, in latter design phases this should be tested in a windtunnel. At this point of the design, the deep stall phenomenon is taken into by selecting a large aspect ratio of the horizontal tail which keeps the tip of the horizontal tailplane out of the wing wake.

Although in Section 5.2 the horizontal tail aspect ratio was set to 4.33, Stanford states that a typical horizontal tailplane for a T-tail configuration is between 5 and 5.5 [29]. As a result, the horizontal tail aspect ratio has been changed to 5.25. However, windtunnel tests should prove whether the wing-tail interference will induce the deep-stall phenomenon. In case this test turns out that the design does not suffer from this phenomenon, a smaller aspect ratio of approximately 4 can be selected.

The vertical tail will be configured as a single vertical tail. This type of configuration is the most efficient configuration in subsonic flight which will decrease the weight of the tail and increases the control force force generated by the tail.

In order to enable a larger center of gravity range, an adjustable tail was selected. Furthermore, as an adjustable tail can be used to trim the aircraft, no trim tabs or other ways of trimming need to be installed. Although the adjustable tail rotates considerably slower than a full movable tail, the sheer complexity of a full movable tail has let it to be discarded as means of trimming the aircraft.

Chapter 6

Hull Sizing

In this chapter, methods used in sizing the hull will be described. After the hull has been sized, it will be designed more thoroughly, calculating stringer spacing and sizing requirements. Also, the displacement of the hull will be calculated in order to enable the determination of clearances and other various parameters.

6.1 Preliminary Hull Sizing

The preliminary hull sizing is based on rules of thumb for flying boats which have been set up in the 1930's and 1940's by several articles and books published by Langley, Locke, Munro and Parkinson [33, 21, 42, 46]. From these rules of thumb the main initial parameters will be estimated for the hull design. These parameters are preliminary values to estimate the sizing of the hull. In a further design stage towing tests are recommended to test the hull's properties.

6.1.1 Beam Length

Computing the first estimate of the beam length, the width at the widest part of the hull, is the starting point of hull designing [42]. The rule of thumb to get an estimation of the beam length is shown in Eq. 6-1 and is based on the load displacement of the aircraft. The beam length will not be computed for the Maximum Take-Off Weight (MTOW) as the aircraft will not perform a fully loaded take off from water when fighting fires. However, in other missions the aircraft may perform, there will be payload that needs to be transported from the water. Therefore, the load displacement will be assumed at the MTOW minus 2,500 kg, which is the loading at which the aircraft will still be able to take off with a runway length of 1,000 meters.

$$b = 4 \cdot \sqrt[3]{\Delta_0} \tag{6-1}$$

6.1.2 Wetted Hull Length

From the beam length, an estimation for the wetted length of the hull can be computed. The wetted length is the part of the hull that will be submerged at zero velocity at zero payload. There are two methods to make a first estimation for the wetted length. The first method is based on Eq. 6-2 and 6-3 which are based on reference flying boats [21].

$$C_{\Delta_0} = \frac{\Delta_0}{\gamma_w \cdot b^3} \tag{6-2}$$

$$L_{wet} = 6 \cdot b \cdot C_{\Delta_0}^{1/3} \tag{6-3}$$

The displaced load is taken as stated above at the MTOW minus 2,500 kg, the specific weight of water at 10 °C and the beam length is obtained from Eq. 6-1. This method will be referred to as 'Method 1' in Table 6-1.

The second method, in Table 6-1 referred to as 'Method 2', uses load coefficients which have been proposed by Parkinson [46]. According to J.B. Parkinson, the values for the initial load coefficient that have the best overall results, lie within the range of 0.5 to 0.8. Parkinson's method yields higher wetted length estimations which vary from a 5.8% to 24.1% increase compared to the Method 1

6.1.3 Fore- and Afterbody Length

The wetted length consists of the fore- and afterbody length, where the forebody length of a flying boat is the distance from the forward perpendicular to the main step at the keel. The rule of thumb for estimating the forebody length for flying boats is shown in Eq. 6-4.

Another way of computing the forebody length is by considering its effects on the spray. The length of the forebody can be computed with the load coefficient which is determined through Eq. 6-6 with k as a spray factor and C_{Δ_0} obtained from Eq. 6-2. The length can be calculated for gradients of spray that vary from excessive ($k = 0.0975$) to light spray ($k = 0.0525$). However, spray can be reduced by other methods than adjusting the ratio between the beam and the forebody length such as spray strips [21].

The afterbody length of a flying boat is the distance from the main step to the second step or sternpost (whichever is shortest). The rule of thumb for estimating the afterbody length for flying boats is shown in Eq. 6-5.

$$L_{fb} = b \cdot 3.5 \cdot \sqrt[3]{C_{\Delta_0}} \tag{6-4}$$

$$L_{ab} = b \cdot 2.5 \cdot \sqrt[3]{C_{\Delta_0}} \tag{6-5}$$

$$L_{fb_{spray}} = b \cdot \sqrt{\frac{C_{\Delta_0}}{k}} \tag{6-6}$$

6.1.4 Shape of Planing Bottom

The V-shape is favored for the planing bottom because of its qualities of absorbing the shock during landing on water [43]. An important angle is the dead rise angle which is the angle of the cross section of the hull with the horizontal, as is explained in Figure 6-1. Angles of 20 to 22.5 degrees have been found to be generally acceptable for large flying boats [21].

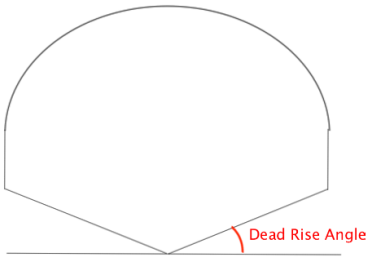

Figure 6-1: Dead Rise Angle

6.1.5 Steps

Steps are abrupt changes in the shape of the bottom of the hull which are essential to break down the water suction and enable the plane to unstick from the water [42]. For the hull design, a configuration with two steps has been selected because the two step hull is steadier and provides enhanced controllability to the aircraft during manoeuvring on the water. The steps will be located slightly behind the center of gravity [33]. The depth of steps will range between 8 to 12 % of the beam length to avoid hydrodynamic instability at high water speeds [46]. Finally, an angle between the fore- and afterbody keels should ensure sufficient clearance after take-off of the tail section. According to Parkinson, the best compromise is between 6 and 7 degrees [46].

Table 6-1: Hull Sizing Parameters Based per Weight Class Estimation

Parameter	Weight Class I Estimation	Weight Class II Estimation
MTOW [kg]	56000	47905
Beam Length [m]	4.65	4.34
Method 1		
Wetted Hull Length [m]	20.9	19.5
Forebody Length [m]	12.2	11.4
Afterbody [m]	8.7	8.1
Method 2		
Wetted Hull Length [m]	22.1 to 25.9	20.7 to 24.2
Forebody Length [m]	12.9 to 15.1	12.0 to 14.1
Afterbody [m]	9.2 to 10.8	8.6 to 10.0
Depth of Steps [m]	0.37 to 0.58	0.35 to 0.52
Forebody Length based on Spray		0
L_{fb} for excessive spray [m]	9.7	9.0
L_{fb} for satisfactory spray [m]	11.6	10.9
L_{fb} for light spray [m]	13.28	12.3

6.2 Preliminary Hull Weight Estimation

As the design is an amphibious aircraft, significant loading on the bottom of the hull is expected which results in a thicker required skin. In order to get a first estimation of this loading and its effects, a MATLAB model was constructed to assess the dynamic and static pressures on the hull below the waterline, as well as the resulting required skin thicknesses.

6.2.1 Assumptions and Model Limitations

Several assumptions were made in order to develop this model which are listed below with an explanation;

- The aircraft is at its maximum draft. In practice, the aircraft's draft will decrease as the aircraft accelerate because the hull will start planing.
- All loads are considered steady, no transient loads are considered.
- The only loads considered are the static and dynamic water pressure loads.
- The shape of the hull is simplified and its cross-section of constant shape. Furthermore, the hull steps are not included.
- The modeled hull is modeled consists of frames and simply supporting stringers which simply support rectangular flat plates under pressure.
- The modeled skin thicknesses are at least 1 millimeter.
- The stringers are modeled as straight beams of I-shaped cross-section with equal-sized flanges.

The main limitation of the model is that it cannot take into account impact loads and stresses in the fuselage due to in-flight bending moments. The impact loads, during for example landing, are relatively hard to quantify but are assumed to be taken up by the keel beam. As the stresses in the fuselage due to in-flight bending will produce a compression force in the fuselage bottom, buckling is the most likely failure mode there.

6.2.2 General Model Structure

The model is based on assumptions and require several inputs such as number and dimensions of frames and stringers, draft, water speed, etc. The model will generate the structure of the hull which is done by evenly distributing the frames across the length of the hull. Next, the local width is determined which, combined with the constant shape, yield a set of center coordinates for the panels and stringers. Based on the coordinates of the surrounding panels and stringers, the angle of each panel with respect to the incoming flow is determined. In order to take into account the pitch angle of the aircraft during landing, an extra angle of 15 degrees is added.

Using this information, the pressure on each skin panel and its required thickness is computed according to the equations are described in the Section 6.2.3. If the resulting thickness is lower than 1 millimeter, the model sets it to this minimum value. With the thickness, panel dimensions and the assumption of a flat rectangular plate, the individual panel weights are found.

The dimensions and weights of the stringers are found in a similar manner. Here, the stringers are modeled as simply supported beams with an I-shaped cross-section with equally sized flanges. In order to determine the load acting on the stringer, the distributed (pressure) force acting on the two adjacent panels in multiplied with the local panel area, yielding the magnitude of the point force acting on the each of the two adjacent panels. Next, it is assumed that half of each point force is acting on the stringer. Using the computed load, the model is able to calculate the required dimensions and weights of the stringers. Finally, the individual panel and stringer masses are summed which provide a first estimate of the hull mass.

6.2.3 Governing Equations

This section will explain the basic principles and governing equations that are the basis of the MATLAB model. The loads used by the program are only pressures resulting from presence in and movement through the water. These are summed to give a pressure for each separate panel, according to Eq. 6-7.

$$P_{tot} = P_{static} + P_{dynamic} \tag{6-7}$$

The static pressure P_{static} is the pressure due to the panel being submerged a certain depth which can be calculated according to Eq. 6-8, where z is the vertical distance below the water line.

$$P_{static} = \rho_{water} \cdot z \tag{6-8}$$

The dynamic pressure $P_{dynamic}$ is the pressure acting due to the movement of the panel through the water, as given by Eq. 6-9.

$$P_{dynamic} = \frac{\rho_{water}}{2} \left(V \sin \alpha_{panel}\right)^2 \tag{6-9}$$

The required thickness can be found according to Eq. 6-10, where the factor s is a Fourier Series. This Fourier Series, given in Eq. 6-11, will be evaluated by the software for the first 9 terms. Eq. 6-10 is a rewritten form of the equation given by Megson for the deflection of a flat rectangular simply supported plate under pressure loads [38]. The rewriting is necessary in order to get the thickness t_{panel} as a function of the maximum allowable deflection w_{max} which is defined by the user. The panel mass m_{panel} is then determined through Eq. 6-12.

$$t_{panel} = \frac{s \cdot 192 \cdot \left(1 - \nu^2\right) \cdot P_{tot}}{\left(\pi^6 \cdot E \cdot w_{max}\right)^{\frac{1}{3}}} \tag{6-10}$$

$$s = \sum_{m=1,3,5}^{\infty} \sum_{n=1,3,5}^{\infty} \frac{sin\left(\frac{m \cdot \pi}{2}\right) \cdot sin\left(\frac{n \cdot \pi}{2}\right)}{m \cdot n \cdot \left(\frac{m^2}{l_{panel}^2} + \frac{n^2}{w_{panel}^2}\right)^2} \tag{6-11}$$

$$m_{panel} = l_{panel} \cdot w_{panel} \cdot t_{panel} \cdot \rho_{panel} \tag{6-12}$$

In order to determine the required size of the stringers, a formula based on maximum allowed deflection is used, as explained by Eq. 6-13 [38].

$$I_{required} = \frac{p \cdot l_{stringer}^4 \cdot 0.625}{48 \cdot E \cdot w_{max}} \tag{6-13}$$

Eq. 6-14 can be used to determine to the thickness of the stringer, based on a given height and width of the stringer and the previously obtained information. The weight of the stringer can subsequently be determined through Eq. 6-15.

$$t_{stringer} = \frac{I_{required}}{w_{stringer} \cdot h_{stringer} + \frac{1}{12} \cdot h_{stringer}^3} \tag{6-14}$$

$$m_{stringer} = \rho_{stringer} \cdot l_{stringer} \cdot (2 \cdot w_{stringer} \cdot t_{stringer} + h_{stringer} \cdot t_{stringer}) \tag{6-15}$$

6.2.4 Results

The number of stringers below the waterline has a large impact on the required skin thickness and the overall weight of the hull. Therefore, a large range of number of stringers have been put in the model, in order to determine the optimum stringer distribution. This assessment yielded a optimum stringer distribution of 40 stringer under the waterline. Using other inputs summarized in Table 6-2, the model provides a first estimate of the hull weight of 635 kilograms.

It should be emphasized that this model does not incorporate any stringers or skin panels above the waterline, nor the keel beam, nor any of the frames. Also, impact loads from waves or landings are not incorporated, neither are the compressive loads that are be expected in-flight.

Table 6-2: Hull structure calculation software input, initial iteration

Input Parameter	Input Value
Fuselage wetted length [m]	34.26
Fuselage beam width [m]	4.21
Fuselage material Young's modulus [GPa]	73.1
Fuselage material Poisson ratio [-]	0.33
Fuselage material density $[\frac{kg}{m^3}]$	2.78
Speed through water $[\frac{m}{s}]$	55
Fuselage maximum draft [m]	1
Maximum allowable plate deflection [mm]	5
Number of fuselage frames [-]	35
Number of stringers below waterline [-]	40
Fuselage deadrise angle [°]	20
Stringer height [mm]	20
Stringer width [mm]	20

As the thickest panels requires a thickness of 2.7 millimeters based on the considered loads, while the panel dimensions range up to 1 meter in length and 10 centimeters in width. However, the compressive loads are expected to significantly increase the required skin thickness. Especially panels near the keel beam are susceptible to compressive loads due to the deformation of the aircraft in flight. As the stringers may suffer from the same phenomenon, they may become thicker than the 1 millimeters as determined through the model.

6.3 Required Hull Volume

According to the Law of Archimedes: "Any object, wholly or partially immersed in a fluid, is buoyed up by a force equal to the weight of the fluid displaced by the object." This law is still in use for different applications, including the next generation water bomber. Archimedes law simply states that

the buoyancy equals the weight of the displaced fluid. As the weight of the next generation water bomber has been determined, an estimation of the displaced water and general dimensions of the fuselage can be performed.

The sizing of the hull in previous section are mainly based on data from reference aircraft. However, as these amphibians aircraft were built to transport only small payloads, these reference aircraft are much smaller and the calculated dimensions may be off. The first calculations of the previous hull sizing method, estimated a fuselage width of 5.1 meters. It has been argued that this width is unrealistic and would result is a large horizontal tail surface in order to ensure longitudinal stability issues. Therefore, the Law of Archimedes is used to review the required dimensions of the hull.

As said, the buoyancy is equal to the weight of the displaced fluid. For the next generation water bomber, the fluid is water which has a density 1000 $\frac{\text{kg}}{\text{m}^3}$. Hence, an aircraft with a weight of 56,000 kilograms needs a volume below the water surface of approximately 56 m^3. As there are three dimensions that determine the volume below the water surface, being the draft and width of the fuselage as well as the wetted length, a consideration should be made between the dimensions. A relation between the dimensions have been established based on reference aircraft, logical reasoning and an iterative process. The iterative process, in which the final values are calculated, will be discussed in Chapter 7. In this same chapter the final dimensions of the fuselage will be presented.

Chapter 7

Iterative Process & Final Configuration

As part of the design process, several design iterations have taken place since the computed variables, such as wing span, tail area, etc., are interdependent. The main aspect of the iterative process is the weight estimation, as the weight directly or indirectly forms the input of other component sizing while the weight in itself again depends on the size of these components. Therefore, the main goal of the design iterations is to optimize the aircraft with respect to weight. This chapter will discuss the approach that have been used with respect to the iterative process and final results will be further elaborated on in the sections below.

7.1 Class II Weight Estimation

In this section, the Class II Weight Estimation for the design will be presented. This estimation forms the basis of the in-depth design process, as the aircraft weight, either directly or indirectly, is the main input parameter for nearly all elements that need to be designed, such as the wing and propulsion system. The Class II method, based on based on the Roskam method for military transport aircraft, is used to obtain a weight estimation of the main aircraft components and therefore the total aircraft weight. This method also estimates the center of gravity location of each component and of the entire aircraft [52].

In order to be able to perform multiple design iterations, a MATLAB model has been constructed and has been used as the main computational tool. The inputs for this method are formed by multiple parameters, of which most been obtained in the Class I Weight Estimation during the Mid-Term Phase [67]. Also, engine data and geometrical properties are used as inputs for this weight estimation. However, it must be noted that during this stage of the design process, the weight estimation is still augmented by statistical data. In order to perform the estimation, some design choices and assumptions have been made and are listed below:

1. The design dive speed equals 1.25 times the cruise speed
2. The design dive dynamic pressure is assumed at sea level
3. Gravitational acceleration equals 9.81 $\frac{m}{s^2}$
4. The incidence angle of the horizontal stabilizer will be fixed
5. The horizontal tail is mounted to the vertical fin at 90% of the vertical fin span
6. The fuselage amphibious weight penalty is 65% [52]
7. The engines will be podded wing mounted turboprops
8. Two floats will be installed, weighing about 100 kg each as explained in Chapter 7 of Part IV
9. One fuel tanks will be installed in each wing
10. The fuel used will be Jet-A (density 804 $\frac{kg}{m^3}$)
11. The engines will have beta controls
12. The wing and tail will have anti-icing systems installed
13. The airplane will be unpressurized
14. The scooping and release system have a fixed weight of approximately 300 kilograms, as explained Chapter 10 of Part III
15. The total weight of all emergency equipment (incl. fire extinguishers, rafts etc.) is assumed to be 200 kilograms
16. Ground support equipment is considered to be part of the payload and is therefore not taken into account for the estimation of the Empty Weight
17. Crew member weights are included in the payload and not in the Empty Weight

With these assumptions and design choices identified, the following component weights could be calculated subsequently:

- Fuselage weight
- Horizontal tail weight
- Vertical tail weight
- Landing gear weight
- Fixed equipment weight
- Wing weight
- Nacelle weight
- Powerplant weight
- Fuel system weight

By summing the individual component weights, the expected design weight could be determined. Using the values obtained from the Class I Weight Estimation as initial inputs, the first design iteration was performed. The iteration results were subsequently used in the iteration process to obtain the final design weight in.

Using the weights of the aforementioned components, the approximate location of the center of gravity of the design could be determined. In order to determine this location, the design was divided in two main components, being a wing group and a fuselage group. The wing group includes the weights of all items attached to the wing (powerplant, nacelle, fuel system, floats) and the wing itself, while the fuselage group includes all remaining items. For every component, its individual center of gravity location was determined using guidelines set by Roskam after which the center of gravity of both groups as well as the total aircraft could be determined [52]. The results of the center of gravity calculations, as well as weight calculations, for multiple iterations can be found in final sections of this chapter

7.2 Iterating Process

The Class I Weight estimation has been used as the main input in a MATLAB computational modelling tool for sizing the wing, tail and powerplant on which different team members had been assigned to [67]. The models of the individual component sizings have been put into a single script with the ability to compute the weight and sizing of the aircraft components and the aircraft as a whole. Setting up this model enabled the design team to constantly vary the initial inputs to reflect iterations in the design. For the first iteration, all sizing was based on the Class I estimation after which a Class II weight estimation was performed. This estimation was subsequently used for the component sizing, after which this iteration process was used again using the new component sizing as input for the iterated Class II weight estimation. This process was continued until the last iteration resulted in a weight difference of less than 50 kilograms.

7.3 Weight and Center of Gravity Results

One of the consequences of using a Class II weight estimation is the need for multiple iterations. The main reason for this lies in the fact that the input of the Class II estimation depends on the component sizing, which in turn depends on the Class II estimation. Therefore, only through repeated iterations, an optimum weight and component size estimations can be obtained. For the first iteration, the results of the Class I were used as input for the Class II estimation. For the subsequent iterations, the results of the Class II estimation and component sizing were used as input. The iterative process was halted after it resulted in a weight difference of less than 50 kilograms. The final results of the weight estimations are presented in Table 7-1. With the final component weights known, their respective center of gravity location could be determined. The center of gravity locations of the aircraft components and the complete aircraft are tabulated in Table 7-2

7.4 Wing, Fuselage and Empennage Dimensions

The sizing of the wing, fuselage and empennage, which includes the horizontal and vertical tail, is based on the estimated aircraft weight. However, the aircraft weight in turn, depends on the sizing of these components. Therefore, whenever a new weight or component sizing estimation was performed, the

Table 7-1: The Final Weights of the Aircraft

Take-off Weight [kg]	54,243
Empty Weight [kg]	30,525
Payload [kg]	15,318
Fuselage [kg]	7,188
Wing [kg]	7,848
Floats [kg]	200
Horizontal Tail [kg]	742
Vertical Tail [kg]	706
Nacelle [kg]	852
Landing Gear [kg]	1,377
Powerplant [kg]	4,824
Fixed Equipment [kg]	5,677
Firefighting [kg]	1,111
Fuel [kg]	8,400

Table 7-2: The Final Center of Gravity Locations

Winggroup [m]	16.80
Wing [m]	17.45
Nacelle [m]	12.12
Powerplant [m]	13.04
Fuelsystem [m]	17.45
Floats [m]	18.40
Fuselagegroup [m]	17.08
Fuselage [m]	14.93
Horizontal Tail [m]	33.74
Vertical Tail [m]	34.41
Landing Gear [m]	17.79
Instrumentation, Avionics and Electronics [m]	3.47
Fixed Equipment [m]	14.93
Fire Fighting Equipment [m]	17.45
Complete Aircraft [m]	16.97

component or weight estimation respectively had to be iterated. Therefore, multiple iterations were performed which ultimately yielded an optimum component sizing for the wing, as shown in Table 7-3. The final dimensions of the fuselage and empennage can be found in Table 7-4 7-5 respectively.

Table 7-3: The Final Wing Dimensions

Surface [m^2]	192.6
Span [m]	39.25
Chord length at the Root [m]	7.01
Chord length at the Tip [m]	2.80
Thickness at the Root [m]	1.19
Thickness at the Tip [m]	0.48
Flap Area [m^2]	27.82
Aileron Area [m^2]	10.73

Table 7-4: The Final Dimensions of the Fuselage

Length of the Nose [m]	1.5
Wetted Length [m]	25.00
Length between Steps [m]	7.26
Total Length [m]	34.72
Length to Half Chord Length of the Wing [m]	18.40
Maximum Width of the Aircraft [m]	3.30
Height above the Water Level [m]	4.87
Height below the Water Level [m]	1.37
Height of the V-Shape part of the fuselage [m]	0.60

Table 7-5: The Final Dimensions of the Tailplanes

Horizontal Tail	
Horizontal Tail Surface [m^2]	43.22
Span Horizontal Tail [m]	15.06
Root Chord Length of the Horizontal Tail [m]	4.10
Tip Chord Length of the Horizontal Tail [m]	1.64
Root Chord Length of the Elevator [m]	1.64
Tip Chord Length of the Elevator [m]	0.66
Elevator Area [m^2]	12.10
Vertical Tail	
Vertical Tail Surface [m^2]	36.08
Span Vertical Tail [m]	6.01
Root Chord Length of the Vertical Tail [m]	8.58
Tip Chord Length of the Vertical Tail [m]	3.43
Root Chord Length of the Rudder [m]	3.52
Tip Chord Length of the Rudder [m]	1.96
Rudder Area [m^2]	15.13

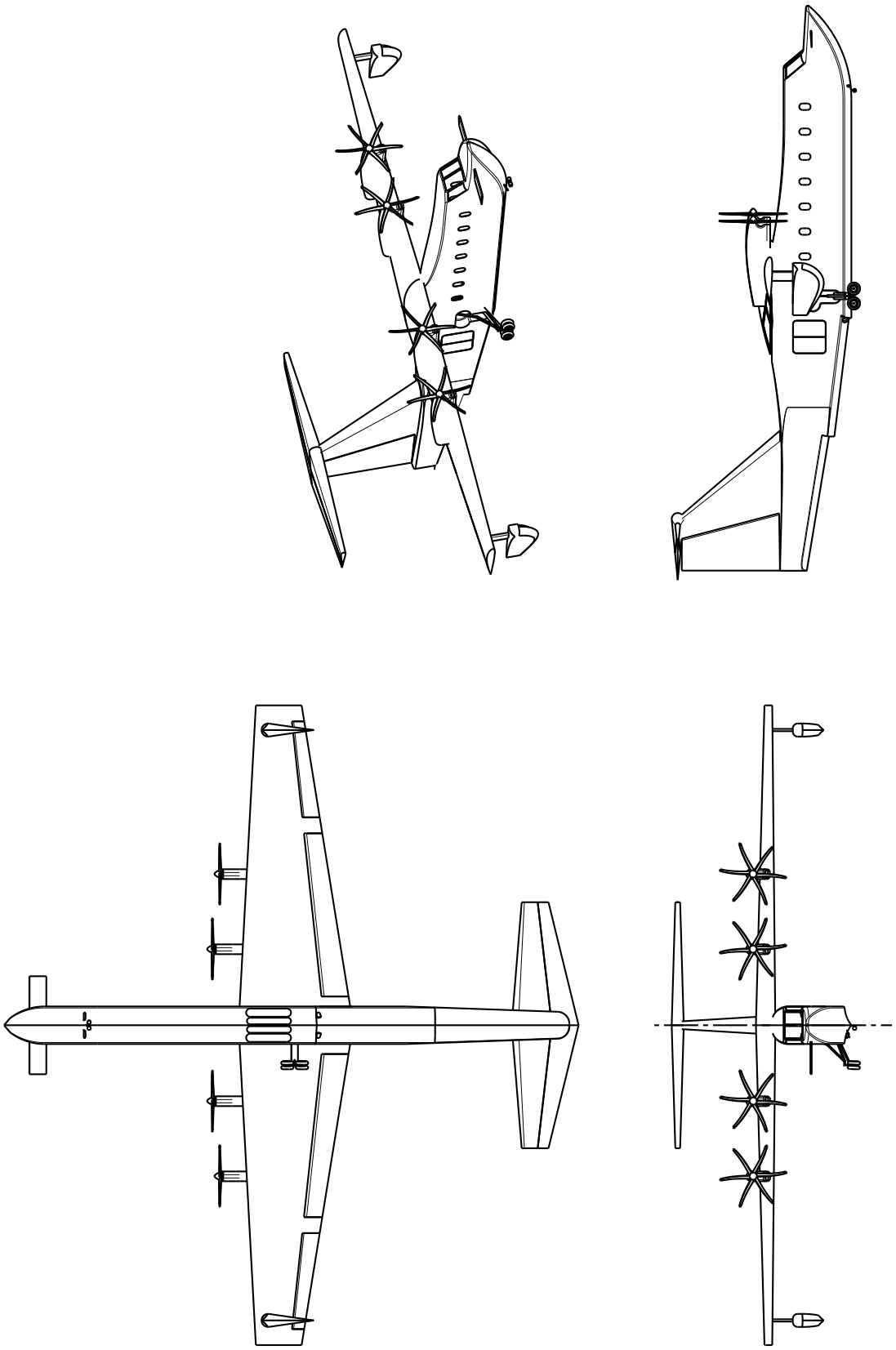

Figure 7-1: Sketches of Final Concept

Part III

System Sizing

Chapter 1

Sizing of Control Surfaces and High-Lift Devices

This chapter contains the sizing of the control surfaces and High-Lift Devices (HLDs).

1.1 Sizing of Control Surfaces

From the parameters mentioned in the previous sections, an initial drawing can be made in order to visualize the space available to position the control surfaces (e.g. ailerons) and the HLDs.

According to Roskam, the allocation of the control surfaces should be based on data from reference aircraft [53]. The same aircraft that have been used to determine the aspect ratio A and wing taper ratio λ_w are used to determine the positioning of the control surfaces, as can be seen in Table 1-1.

Table 1-1: Control Surface Data of Reference Aircraft

Aircraft Type	Wing Surface Area [m^2]	Spanwise Location of Ailerons	Surface Area of Ailerons [m^2]
Bombardier 415	100	$0.61 - 0.93$	8.05
ShinMaywa US-2	135.82	$0.71 - 0.97$	6.40
Beriev Be-200	117.44	$0.77 - 0.95$	3.56

From Table 1-1, it has been decided that the ailerons will run from 0.65 to 0.95 $\frac{b}{2}$ spanwise, and 0.75 to 1.00 c chordwise.

1.2 Sizing of High-Lift Devices

In Chapter 2 an airfoil has been selected which will deliver a $C_{L_{clean}}$ of **1.3**, while the required $C_{L_{land}}$ is **2.6**. The required $C_{L_{TO}}$ is **1.7**, however, as the $C_{L_{land}}$ is higher this value will be used for sizing since it is critical. In order to attain the large lift coefficients required for landing and take-off, HLDs are installed to increase the $C_{L_{clean}}$ to the required $C_{L_{land}}$ and $C_{L_{TO}}$.

Selection of Flap Type, Flap Angle and Flap Chord

The available flap types vary from simple plain flaps to complex triple-slotted flaps. However, as the design of the water bomber should remain a simple as possible in order to be more reliable and easy to maintain, the complex flap systems are dismissed and a simple single slotted flap systems has been chosen. Furthermore, the following calculations show that this flap systems will be able to provide a sufficient increase in lift coefficient.

Eq. 1-1 can be used to determine the incremental values of maximum lift coefficient which need to be produced by the high lift devices. In Eq. 1-1 the factor 1.05 accounts for the additional trim penalties due to the deployment of flaps.

$$\Delta C_{L_{\max_L}} = 1.05 \left(C_{L_{\max_L}} - C_{L_{\max}} \right) = 1.05 \left(2.6 - 1.3 \right) = 1.365 \tag{1-1}$$

The required increment in maximum lift coefficient with flaps down, is determined through Eq. 1-2.

$$\Delta C_{l_{\max}} = \Delta C_{L_{\max}} \left(\frac{S}{S_{wf}} \right) K_\Lambda \tag{1-2}$$

where the factor K_Λ accounts for the effects of sweep angle and is given by:

$$K_\Lambda = \left(1 - 0.08\cos^2\Lambda_{c/4}\right)\cos^{\frac{3}{4}}\Lambda_{c/4} = 0.92$$

Next, for two values for $\frac{S_{wf}}{S}$, the $\Delta C_{l_{\max}}$ are determined, as can be seen in Table 1-2.

Table 1-2: Values of $\Delta C_{l_{\max}}$ for Different $\frac{S_{wf}}{S}$

	Landing Flaps	
$\frac{S_{wf}}{S}$	0.3	0.6
$\Delta C_{l_{\max}}$	4.186	2.093

As has been explained, a single-slotted flap system has been selected for the required ratio of $\frac{S_{wf}}{S}$, which can be determined using Table 1-2 to 1-4.

Table 1-3: Constants in Table 1-4

$\frac{z_{fh}}{c}$	0.1
$\frac{c_f}{c}$	0.25
δ_{f_L}	40°
C_{l_α}	2π
α_{δ_f}	0.43 rad
K	0.93

Table 1-4: Governing Equations Determining Dimension of High Lift Devices

$$\left(\frac{c'}{c}\right) = 1 + 2\left(\frac{z_{fh}}{c}\right)\tan\left(\frac{\delta_{f_L}}{2}\right) = 1.0728$$
$$C_{l_{\alpha_f}} = C_{l_\alpha}\left(\frac{c'}{c}\right) = 6.741$$
$$\Delta C_l = C_{l_{\alpha_f}}\alpha_{\delta_f}\delta_f = 2.0235$$
$$\Delta C_{l_{\max}} = \Delta C_l \cdot K = 1.8818$$

Through interpolating $\Delta C_{l_{\max}} = 1.8818$ using the results from Table 1-2, can be found that the required "flapped wing area" ratio becomes:

$$\left(\frac{S_{wf}}{S}\right) = 0.6303$$

from which it has been decided that the single slotted flaps will run from 0.09 to 0.60 $\frac{b}{2}$ spanwise, and 0.75 to 1.00 c chordwise.

However, as lateral controllability issues may arise during on-water operations such as landing and take-off, it has been decided to use " flaperons" instead of the single slotted flap. Flaperons are a type of control surface that combines aspects of both flaps and ailerons and will be installed in positions where the single slotted flaps were originally planned (0.09 to 0.60 $\frac{b}{2}$ spanwise direction, and 0.75 to 1.00 c chordwise). Since the flaperons are installed behind the wash of the propellers, they will experience a faster airflow during low-speed operations such as landing and take-off and will therefore be more efficient in ensuring lateral stability.

Leading Edge Slats

As the flaps potentially cannot provide a sufficient C_L increase during hot atmospheric conditions and the airflow does not remain attached to the wing profile at high angles of attack, the wing should also be equipped with a leading edge lift-enhancing device. There are two leading edge lift-enhancing devices that may be installed on the wing of the next generation water bomber, being a *Krüger Flap* and a *Slotted Leading Edge Flap*, also known as slat.

According to La Rocca, the slats are the most effective leading edge devices which actually increases $C_{L,max}$ and provides an increase in stall angle [51]. As a result, it has been decided to prefer slats over Krüger flaps. Finally, taking into account the positioning of the engine, it has been decided to install the slats running from 0.60 to 0.95 $\frac{b}{2}$ spanwise, and 0.00 to 0.15 c chordwise.

1.3 Actuation of Control Surfaces

In the late 90s, the NASA Dryden Flight Research Center conducted experiments concerning electric actuation of control surfaces instead of using a complex hydraulic system, used by most current aircraft

[11]. The hydraulic system is a complex system with high maintenance requirements, making it costly and prone to failure. Electric actuation turned out to be lighter, more efficient, less complex and more reliable. The electric actuation leads to five to nine percent of fuel savings and a 30 to 50 percent reduction in required ground equipment. Reducing ground equipment is a big advantage of this design which often operates from different bases. As such, the control surfaces will be electrically actuated. Also, the actuation of high lift devices, which requires a constant hydraulic pressure instead of short pulses, is something to be investigated.

Chapter 2

Engine Sizing

With a power loading selected and an initial weight sizing performed, it is possible to select engines. First, the number of engines needs to be determined. Once the number of engines has been determined, the engines can be sized accordingly.

2.1 Engine Type Revisited

Using Roskam [54], a preliminary choice for a turboprop powered design was made in the Mid-Term Report. As Roskam only mentioned pistonprops, turboprops and several types of jet engines, no other engine types were taken into consideration. In this section, other engine types are taken into account.

A Wankel engine is a very compact engine using few moving moving parts. This means less wear and tear and thus less maintenance, but also a lower susceptibility to failure. On top of that, Wankel engines feature a high power to weight ratio. They also run with almost no vibration. On the other hand, very precise manufacturing is needed to ensure little power losses, due to the nature of the inner workings of the engine. The nature of a Wankel engine is such that one side will reach high temperatures whilst the other sides will remain cool. Combined with the large size this will cause deformations in the engine, which may lead to failure of the engine. Due to these reasons the design choice will not be changed to a Wankel engine design.

Besides the Wankel engine, electric engines have also been taken into account. However, as calculated earlier in the MTR [67], a battery weight of 50,000 kilograms is required for an hour of flight. Generating electricity in-flight using on-board generators instead of storing the required energy is inefficient compared to direct fuel burn; it adds unnecessary weight and costs in terms of engines. Also, energy is lost in two processes instead of one. Besides that. electrix engines have to be developed for the power regime the design requires.

In the end, the design choice will remain a turboprop. They are most beneficial in terms of efficiency at operating altitude, power required and weight and size compared against power produced.

2.2 Choice on Number of Engines

Several important design choices are based on the engine count, therefore, the choice of the number of engines should be well-considered. In the selection process, structural, aerodynamic and performance characteristics should be kept in mind. A larger number of engines not only results more but less intense loads, but also results in a lower propeller loading, which allows to vary the propeller blade count. More blades means a lower blade loading, which allows for thinner blades. On the other hand, more engines raise the possibility of running out of space on the wingspan. Also, more engines require a larger vertical tail area to counteract a One Engine Inoperative-induced (OEI) yaw moment. Finally, although it might seem counter-intuitive, more engines do not necessarily result in a significant higher weight, as less powerful engines weight less, but require a higher count.

From a aerodynamic point of view, a larger number of blades causes more interference between the blades. The vibrations, which are the result of this interference, possibly require heavier blades opposed to the weight reduction explained earlier. Besides the propeller blade issues, more engines also causes a higher drag coefficient.

From a performance point of view, the OEI scenario is of interest. As will be explained in more detail in Chapter 2 of book IV, a OEI scenario for a four-engined design still allows for a ZPLW takeoff within 1,000 meters, whereas a two-engined design is only capable of taking of in 1,250 meters without payload and $\frac{1}{3}$ of its fuel capacity. Being able to still comply with the takeoff distance requirement with an engine failure, is favorable from a mission point of view; if the aircraft lands with an inoperative engine

on an airfield with limited accessibility, it can autonomously move to another, more accessible airport for repairs.

The blade loadings required were estimated using Eq. 2-1 in Section 2.5. For two engines, the blade loading only came within a range defined Roskam for a diameter of 5.0 meters in combination with 10 blades [53]. As this large diameter and number of blades are considered unrealistic, the design choice has been further pushed towards a four-engined configuration. Based on the reasoning above, the final design choice was four engines. This configuration ensures sufficient clearance with respect to the water and has a favorable OEI-performance. The possible weight savings due to lower point loads on the wing however, are offset by the need for a bigger tail surface.

2.3 Engine Selection

From the sizing methods, a power requirement of P_{req} of 11.9 MW and a four engine configuration have been established, which yields a required engine (shaft) power P_{shaft} of 3.0 MW. Jane's Aero-Engines have been consulted to select an engine that meets these this requirement which resulted in the RR Allison T56-A-10WA [9]. In Figure 2-1 the T56-A-427, an engine of the same family, is depicted.

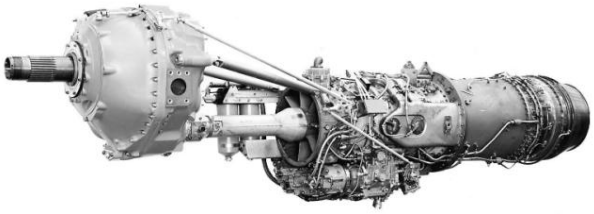

Figure 2-1: Picture of RR T56 Engine, Type A-427

The A-10WA features a reduction gear below instead of above the power section. This selected engine has P_{shaft} of 3.2 MW, weighs 848 kilograms and has a length of 3.7 meters, which is assumed equal to the engine nacelle length. These parameters were subsequently used in the weight iterations. As the weight iterations yielded as reduction in weight, the power requirement yielded a smaller P_{shaft} and an engine re-selection had to take place.

2.4 Engine Re-Selection

After the weight estimates are iterated, a power requirement of P_{req} of 11.6 MW is obtained, requiring four engines rated at 2.9 MW. Jane's Aero-Engines does not list such a turboprop engine. Therefore, the engine chosen before will remain the preferred design choice for now. Of course, a new engine could be developed. However, such a development is a costly process, especially considering the low predictions of sales numbers. If another manufacturer appears to be in need of a similar engine, a joint development program could be started.

Another aspect to take into account when a new engine will be developed is the availability of the required fuel type. If this aircraft is to operate in scarcely populated regions or disaster areas, some fuels might be limited in availability.

2.5 Propeller Sizing

The purpose of a propeller is to transfer energy to the air efficiently to produce thrust. Several propeller parameters can be altered to achieve a desirable propeller configuration, for which Eq. 2-1 can be used [53]. In this equation, the design parameters are propeller diameter D_P, propeller blade count n_{bl} and propeller blade loading P_{bl}. Furthermore, in this equation, $P_{max} = P_{shaft} = 3,117$ kW.

$$D_P = \frac{4P_{max}}{\sqrt{\pi n_{bl} P_{bl}}} \tag{2-1}$$

Existing blade loading ranges are provided by Roskam for different types of aircraft [53]. The category most closely resembling this design is the regional turboprop aircraft, of which P_{bl} range varies from 3.4 to 5.2 $\frac{\text{lbs}}{\text{ft}^2}$. For a diameter range of 3.7 meters to 5.0 meters and a blade count ranging from 4 to 8, feasible combinations have been summarized in Table 2-1.

Table 2-1: Wing Loading for Different Combinations of D_P and $n_b l$

D_P/n_p	4	5	6	7	8
3.7				5.16	4.52
3.8				4.89	4.28
3.9				4.64	4.06
4			5.15	4.42	3.86
4.1			4.90	4.20	3.68
4.2			4.67	4.00	3.50
4.3			4.46	3.82	
4.4		5.11	4.26	3.65	
4.5		4.88	4.07	3.49	
4.6		4.67	3.89		
4.7		4.48	3.73		
4.8		4.29	3.58		
4.9	5.15	4.12	3.43		
5	4.94	3.96			

From reference data, the diameter D_P should be approximately 4.1m. From Table 2-1, this value is feasible for a blade count from 4 to 8 blades. General Electric Aviation has developed a 6-bladed propeller, the C-130J Advanced Propeller System, featuring a diameter of 4.1 meters [7]. This propeller is designed for "excellent take-off and climb performance", low maintenance requirements, easy control to relieve the pilots, whilst featuring a sturdy, fail-safe system. As such, it suits the design of the next generation water bomber perfectly. In light of keeping unnecessary development costs to a minimum, integrating this propeller system into the design is a proper solution.

If better performance is desired it is an option to redesign the propeller blades of the General Electric C-130J engine. A trade-off was made by the manufacturer in favour of noise reduction instead of structural, aerodynamic and costs aspects. So a more efficient propeller could be designed by dropping the noise constraint and instead focusing on a weight reduction or aerodynamic efficiency increase. It is recommended to do research in the redesign of the propellers and its costs for future development stages.

2.6 APU Sizing

The aforementioned power requirement wasvthe power required for propulsion. There are however, other aircraft systems that require power, specifically electric power. This power is provided for by the Auxiliary Power Unit (APU). These other systems usually include environmental control, air starters to start the engines, avionics and miscellaneous electrical systems such as exterior lighting. Whilst definite values are hard to obtain without proper design of these components, some qualitative aspects can be described to certain a extent.

Air starters spool up the turbines of the engines such that a mass flow sufficient to sustain operation, is obtained. The power required for this is not listed in the engine specification of Jane's. However, the power can both be taken from the APU, on-board batteries, running engines, available ground power sources or combination of these. Environmental control systems such as pressurizing systems and air conditioning systems require a significant amount of power in case these are installed. As the aircraft will be operating in warm environments, it is decided to install an air conditioning systems to provide crew comfort. However, as the flight ceiling will be around 4,000 meters, there is no need for a pressurized fuselage and the pressurization systems can be discarded. Avionics and other electrical

Table 2-2: C5-M Auxiliary Power Unit Characteristics [26]

Length	1.247 m
Width	0.853 m
Height	0.757 m
Weight	140 kg
Power output	126.7 kW

systems significantly vary in power requirements, depending on what systems are installed. However, these systems will only put a minor demand on the electrical system. These systems usually obtain power from the main engines. In addition, the non-essential systems do not need power from the APU in case of an engine failure.

In Chapter 1, a design choice is made to use electrical actuation instead of a full-hydraulic system throughout the aircraft. Usually, the hydraulics are powered by the main engines in normal operation, with few critical hydraulics backed up by the APU in case of engine failure. Whilst electrical actuation reduces the power required for hydraulic systems, it puts extra strain on the APU and has to be taken into account when selecting an APU in the future.

The placement of the APU within the fuselage requires some consideration. Obviously, the APU has certain dimension constraints. As no APU has been yet selected, these dimensions are yet unknown. However, judging by APU's in other aircraft, it should be able to fit an APU within this designs fuselage. An indication of typical weights and dimensions is listed in Table 2-2, which contains specifications of the APU in the Lockheed C5-M, which is of significant larger size than the proposed design.

Other considerations concern the weight distribution, air intake and exhaust outlet. The weight distribution is practically unaffected by a weight below 150 kilograms. The exhaust outlet has a temperature of up to 1000° Celsius. This deems any usage of blown effects non-feasible. Also, the exhaust must be placed as such that no water flows in when the aircraft is afloat which implies either a high-placed exhaust, some sort of flowback prevention or a combination thereof have to be used. The air intake has the same issue; water must be prevented from flowing in whilst afloat.

Chapter 3

Engine Positioning

As the type and number of engines have been selected, the positioning of the engines need to be determined. The position of the engines has a large effect on the longitudinal and the lateral control and stability during flight as well as on the on-the-water operations. During the conceptual phase it was decided that the design will feature a high-wing configuration with the engines mounted on top of the wings in order to minimize the risk of contact with water during on-water operations. Since the design process has evolved, a more detailed research is performed to determine the location of the engines which will be described in this chapter. First the configuration of the engines is determined, after which the vertical position of the engines will be discussed. Thereafter, the span wise location of the four engines will be elaborated on, after which the longitudinal position will be will be discussed.

3.1 Engine Configuration

When the propeller is located ahead of the engine, the propulsion system is considered to be a tractor configuration. In contrast, when the propellers are behind the engine, the system is referred to as a pusher configuration. When choosing the configuration type the advantages and disadvantages of each configuration should be taken into account.

The pusher engine moves the center of gravity of the entire aircraft aft which is unfavourable for the longitudinal static stability. In contrast, a tractor engine configuration moves the position of the center of gravity forward. Keeping in mind that during flight over the wildfire the aircraft might be subjected to updrafts affecting the stability of the aircraft, a longitudinal stable aircraft is desired. Furthermore, for a tractor configuration, the resulting thrust is higher than that of a pusher configuration as a propeller after the wing is subjected to the disturbed airflow over the wing. Finally, during scooping operations and water take-off, the aircraft flies under an angle of attack. This angle results in the fact that for a pusher configuration the rotor disks is closer to the water while for a tractor configuration there is more clearance with respect to the water.

On the other hand, during take-off operations a pusher configuration has a better longitudinal controllability as it requires less elevator deflection [56, p. 446]. However, based on an assessment of the advantages and disadvantages of each configuration, it has been decided to opt for a tractor configuration.

3.2 Rotation Direction

Now that a engine configuration has been selected, the rotation direction of the propellers need to be determined. Extensive research has been performed concerning the interaction between the propellers and the wings from which concluded that an inboard up rotation is beneficial since higher lift over drag ratios can be obtained. It has been shown that the inboard-up rotating propellers have a superior performance compared to co-rotating or an outboard-up rotating configuration [68]. The section of the wing which is situated in the region behind the up moving rotors is subjected to a local increase in angle of attack, which leads to an increase in local lift coefficient. Moreover, the force vector is tilted forward which leads to a negative drag component. The part of the wing that is located behind the down moving rotors experiences a local angle of attack decrease. Consequently, this leads to a decrease in local lift coefficient and the force vector is tilted backwards producing more drag. The wing lift loading is larger inboard than outboard [36]. Subsequently. the net drag of an inboard-up rotating propeller is reduced and the net local lift coefficient is increased. As a results, an inboard-up rotating configuration is chosen.

Moreover, it is chosen to use a counter-rotating propeller configuration as it can be reasoned that the moment on a single wing induced by the first engine. is counteracted by the second engine. In case both engines at one side of the wing have the same rotation direction, the moments are not counteracted

and therefore stresses at the root of the wing will be larger compared to counter-rotating propeller configuration. Therefore it is argued that a counter-rotating orientation will result in a lighter structure at the root of the wing. This design decision is supported by the fact that the A400M transport aircraft is also equipped with counter-rotating propeller for structural weight reduction reasons. Furthermore, this orientation allows a reduction of the size of the vertical tail surface, hence reducing weight and drag [40]. In the next design phase, it is recommended to perform further research to determine the exact effect of this rotation direction on the wing structure and the aerodynamic characteristics of the aircraft.

3.3 Vertical Position

In this section the effect of the vertical position of the engines on the design will be elaborated on. The vertical position of the engines is limited by several factors of which clearance is the most important factor. During the conceptual phase it was decided that the engines should be located on the top of the wing for clearance with the water reasons. In this section, a more detailed analysis of the vertical position of the engines will be made.

3.3.1 Water Clearance

With respect to safety and maintainability, it is of importance that the rotor blades have sufficient clearance with respect to the water. During the on-the-water procedures, rotorblades breaking due to interference with heavy water spray or just simply touching the water will have disastrous consequences. Therefore the engines must be positioned such that, even under a bank angle, the rotorblades will never touch the water or be subjected to heavy water sprays. During on-the-water operations a maximum bank angle of 7 degrees is allowed before the floats completely submerge, as will be explained in Chapter 7. Even when the aircraft is subjected to this maximum bank angle, the rotorblades need sufficient clearance with respect to the water. In the Federal Aviation Regulations part 25 (FAR25) it is specified that there must be a clearance of at least 45.72 cm between each propeller and the water [6]. To determine the lower limit of the position of the rotor disks, this clearance is added to the bank angle. In Figure 3-2 this lower limit and the clearance with the water are shown.

3.3.2 Longitudinal Stability

During on-the-water operations, a high vertical position of the engines with respect to the center of gravity will create a diving moment which is unfavourable for the longitudinal stability. Especially during acceleration for take-off this is unfavourable since it is intended to get the aircraft as soon as possible out of the water whilst this moment would actually counteracts this motion. Furthermore, during normal flight conditions, a high position of the engines with respect to the center of gravity is also destabilizing for the longitudinal stability. Therefore, it is required that the engines are located close to the vertical plane of the center of gravity. Secondly, as for longitudinal controllability reasons the horizontal tail surface should be be within the wake of the engines, a high position of the engines is not desired.

On the other hand, in case the engines are located at the top of the wings, the trust vector creates a negative torsion around the wing which adds to the pitch down moment of the wing. If the engines are located at the bottom of the wings the trust balances the negative pitching moment of the airfoil. As a result, the structure in the wing might be lighter.

3.3.3 Propeller Wing Interaction

The air directly behind the propellers of the engines is accelerated, creating thrust. However, this accelerated air can also be directed over the wing. With respect to the propeller wing interaction, two vertical configurations are considered. In the first situation the propellers and engines are located higher than the wing as with the Bombardier 415. The second case is that the propellers are positioned below the wing, thereby accelerating mainly the air below the wing, comparable to the Lockheed C-130 Hercules. Both situations are shown in Figure 3-1.

For the high propeller position, both the drag and the required thrust are smaller compared to an wing in free stream. In the second case, the wing is subjected to an increase in drag and required thrust [68]. This is explained by the fact that behind the propeller disk the slipstream contracts since the air is accelerated resulting in a lower static pressure. In the first situation this contraction induced an upwash. Similar to the upwash due to the moving propeller up which leads to a lift increment and a lowering of the drag as the force vector is pointed forward. For the low propeller position the exact opposite occurs and the wing experiences a local decrease in angle of attack decrease. Hence a decrease in lift coefficient and more drag [36].

A high position of propeller thus results in an overall gain in propulsive efficiency and increase in lift over the wing. If the same total lift is required over wing, other parameters such as the lift coefficient C_L, the surface of the wing S_w or the velocity V may be reduced. During the next design phases, the effects of the propeller and wing interaction on the aerodynamic properties of the wing and possible changes to its design should be assessed in more detail.

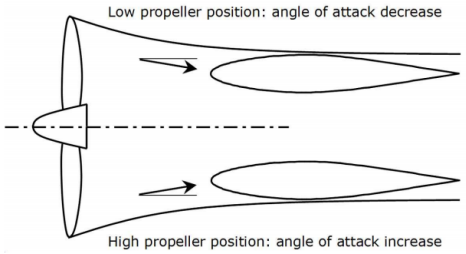

Figure 3-1: Effect of High and Low Propeller Position [68, p.43]

Furthermore, research has shown that the propeller slipstream has a strong effect on the stall angle [30]. The air effected by the propeller is always blown under the same angle of attack with respect to the wing as the engine is directly attached to the wing. At high angles of attack, the freestream over the wing is not able to follow the curvature of the wing. As a result, the flow may separate which eventually causes a stall of the aircraft. However, the air affected by the propeller is still under the same angle of attack with respect to the wing and therefore the effective angle of attack is lower than the angle of attack with respect to the freestream. Therefore higher stall angles can be reached. This increase in stall angle is especially desirable during operations approaching the stall speed such as scooping and release of the fire retardant.

Based on the reasoning discussed above, it is decided that the engines should be positioned on top of the wings. The positive effects this placement has on the stall characteristics, the propulsive efficiency and the clearance with the water were valued as critical.

3.4 Spanwise Position

The spanwise position of the engines is determined by the amount of engines, the clearance required with respect to the fuselage and between the engines themselves. During a one-engine-out scenario it is highly desirable that the engines are placed as close to the center line of the aircraft as during an one-engine-out scenario the induced yawing moment is smaller when the engines are positioned close to the center of the aircraft.

During such scenario differential power settings and the rudder correct for this yaw-moment. Hence, if the engines are located too far from the center this might possibly lead to an undesired increase in the rudder size. As a design guideline a minimum distance between the tip of the propellers and the fuselage of 0.5 meters is used which is the same distance used between the tips of each propeller. However, during the next phases of the design process, computational fluid dynamics tests should be performed in order to determine the optimal distance between the propellers with respect to the aerodynamic effects of the counter-rotating propeller configuration.

3.5 Longitudinal Position

Although previously has been discussed that the four engines are mounted onto the wings, a preliminary estimation of the location of the engines should be made.

Firstly, as the slipstream behind the propellers need a distance behind the propeller to develop, the propellers have to be placed in front of the leading edge (LE) [68].

In Table 3-1 the ranges of the propeller positions are given from which the distance between the propeller and the leading edge can be determined. Given the fact that the diameter of the chosen propeller disk is approximately 4.1 meters, the distance with respect to the LE ranges from 1.66 meters to 3.20 meters. Research further indicates that the best performance of the wing in the wash of the propeller is obtained when the propeller is installed close to the wing [30]. However, quantitative design guidelines have not been derived.

Table 3-1: Ranges for Propeller Position on Aircraft [68, p.42]

Dimension	Range
x_p/R	0.81 - 1.56
$y_p/(b/2)$	0.23 - 0.36
z_p/R	-0.25 - 0.42

The longitudinal position of the engines contributes to the torsion of the wing. The wing airfoil has a negative moment coefficient due to its pressure distribution. As a consequence, the wing is subjected to a pitch down moment. Locating the engines more to the front will result in a pitch down torsion on the wing due to their weight. As a result the structure must be reinforced in order to deal with these torsional loads. Hence, from a structural point of view, it is favorable to locate the engines as much as possible to the rear. Furthermore, it is desirable to locate the engines in front of the high lift devices (HLD's). During take-off and on-the-water operations the velocity of the aircraft itself is relatively low. As the air behind the propellers is accelerated, the high lift devices will be located in the wash of the propellers which makes them more effective.

The engines are 3.7 meters long while the high lift devices cover 25% of the chord length at the engine location (there are no slats at the engine locations). For the most inner engine, located at 3.77 meters from the root in spanwise direction, this provides 4.59 meters of chord length in space measured from the leading edge. In case of the outer engines, located at 8.37 meters from the root in spanwise direction, 3.84 meters of chord length remains available for engine positioning. Given the available space, the range for the position of the propeller in front of the leading edge and the pitch down moment, it is decided that the propeller should be situated as close to the leading edge as possible. As a result, the center of the propeller will be located at 1.66 meters in front of the leading edge with the engines directly attached to it. In Figure 3-2 a front view of the aircraft is given illustrating the vertical and spanwise positions of the engines.

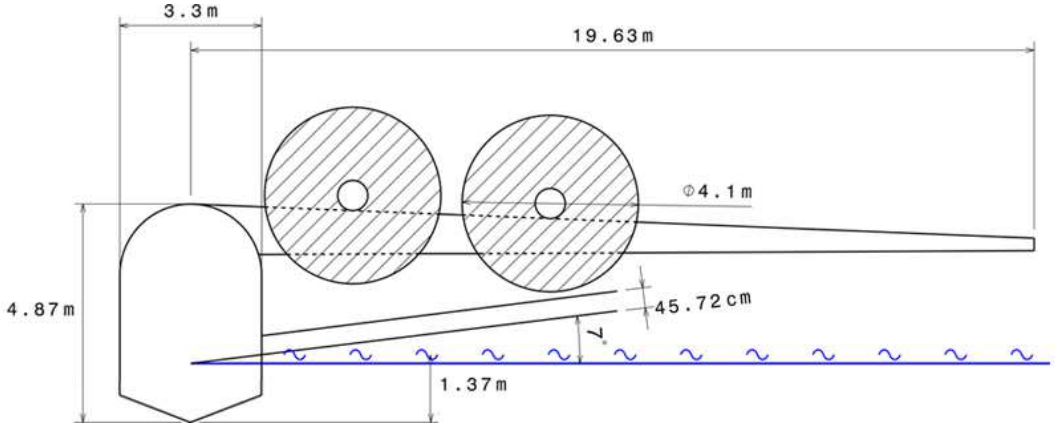

Figure 3-2: Illustration of the Positioning of Engines with Respect to Waterline

Chapter 4

Landing Gear

Landing gears are used to absorb landing shocks and taxiing shocks. A first estimation of the landing gear is calculated with the method used in Roskam [55]. With this method, the weight of the nose and main gear is calculated first, after which the size of the tires are estimated. Furthermore, the strut length and diameter is calculated and the landing gear configuration is determined.

4.1 Weight distribution

For the landing gear a tricycle configuration will be used which means the aircraft will have a nose gear in the front and the main gear behind the center of gravity. For the first estimation the maximum take-off weight is used for the weight distribution. Figure 4-1 shows a sketch of the weight distribution. The nose gear will be located 5.25 meter from the nose and will have one strut with two tires. This distance is chosen because the nose gear needs to carry at least 8% of the MTOW. The main gear will be located 17.95 meter from the nose and will feature two struts, one on every side of the hull. Finally, the struts will hold four tires each. The distance of the main gear from the center of gravity is chosen because it is typically positioned 45 to 50 % of the MAC [50].

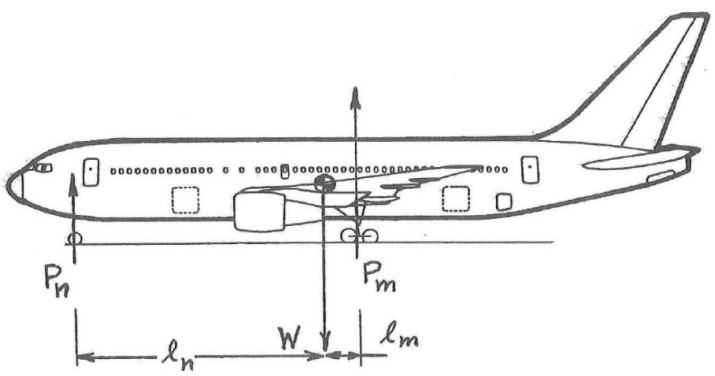

Figure 4-1: Sketch of the Weight Distribution [55]

The weight every strut needs to be able to handle is shown in Figure 4-1 . P_n indicates the total weight the nose strut needs the handle. The P_m stands for the weight one main gear strut needs to handle. This means the total weight of the aircraft is equal to $W = P_n + 2 \cdot P_m$. The weight distribution is shown in Table 4-1.

Table 4-1: Static Loads per Strut at MTOW

Static Load	[lbs]	[kg]
P_m	55,179.0	25,028.8
p_n	9,227.8	4,185.7

4.2 Tire sizing

Now the amount of weight every struts needs to handle is known, the size of the tire can be determined for which the maximum loading for each tire needs to be obtained. The static load of one tire is the weight distribution per tire determent above multiplied by 1.07, according to FAR25 regulations. For the first estimation of the dynamic load per tire, 1.5 times the static load per tire can be assumed. For the tire sizing the largest load value will be used.

Not only the maximum load value is a factor for tire sizing, also the inflation pressure of the tire is of importance which is done using Figure 4-2. First, the *Equivalent Single Wheel Load (ESWL)* needs to be obtained. The ESWL of a group of two or more wheels is equal to the load of a single wheel with the same pressure causing the same pavement stresses. As for this design every strut has two tires, the ESWL is obtained by dividing the P_n or P_m by 1.33 [55].

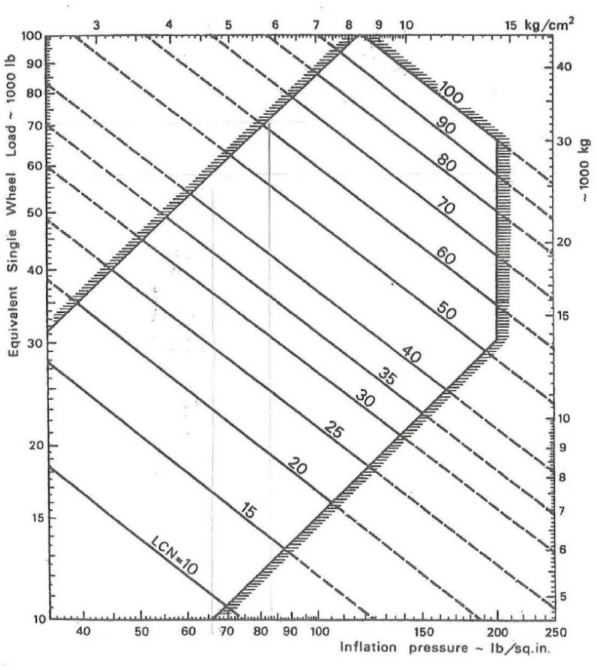

Figure 4-2: Inflation Pressure [55]

The last condition the tire needs to meet, is the maximum tire operating speed. The landing and take-off speed are calculated through Eq. 4-1 and 4-2.

$$V_{max,landing} = 1.2 \cdot V_{s,land} \tag{4-1}$$

$$V_{max,Take-off} = 1.1 \cdot V_{s,TO2} \tag{4-2}$$

The sizing of the tires is done with the help of tire data tables in Roskam [55]. Tire sizes for the main and nose landing gear were obtained by applying the previously determined conditions. The final tire size was selected from multiple options. The main argument to choose the final tire size is that the diameter of the tire should be as low as possible. The final tire design choices are shown in Table 4-2.

Table 4-2: Final Tire Design Choices

	Tire diameter		**Tire width**		**Max Loading**		**Weight**	
	[inch]	**[m]**	**[inch]**	**[m]**	**[lbs]**	**[kg]**	**[lbs]**	**[kg]**
Main gear	30	0.76	8	0.20	24,100	10,932	58.0	26.3
Nose gear	8	0.20	8.5	0.22	8,000	3,629	23.0	10.4

4.3 Strut Sizing

During landing as well as taxiing, not only the tires but also the shock absorbers absorb the loads. For a first estimation of the shock absorber length equation 4-3 can be used. Furthermore, it is suggested to add one inch to this length by Roskam[55]. In order to calculate the diameter of the shock absorbers, equation 4-4 is used. It should be noted that for these equations an oleo-pneumatic shock absorber is considered. The oleo-pneumatic shock strut is the most common type of shock absorber used today. The oleo combines a spring effect, using compressed air, and a damping effect, using a piston which forces oil through a small hole. It has the highest absorption efficiency compared to air springs, metal springs or liquid spring. The results of the shock absorber length and diameter can be found in Table 4-3.

$$S_s = [(\frac{0.5 \cdot (\frac{MTOW}{g}) \cdot (w_t)^2}{(n_s \cdot P_m \cdot N_g)}) - \eta_t \cdot s_t]/\eta_s \tag{4-3}$$

$$d_s = 0.041 + 0.0025\sqrt{P_m} \tag{4-4}$$

Table 4-3: Dimensions of Shock Absorbers

	Required length		Required diameter	
	[ft]	[m]	[ft]	[m]
Main gear	2.0	0.61	0.63	0.19
Nose gear	2.2	0.67	0.22	0.07

4.4 Landing Gear Lay-Out

For the landing gear lay-out, the lateral tip-over criterion is very important. In order to ensure that the airplane will not tip-over during a turn, the line from the nose tire to the main tire and the line perpendicular to the first line should have an angle equal or smaller than 55°, as explained by Figure 4-3.

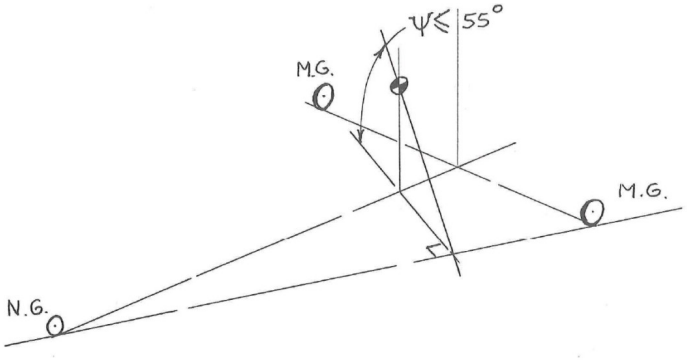

Figure 4-3: Lateral Tip Over Criterion[55]

Since the distance between the nose and main gear is known as well as the height of the center of gravity, the distance of the main gear from the center line can be calculated. This yielded a distance from the center line to the main gear of at least 2.94 meter. As the width of the hull is less than the distance the main gear needs to be from the center line, two options of storing the landing gear are considered. The landing gear can be stored in the wing while the second option is folding the landing gear up in the fuselage. As the wings are designed to be high above the ground, folding up the main gear in the fuselage will be the best option.

For the first estimation of the main landing gear configuration, the Bombardier 415 is used as reference landing gear. The main difference between the Bombardier 415 landing gear and the new design, is the

number of tires per strut. As each strut will feature four tires of which two tires are placed next to each other, a gap in the fuselage is required to store the inner tires. The main gear configuration will look similar to the one depicted in Figure 4-4a. To maintain a fuselage in which the cabin crew is able to walk from the front to the rear the internal structure of the main landing gear will be altered.

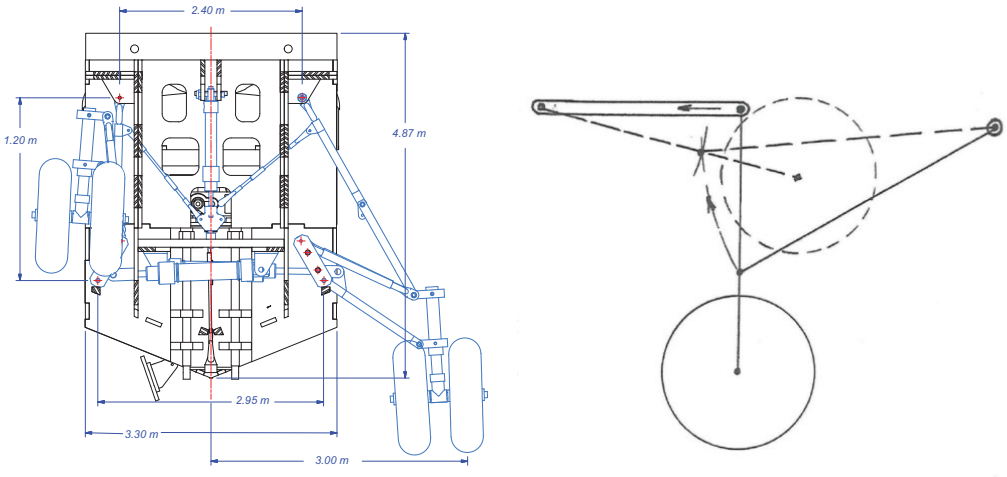

(a) Main Gear Configuration **(b) Nose Gear Configuration**

Figure 4-4: Landing Gear Configuration for Proposed Design

The nose gear will have a simple configuration as shown in Figure 4-4b. As soon as the aircraft is in the air, the nose gear will be retracted into the fuselage and two hatches will be used to seal the nose gear gap such that the aircraft can land on water. The nose gear will consist of two tires, which will be in twin configuration connected on both side of the strut.

4.5 Conclusion

The initital sizing of the landing gear has been done using of the method from Roskam [55]. The main gear will consist of two struts with each four tires. The main gear tires will have a diameter of 30 inch (76 cm) and width of 8 inch (20 cm). The shock absorber will have a length of 2.0 feet (61 cm) and a diameter of 0.63 feet (19 cm). The nose gear will consist of one strut with two tires. The diameter of the nose gear tire will be 8 inch (20 cm) and the width 8.5 inch (22 cm). The nose gear shock absorber will have a length of 2.2 feet (67 cm) and a diameter of 0.22 feet (7 cm).

Chapter 5

Hydrofoils

As water is a denser medium than air, maneuvering through it requires more energy compared to maneuvering through air. However, this denser medium can also be used to an advantage. By using hydrofoils, the aquatic handling characteristics of the aircraft can be altered dramatically. Using small control foils at the front of the aircraft, the maneuverability or stability can be greatly increased, although use of these is questionable for this design, that mainly skims over the water surface instead of actually submerging part of the hull.

Hydrofoils can also be used as lifting surfaces, as seen on the TU Delft Solar Boat in Figure 5-1. For this particular design, lifting surfaces are useful in improving take-off performance. Raising the main hull of the aircraft out of the water at low speeds, reduces drag forces considerably, allowing for greater acceleration and shorter takeoff distances from water. Using two hydrofoils, one near the main gear and a smaller one near the nose gear, the aircraft should be able to achieve a stable lift out of the water.

Figure 5-1: Example of Application of Hydrofoils on TU Delft Solar Boat [61]

During flight, the hydrofoils increase the profile drag. Also, once on a scooping run, the hydrofoils will actually prevent the aircraft from submerging the scoops. In addition, the landing procedure will require as much drag as possible in order to slow down as quickly as possible. The extra lift generated by the hydrofoils is minimal, rendering in-flight hydrofoils a disadvantage. Also, when operating from a land airfield, hydrofoils can prevent touchdown completely when they are made too large.

Concluding, as the hydrofoils are only advantageous when taking off from water, they should be retractable. This can be done using a screwing or tilting system, where the foils fit flush in the fuselage in order to minimize in-flight drag. Also, in order to lessen aircraft damage due to floating debris, it is opted to attach the hydrofoils through springed hinges, so they will yield upon impact without being damaged.

Chapter 6

Fuel System

In this chapter the position of the fuel tank and the size are estimated as this affects the initial sizing, the maximum range and the stability of the aircraft. Section 6.1 will discuss the positioning of the fuel tanks while Section 6.2 concerns with the actual size of the fuel tank.

6.1 Position

The position of the fuel tanks and the design of the fuel system have a strong correlation with the the structural layout of the wings and the center of gravity of the aircraft. Therefore, knowing the general geometry of the wing, a first order estimation for the available volume for the fuel tanks and system can be made.

The fuel tanks are placed within the empty space of the wings for three important reasons. Firstly, placing the fuel tanks in the wings causes wing bending relief, subsequently the structure can be designed lighter. Furthermore, the engines are commonly attached at the wing or placed closely to the wing. Placing the fuel tanks in the wings imposes the advantage of a smaller fuel system, thus shorter fuel ducts. Finally, as the wings are usually close to the center of gravity, the fuel consumption will not have a strong affect on the center of gravity range.

6.2 Sizing

The fuel tanks and fuel systems are placed within the wing-box, so therefore the sizes of the wing box are governing for the size of the fuel tanks. For a first order approximation the dimensions of the wing box are estimated using general guidelines, reference aircraft and the first approximated airfoil. The front spar of the wing-box is approximated at about 15% of the chord, the rear spar at 75%.[49] The height of the spars are approximated by the local thickness of the wing. Furthermore, it is given that approximately 4% of the fuel tank volume is required for the wing structure and fuel systems. Simultaneously 5% of the tank volume must be left empty to account for fuel expansion. As a third guideline it is given that the tanks extend up to approximately 85% of the wing span as the tip area of the wing is subjected to a higher risk of lightening strikes. Because the aircraft will fly above fire, a fire hazard foam needs to be placed inside the fuel tank which takes up about 2.5% of the fuel volume will be replaced by foam. Finally, 2.5 % of the volume is lost because the foam tends to absorb fuel [49]. When the aircraft is not carrying any payload, the amount of fuel that can be carried during flight can be increased as the wings are large enough to include this additional fuel.

Sloshing of fuel during an aircraft manoeuvres should be prevented as this can cause fluctuations of the center of gravity. The risk of liquid sloshing would be particularly high in the wing tanks and should reduced as much as possible. To prevent the fuel from sloshing during an aircraft manoeuvres anti-slosh baffles are used in the tank. The risk of significant liquid sloshing can also be reduced by using ribs.

For controlling the fuel in the tanks, two types of pump system, the transfer and boost pumps, are installed. The transfer pumps are used to control the fuel level in the tanks where the fuel is gathered before the engine is fed. Furthermore, these pumps can be used for pitch and roll trim reasons by balancing the fuel distribution in the tanks. The boost pumps feed the engine, not directly into the engine combustion chamber but to provide the fuel rate that is requested by the engines. Normally one booster pump is used to feed one engine. However, in case of malfunction of one feeding branch, the other must be able to supply fuel to both engines. [49]

Using these guidelines and Eq. 6-1 and 6-2, a first estimation for the available volume for the fuel tank and fuel systems can be made as is illustrated in Figure 6-1.

$$V_{ftw} = \frac{L}{3}(S_1 + S_2 + \sqrt{S_1 S_2}) \tag{6-1}$$

$$S_1 = \frac{1}{2}(h_{r1} + h_{r2})w_r \tag{6-2}$$

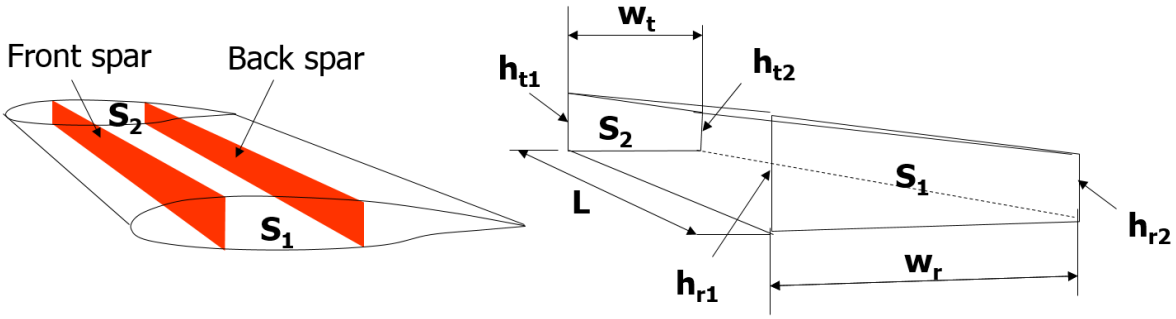

Figure 6-1: Method for Approximating Fuel Volume

The method yields a maximum volume of 13.2 m^3 per wing and the size of the fuel system will be approximately 0.53 m^3 per wing.

6.3 Conclusion

The position and design of the fuel system has a strong influence on the structural layout of the wings and center of gravity. As the wings of this aircraft quite large, a large volume is available to install the fuel tanks in. These large wings also result in the opportunity to increase the amount of fuel by reducing the payload and increasing that amount of weight of fuel in the fuel tanks, which increases the range of the aircraft. From a first estimation of the fuel sizing can be concluded that the maximum volume of the fuel tanks will be 28.5 m^3 and the fuel system requires 1.14 m^3 in the wing.

Chapter 7

Water Stability Devices

7.1 Basic Principles

For the lateral stability, the *center of buoyancy* (B) and the *center of gravity* (G) are important, as can be seen in Figure 7-1. The center of buoyancy is the center of the volume of water which the hull displaces, as shown in Figure 7-1a. With a shift in payload, the center of gravity changes. This generates a rotation of the hull compared to the load water level. The volume below the water level stays the same, however due to the shape of the hull, the center of buoyancy changes. When a line is drawn through the center of buoyancy B and center of gravity G for the first position and the second position, these lines will intersect in the *metacenter* (M), as depicted in Figure 7-1b. The shifting of the center of buoyancy in the second position generates a righting moment, the gravity pulling the hull down and the Buoyancy pushing the hull up, as shown in Figure 7-1c.

The distance between the center of gravity and the metacenter is called the metacentric height. For a good stability, the metacentric height should be as high as possible. The distance between the center of buoyancy and the metacenter can be determined through Eq. 7-1 where I refers to the longitudinal Moment of Inertia of the hull at the load water plane. The V refers to the underwater volume of the hull, which is equal to the weight of the flying boat. As the metacentric height should be as large as possible, the center of gravity should be as close to the water as possible. This is a difficult design problem because heavy subsystems, such as fuel storage, wing and engines, are designed high above the water, which will result in an negative metacentric height [1].

$$B.M. = \frac{I}{V} \tag{7-1}$$

7.2 Types of Stabilizers

Stabilizers are used to improve lateral stability. There are three types of stabilizers, floats mounted out along the wing on each side, stubs and twin hulls [42, 33].

Floats mounted out along the wings can be divided into wing tip floats and inboard wing floats, as can be seen in Figure 7-2. The inboard wing floats are a compromise between stubs and wing tip floats, as depicted in Figure 7-2a. The inboard wing floats are often larger and less aerodynamic than wing tip floats, as illustrated by Figure 7-2b. From a study conducted by the Air Ministry can be concluded that wing tip floats are 9% more efficient than inboard wing floats [32].

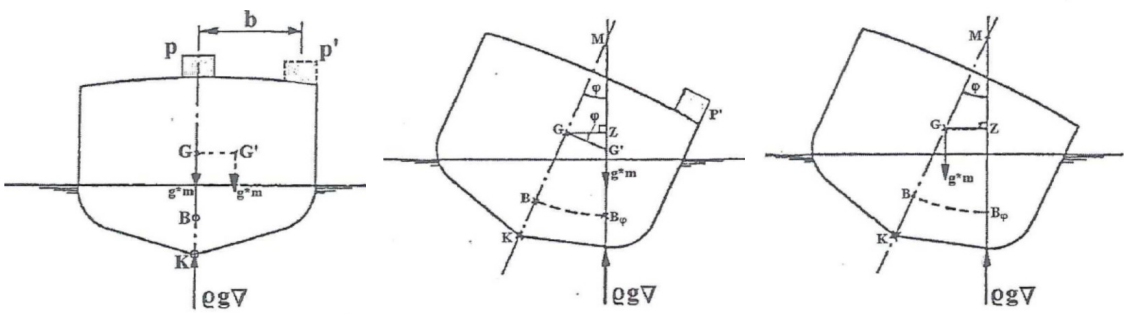

(a) Position 1 **(b) Position 2** **(c) Righting Moment**

Figure 7-1: Basics Lateral Stability [1]

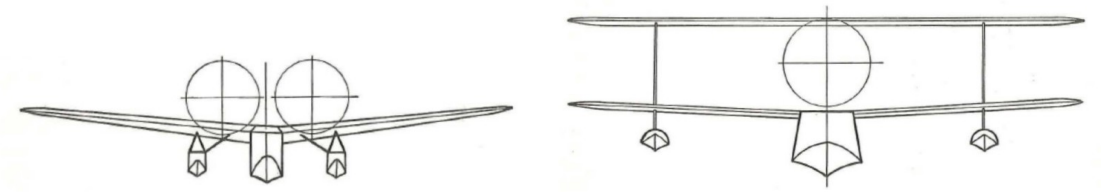

(a) Inboard Wing Floats **(b) Wing Tip Floats**

Figure 7-2: Types of Floats Mounted Along the Wing [33]

(a) Twin Hull **(b) Stubs Floats**

Figure 7-3: The Twin Hull and Stubs Floats [33]

The twin hull, shown in Figure 7-3a, provides good stability, yet spacing is required to avoid interference. The disadvantage of a twin hull is the increase of the control loads, as the maneuverability is reduced. A twin hull design also causes heavy wracking loads across the center section of the wing.

Stubs are stabilizers which are connected to the hull on each side at about the mid length of the fuselage, as explained in Figure 7-3b. Stubs provide greater seaworthiness, because they are less likely to take serious damage in rough water. Furthermore, stubs can be used as a stair to get inside the aircraft. Due to the rigidity of their attachment to the hull, the weight of the flying boat will increase and the water resistance will be greater than a hull of similar shape fitted with wing tip floats. From the Air Ministry study can be concluded that the efficiency of studs is 17% less compared to wing tip floats [32].

7.3 Placing of Floats

Vertical position of the stabilizing floats is important. With respect to the water line, the wing tip float should not be too close to the water. This will result in an increase in drag when the flying boat is accelerating. Also the wing tip float should not be mounted too high above the water line because the flying boat should be prevented from large tipping angles. The position is usually determined by assuming that the boat floats at its water line and then allows one degree of roll before the keel of the wing tip float touches the water [33].

7.4 Float Sizing

For the first estimation of the float sizing, the requirements set by The Air Ministry are used as described in Langley [33]. They require that the buoyancy of completely submerged wing tip floats induces a righting moment, $R.M.$, larger than the value obtained from Eq. 7-2, The values in this equation all are expressed in imperial units.

$$R.M. = R \cdot W(h + \sqrt[3]{W}) \sin(\theta) \tag{7-2}$$

The W in Eq. 7-2 refers to the Maximum Take-Off Weight (MTOW) of the aircraft in lbs. The h refers to the negative metacentric height of the hull in upright position in ft. Furtermore, θ represents the angle of heel or roll which is required to completely submerge a wing float. As the wing floats are almost completely submerged at an angle of 7°, angle θ is set to be 8°. Finally, the R is a coefficient depending on the value of W and is equal to 1.

Dividing Eq. 7-2 by the distance of the wing tip floats from the center line in feet, yields the displacement a single float given in pounds salt water. Using the density of salt water, this value can be convert to cubic feet. This volume converted to SI units gives a volume of 4.8 m^3.

The dimensions of the floats can vary widely, it is suggested that floats with a the short wide have a better performance [33]. The depth of the floats is assumed to be 7° when it is completely submerged. This gives an fixed depth of the floats when the distance of the floats from the center line is known. The length of the floats is assumed to be four times the width of the floats. This result in the wing top floats measuring $3.20 \times 0.80 \times 1.90$ meters.

7.5 Potential Innovations & Recommendations

Although the wing tip floats are sized as aerodynamically as possible, retracting during flight will reduce the overall drag of the aircraft. Furthermore, as the length of the floats is larger than the wingtip, foldable or inflatable floats should be designed. This will generate a smaller sized unit that can be stored in the wings during flight. During on-water operations, the wing tip floats will be unfolded or inflated to provide lateral stability. However, due to limited resources, no detailed design of such floats could be made and therefore it is recommend to conduct a more detailed assessment of such floats.

7.6 Conclusion

For a good lateral stability the metacentric height should be as high as possible. Due to the design of a flying boat, the center of gravity lies high above the water which makes the flying boat less stable. Stabilizers are used to improve the lateral stability of the aircraft while on the water. From a study conducted by the Air Ministry can be concluded that the wing tip floats are the most effective stabilizers [32]. From the first estimation can be concluded that the dimensions of the floats will be $3.20 \times 0.80 \times 1.90$ meters and they will be placed 18 meters from the center line.

Chapter 8

Choice of Retardant Types

Heat and wind induced by wildfires will result premature evaporation of water when dropped over the wildfire location. Furthermore, wind causes drift and a decreased drop accuracy. Therefore, research has been done in order to use the water more efficiently. In 1955 was found that adding sodium calcium borate to the mixture, will hold the retardant together such that more retardant will reach the wildfire. However, as this mixing agent was found to be corrosive and soil-sterilizing, other retardants were developed in the 1960's. These were fertilizer-based retardants containing diammonium phosphate, ammonium phosphate and ammonium sulfate. The current long-term retardant still partly consists of these ammonia-based compounds. Besides these long-term retardants, gels and foams are being used in aerial firefighting. This chapter will discuss the advantages and disadvantages of each of these fire-suppression types [58].

8.1 Long-Term Retardants

Long-term retardants consists of approximately 85 to 90 percent water, while the remainder of the product consists of about 60 to 90 percent ammonia compounds such as ammonia sulfate or ammonia polyphosphates (both inorganic fertilizers). Other ingredients are thickeners (generally guar gum or attupulgite clay), dyes and corrosion inhibitors.

Using a long-term retardant has several advantages over using water as fire retardant. Firstly, although the water serves as cooling, the long-term retardant does not depend on water for effectiveness. Even after losing its moisture, the retardant remains effective. Secondly, in the presence of heat, the long-term retardant reacts with the fuel (vegetation) which reduces its flammability since retardant-treated cellulose decomposes into non-flammable gases, carbon and water vapor. Finally, the additives in the retardant will improve drop characteristics (e.g improved dropping accuracy), lower the corrosive behavior of the retardant and will reduce the retardant's impact on the environment

On the other hand, long-term retardants cannot not yet be mixed during flight and need to be loaded on the ground. This does not make it as attractive to scooping aircraft as, when using this type of fire suppressant, the scooping capabilities of the aircraft cannot be used.

8.2 Water Enhancers

Water enhancers, or gels, thickens water and have been used since the 1960's in aerial firefighting. Firstly, gels allow water to even stick on vertical surfaces, preventing runoffs. Secondly, gels reduce premature evaporation of the suppressant, provide improved insulation and increases the heat absorbing capacity of the suppressant. As a result, the suppressant has a longer effectiveness (10 to 40 minutes under fire conditions) compared to water. Finally, the gel results in enhanced dropping characteristics.

On the other hand, gels are only effective when water is present. Hence, in contrary to the long-term retardant, as soon as the water is evaporated, the gel will lose its effectiveness. Furthermore, the gel treated suppressant can only be loaded on the ground and therefore may not be attractive to a scooping aircraft.

8.3 Class A Foams

Class A foams where developed in the 1980's for fighting wildfires and are currently used on scoopers such as the Bombardier 415. Class A foam concentrates are a mixture of foaming and wetting agents. These foam concentrates are generally non-hazardous and non-flammable and are often used in small concentration in fire suppressants (typically 0.1 to 1 percent).

Since the Class A foams are wetting agents, they lower the water surface tension. As untreated water has a high water surface tension, as soon a water is dropped on the surface of a fuel (e.g. wood), the water tends to roll off the surface without penetrating the fuel and therefore does not absorb a lot of heat or cool the fire. A lower water surface tension enables the water to penetrate the burning surface and thereby effectively absorbing heat and cooling the fire (up to three times more heat than plain water). As a result, less water is required to contain the same wildfire. Secondly, the bubbles induced by the foam concentrate increase insulation and slow down premature evaporation of the suppressant. Finally, premixing foam concentrate with plain water is relatively simple and inexpensive method of creating an effective suppressant.

On the other hand, Class A foams may be corrosive to some metals and may speed up the deterioration of some types of sealing material. Furthermore, due to the fact that the foam has various toxicities with respect to fish and due to sensitivity of aquatic habitats, spilling high concentrated foam suppressant into bodies of water must be avoided.

8.4 Conclusion

Class A foam suppressants are suitable for scoopers as it can be mixed during flight. Therefore it has been opted to incorporate a foam system into the design of the next generation water bomber. According to Edward Goldberg, every type of suppressant is suitable for a different specific mission. Long-term retardant and Class A foam suppressants seem to capable of handling numerous firefighting missions.

In order to be flexible with respect to what types of firefighting missions can be performed, it has been decided that the water bomber should also be able to carry long-term retardant suppressants which should be carried in the tanks that are generally destined for water. As the long-term fire retardant suppressant is only available at the airport, the water bomber will probably perform less drops per hour. Therefore, it may be opted to perform a single long-term fire retardant suppressant drop, after which the crew starts dropping regular foam suppressant. However, the long-term retardant and foam may reacts with each other. Therefore, it is important that the system is "cleaned" first by means of scooping a load of water and dropping this load without adding class A foam. After this, the crew can safely switch to dropping regular Class A foam suppressants. Furthermore, the water tanks should be coated in order to prevent the tanks from corroding due to the corrosive behavior of the long-term retardant suppressant.

However, being able to drop both types of suppressant greatly improves versatility of the water bomber and will make it more attractive to potential customers.

Chapter 9

Retardant Intake System

The water bomber will feature a retardant intake system in order to refill its water tanks during scooping. This section will discuss what this intake system consists of and what problems have to be anticipated for.

9.1 Dimension of Inlet Probes

A conventional and simple way of refilling is by means of inlet probes, as depicted in Figure 9-1. These probes will be dropped into the water during the scooping motion and water will be directed to the water tanks.

Figure 9-1: Example of Water Inlet Probe of the Bombardier 415 [9]

The number and size of inlet probes and its dimensions depend the scooping distance s_{scoop}, scooping velocity V_{scoop} and the water tank volume V_{water}. The required inlet probe cross-sectional area A_{probe} required to refill the retardant within a specified scooping distance, can be determined through Eq. 9-1 to 9-3.

$$t_{scoop} = \frac{s_{scoop}}{V_{scoop}} \tag{9-1}$$

In Eq. 9-1, the scooping velocity V_{scoop} is set to 55 $^{m}/_{s}$ since the stall speed in take-off configuration is 48.7 $^{m}/_{s}$, such that a sufficient safety margin is provided. Furthermore, the scooping distance s_{scoop} has been set to 60 percent of the take-off field length, yielding a s_{scoop} of 600 meters.

$$\dot{m} = \frac{V_{water}}{t_{scoop}} \tag{9-2}$$

The mass flow $\dot{m}$ that needs to be fed into the water tanks during the scooping motion, can be determined through Eq. 9-2 where the water tank volume V_{water} is specified to 15 m^3.

$$A_{probe} = \frac{\dot{m}}{\rho_{water} V_{scoop}} \tag{9-3}$$

According to Eq. 9-3 the required probe cross-sectional area is 250 cm^2. In order to fill water tanks which are located on both sides of the fuselage, two probes will be installed with an height of 8.2 cm and a width of 15.2 cm.

Chapter 10

Release Systems

The firefighting capabilities of the aircraft is what sets it apart from conventional aircraft. An important characteristic therefore is the ability to release retardant on target. This section provides a description of the retardant tank and the release system.

10.1 Design Approach

Initially, the design approach with respect to the release system was to set a desired drop pattern and based on this pattern design the water tank and release system. This approach was further underpinned as it turned out that different drop patterns are desired in various situations. However, an article by Liu and Kim on water mist fire suppression systems the stated: "As water mist does not behave like a true gaseous agent, it is difficult to establish the critical concentration of water droplets to extinguish a fire. The amount of mist reaching the fire is determined by many factors. These include the spray momentum and angle, shielding of the fuel, fire size, ventilation conditions and compartment geometry" [31]. Therefore, the new approach is to design the water tank and release system conforming to the aircraft and subsequently tune it to produce a practical drop pattern.

10.2 Retardant Tank Design

Scooping and releasing the retardant will cause the center of gravity of the entire aircraft to shift, influencing the longitudinal stability. Preferably, the center of gravity of the water tank is placed underneath the center of gravity of the aircraft in order to limit the shift in center of gravity. However, this is not possible since the retardant tank had to be designed around the landing gear. As a result, the tank is designed such that the center of gravity of the retardant body lies within a range for the aircraft to be stable at all times. From a lateral stability point of view, the tank had to be of symmetrical shape. On top of that, the tank is located as low as possible in the aircraft to lower the center of gravity which is preferable for stability reasons.

As the landing gear obstructed the retardant tank, the tank had to be moved forward and is formed around space occupied by the landing gear to keep the tank as low as possible. Furthermore, as the the tank is limited in length for stability, the height of the retardant tank had to be increased to provide the necessary volume for the retardant.

The aircraft is designed for a retardant payload of 15.00 m^3. However, due to thermal expansion and structures within the tank and foam additive, the tank volume is increased by 6% resulting in a volume of 15.96 m^3. The tank will have a maximum height of 2.13 meters, leaving 2.75 meters of space to the top of the fuselage. The floor is positioned at 1.47 meters from the bottom of the hull which is done such that the door thresholds are 10 cm high, enabling easier to loading of the aircraft. As a result, the water tank rises 66 cm above the floor, leaving sufficient height above the tank to stand up straight. A couple of stairs are used to aid personnel crossing over the tank. The part of the tank perturbing the floor can be removed in the case the tank is not needed, allowing a leveled floor throughout the fuselage.

The scoop duct is directly connected to the top of the water tank, where the water enters the tank, filling the tanks during the scooping. Water in excess of 15 m^3 will leave the aircraft through vents connected between top of the tank and the sides of the fuselage, in order to prevent the tank from overloading. On top of that, the vents are used to allow air into the tanks during releasing.

The tank is divided into four subtanks as can be seen in Figure 10-1. Anti-slosh baffles with holes are placed in the tanks to prevent longitudinal sloshing. Each tank can be opened independently. Tank opening combinations can be formed to produce different drop patterns and allow for more efficient firefighting. The opening of release is computer controlled as the computer can determine which tanks to

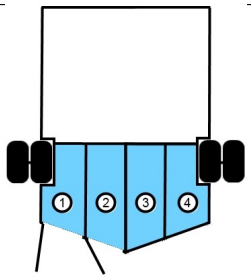

Figure 10-1: Sketch of Four Tanks with Release Door 1 and 2 Opened

open for a desired drop pattern whilst maintaining stability. Depending on the combination, a maximum moment of 55 kNm will be produced in the lateral direction. Testing and simulations should determine whether the aircraft can handle this moment. The outer tanks will have a slightly smaller volume than the inner tanks as they make way for the wheels of the landing gear.

Mixing of a foam or a gel with the water are options for increased firefighting effectiveness. The foam additive will be injected and mixed in the tank. Once the release doors are opened and the mixture is exposed to air, the foam mixture will start foaming.

10.3 Release System and Drop Pattern

The most important aspect of the release system is the drop pattern. The drop pattern is the mark on the ground created by the dropped water. This is largely dependent on the mass flow of retardant through the exits of the tanks and the area of the exits. Other main factors influencing the drop pattern are:

- Relative wind
- Height
- Dispersion of retardant
- Dropping velocity
- Dimension of the fire
- Evaporation of the retardant

Mass flow depends on the exit velocity of the retardant and the area of the release doors. As the system is based on gravity and the pressure difference above and below the tank is negligible, the release door areas are the only variable. Although the exit area is fixed, by varying the angle of the release doors, the effective exit areas can be changed in order to regulate to a certain extent.

Each tank has its own release door covering nearly entire bottom of the retardant tank. The doors are attached through hinges and are opened and closed by two hydraulic actuators per tank. The actuators are computer controlled in order to drop the retardant as accurately as possible. However, as the drop pattern is dependent on a large number of factors, it is difficult to model the actual drop pattern. Assumptions have to be made for a good approximation which include:

- The water jet stays constant until the break-up location
- At the break up location the water jet breaks up instantly
- The aircraft has a constant dropping velocity
- Inviscid, incompressible, irrotational and steady vertical flow in the tank

In general, the drop pattern is approximated as an ellipse where the water layer gets thicker towards the center of the ellipse, as depicted in Figure 10-2. Furthermore, results of the drop patterns at different release door configurations are shown in Table 10-1. These results provide a good approximation of the drop patterns the aircraft, however real testing should be done in order to produce the actual drop characteristics. One of the tests that is recommended test, is the cup-and-grid method which will be discussed in chapter 5.1.7.

Table 10-1: Drop Pattern Data for Different Release Configurations

Configuration	Pattern Length L [m]	Pattern Width λ [m]	Max. Retardant Height h [m]
1x inner tank	144	64	22.6
1x outer tank	149	68	25.9
1x inner tank and 1x outer tank	201	93	17.1
2x inner tank and 1x outer tank	241	113	13.7
1x inner tank and 2x outer tank	245	115	14.3
All tanks	278	132	12.1

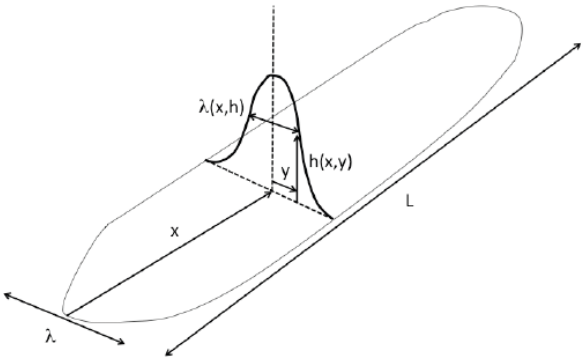

Figure 10-2: Diagram of Drop Pattern with Symbols Explained in Table 10-1

10.4 Water Cannon

The ability to choose between a concentrated release and a large coverage release, will distinguish this design from current aerial firefighters. Installing a water cannon enables the aircraft to perform concentrated releases which allows precision and accurate aerial firefighting, for example in urban areas.

Current water cannons are accurate up to a range of approximately 85 meters at ground level [64]. In order to maximize exposure time to the fire for the use of the water cannon, the aircraft has to circle the wildfire location. However, a preliminary assessment of circling the wildfire has shown that this is not possible with a bearable load factor and range combination. As a result, the aircraft will have to fly an arc around the fire with a reasonable load factor and stay in range as long as possible. This maneuver is explained in Figure 10-3 for a load factor n of 1.5 (or a 45 ° bank angle), a jet range of 85 meters and an aircraft release velocity of 54.8 $\frac{m}{s}$. This set of data yields a time frame of about 3.1 seconds per pass during which a total amount of 284.2 liters of water can be ejected.

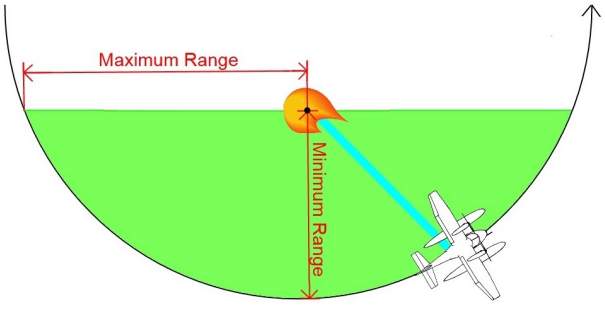

Figure 10-3: Extinguishing Maneuver

When using a water cannon such as the Unifire Force 80, the reaction force of the jet can be up to 5000 N where the support must be able to withstand 25 kN. Furthermore, the exiting mass flow will be

around 5500 $\frac{L}{min}$ [65].

As the IFEX 3000 system is an excellent extinguisher for firefighting operations on the ground, it was assessed to what extent this system can be used in an areial firefighting vehicle. This assessment showed that this system requires significantly less water than conventional water cannons [2]. However, the IFEX 3000 only ejects water by means of impulse shots lasting several milliseconds, after which the systems requires 6 seconds to reload. Even though the gun has a 60 m range, the system is most effective between 10 and 40 m [3]. Furthermore, a single impulse shot releases a maximum of 12 liters. Hence, the system can only eject 12 liters of water every 6 seconds. Concluding, the IFEX 3000 systems is not suited for aerial firefighting purposes as it can only deliver small quantities of water during each pass. Furthermore, the limited range of the systems poses restrictions on the operation capabilities of the aircraft.

The major advantages of a water cannon are its accuracy and precision. Precision is achieved using a concentrated jet of water while accuracy is achieved by a computer controlled aiming system. The nozzle of the cannon should have 360° degrees horizontal movement and 180° vertical movement which allows it to aim in every direction.

However, several complications arise with the use of a water cannon. Several factors that may prevent extinguishant from reaching the wildfire include:

- Wind
- Dispersion of water jet
- Banking of aircraft
- Wing obstruction

The wind will cause the jet of water to drift away from the target which could be compensated by means of a computer that uses of a camera or wind measurement systems to anticipate for the wind direction and velocity. Using such computer, the nozzle of the water cannon will be re-calibrated constantly throughout the operating of the cannon. On the other hand, the effect of gusts can not be accounted for.

Dispersion of the jet stream due to the drag of the water droplets also effects the precision of the extinguishing. A wide spread is not necessarily undesirable as it will be better at cooling the target, but if the dispersion is too large it will no longer extinguish the fire. On top of that, the water cannon's purpose is concentrated extinguishing.

As the aircraft will be banking when extinguishing, it should be taken into account that the long wings of the aircraft stay clear of ground objects. As a result, the aircraft may have to extinguish from a greater altitude, which in turn increases the distance to the target adversely affecting accuracy and precision. In certain situations the proximity of ground obstacles disallows banking flights, having to resolve to symmetrical flight instead whilst releasing. This in turn decreases exposure time to the target.

Another challenge whilst banking is that the wing might get in the line of "firing" which can be resolved by taking it into account in the computer controlled aiming system. The jet stream can be turned off when the wing is in the way of the target. The downside of this is that it will decrease the amount of time water can be released.

10.4.1 Double Water Cannon Configuration

A double water cannon configuration where a cannon is mounted on each side of the fuselage is recommended since the orientation with respect to the wildfire location of one of the two nozzles is usually better than that of a single nozzle, during a pass around the fire. On top of that, the double water configuration does not need the nozzle heads to have an extended distance from the fuselage, therefore having smaller moments on the aircraft during releasing. Installing a second nozzle will not significantly increase the overall weight as the nozzle itself weighs around 20 kg and the controlling equipment even less.

10.5 Foam Mixing System

As explained in Chapter 8, a Class A foam additive is used to enhance to properties of the retardant. As a result, a foam concentrate tanks and a foam mixing system should be installed. The foam concentrate

will be used in relative small concentrations up to 1 percent, hence the foam concentrate tanks can be designed relatively small. As it has been argued that the aircraft should be able to perform a large drops before returning to base, two 500 liter foam concentrate tanks are installed enabling the aircraft to perform 10 to 15 drops foam retardant drops.

Figure 10-4: Example of a Foam Mixing System [24]

In order to generate a foam retardant, the foam additive should be pressurized and subsequently be injected in the water flow at a predetermined concentration. For this, a foam mixing systems as depicted in Figure 10-4.

10.6 Conclusion

Having the capability to perform of large coverage releases as well as concentrated releases, is a major advantage over current aerial firefighting vehicles. The design can therefore be used in almost every aerial firefighting mission. However, the water cannon is rather impractical and its effectiveness limited. Bombing the target with large amounts of extinguishant through the release door will probably be more effective in most cases. Therefore including the water cannon option is not recommended, but definitely does not hurt having it included.

Chapter 11

Electrical Block Diagram

As the next generation water bombers features a large number of electrical systems, their mutual relations and interactions need to be determined through an *Electrical Block Diagram*. The Electrical Block Diagram for the next generation water bomber consists of four main parts, being the power system, Visual Flight Rules (VFR) system, Instrument Flight Rules (IFR) system and the miscellaneous systems. These four different systems and their interactions will be discussed in this chapter.

11.1 Power System

The electrical system is powered by the primary power generating system, which consists of the engine generators, as explained in Figure 11-1. The engines are started using energy from this battery. The battery and APU are part of the secondary power generating system which starts working in case the primary power generating system fails. The power generated by the primary power generating system is subsequently used for all the components described in the remainder of the electrical block diagram.

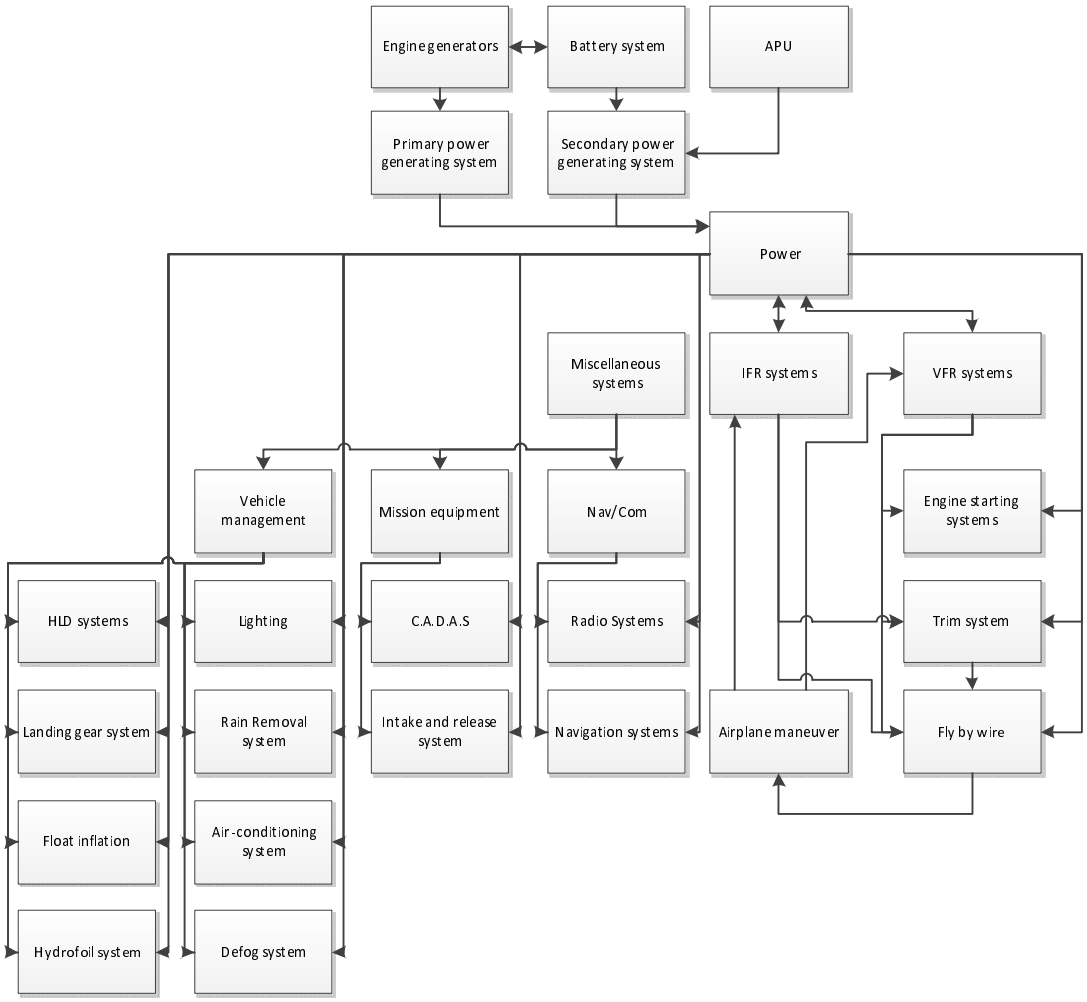

Figure 11-1: Electrical Block Diagram

11.2 VFR & IFR System

The main function of the airplane is to fight fire, which requires a lot of flying without autopilot. Therefore it is decided that the main way of flying will be VFR flying. The VFR system includes the steering components and basic flight instruments which include the altimeter, airspeed indicator, turn and bank indicator, vertical speed indicator, artificial horizon and a heading indicator.

The VFR system provides input to the power systems, engine starting, trim system whereas the pilot provides inputs for the steering components and the trim system through a fly-by-wire system. As a result of the inputs by the pilots, the aircraft starts maneuvering in response to outputs of the trim and fly-by-wire input. The aircraft maneuvers are a direct result of changes to the ailerons, elevators, control canards and rudder position. The aircraft maneuvers are subsequently used as input for the VFR and IFR system.

The IFR system, on the other hand, is an additional system which is only used while flying at night or in bad weather conditions. The IFR system provides inputs to the power, trim system and the fly-by wire-system.

11.3 Miscellaneous Systems

The miscellaneous systems are divided into three subcategories, being Navigation and Communication (Nav/Com), Mission Equipment and Vehicle Management. The radio system and navigation system are considered part of the Nav/Com category. The CADAS and the intake and release systems are considered part of the mission equipment. The vehicle management is divided in two columns where the left column refers to systems systems that are attached to the outside of the aircraft and are only used during specific stages of the flight. Examples are the High-Lift Devices (HLD's) and landing gear.

11.4 Conclusion

The electrical bock diagram consist of four main blocks, being Power, VFR System, IFR System and Miscellaneous Systems. The Miscellaneous Systems are further divided into Nav/Com Systems, Mission Equipment and Vehicle Management Systems. Each individual system requires power to operate, yet not all systems perform primary functions for the aircraft maneuvers.

Part IV

Design Performance Analysis

Chapter 1

Control & Stability

During flight the aircraft should remain stable as well as controllable. This chapter will discuss the approach that has been used to assess the stability and controllability of the aircraft.

1.1 Scissor Plot

Besides using data of reference aircraft, another method, called a "scissor plot", is used to size the tailplane for stability and controllability. A scissor plot can be used to determine a required $\frac{S_h}{S}$ for a desired center of gravity range. The scissor shape of the plot is determined by plotting two equations as described by Eq. 1-1 and 1-2. Eq. 1-1 relates to the most aft position of the center of gravity for which the aircraft is stable. Eq. 1-2 on the other hand, is used to determine the most forward position of the center of gravity for which the aircraft remains controllable.

$$x_{cg} = x_{ac} - \frac{C_{m_{ac}}}{C_{L_{A-h}}} + \frac{C_{L_h}}{C_{L_{A-h}}} \frac{S_h l_h}{S\bar{c}} \left(\frac{V_h}{V}\right)^2 \tag{1-1}$$

$$x_{cg} = x_{ac} + \frac{C_{L_{\alpha_h}}}{C_{L_\alpha}} \left(1 - \frac{d\varepsilon}{d\alpha}\right) \frac{S_h l_h}{S\bar{c}} \left(\frac{V_h}{V}\right)^2 \tag{1-2}$$

Most of the coefficients mentioned in these equations are already established. However, several parameters such as l_h and $\frac{S_h}{S}$ are yet to be determined as they greatly depend on the size and relative position of the (horizontal) tailplane. During the iteration process, the scissor plot has been used to verify whether the overall configuration of the aircraft meets the controllability and stability requirements. Furthermore, if these requirements were not met, the parameters mentioned above could be altered such that the design is stable and controllable for the center of gravity range considered.

The method described above only focuses on the *longitudinal* controllability and stability. Hence, the *lateral* controllability and stability is not considered. A search for a first-order estimation method for assessing the lateral controllability and stability was held but, unfortunately, no first-order methods were readily available to assess this. Since the amphibious aircraft operates close to the water during potential strong crosswinds, the lateral stability is of importance and therefore should be tested in later stages of the design process.

1.2 Results

Plotting Eq. 1-1 and 1-2 for different center of gravity locations yields a scissor plot depicted in Figure 1-1 in which the design point is indicated. This design point is based on a desired center of gravity range which in turn requires a certain $\frac{S_h}{S}$ to remain stable as well as controllable.

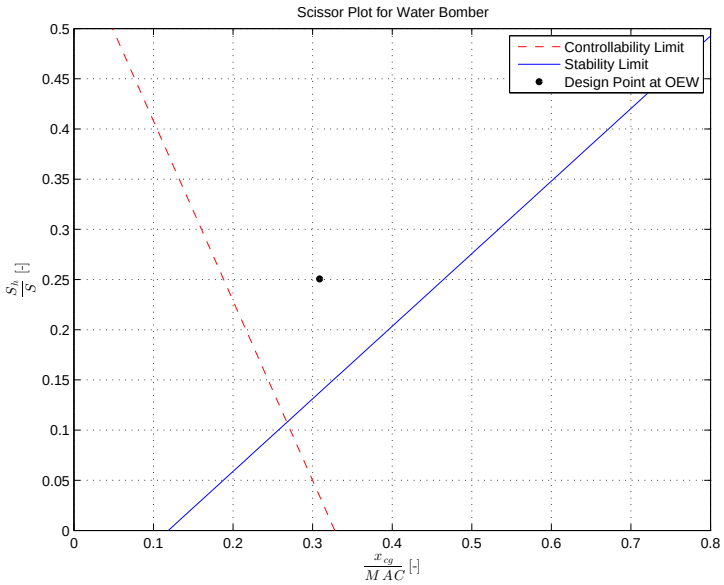

Figure 1-1: A Scissor Plot of the Proposed Design of a Waterbomber

Chapter 2

Flight Performance

As the installed power and wing area are determined, the performance envelope of the aircraft can be established. Several key performance envelopes have been selected to be evaluated, based on the mission requirements. These are a *maneuver envelope*, *payload-range diagram*, *several altitude diagrams* and a *takeoff field length diagram*. The flight conditions have been taken at sea level if else unspecified for steady flights.

2.1 Maneuver Envelope

As the client imposed a minimum and maximum allowable loading of $n_{min} = -2$ and $n_{max} = 5$, the maneuver envelope can be established based on CS-25 and calculated limits, as depicted in Figure 2-1.

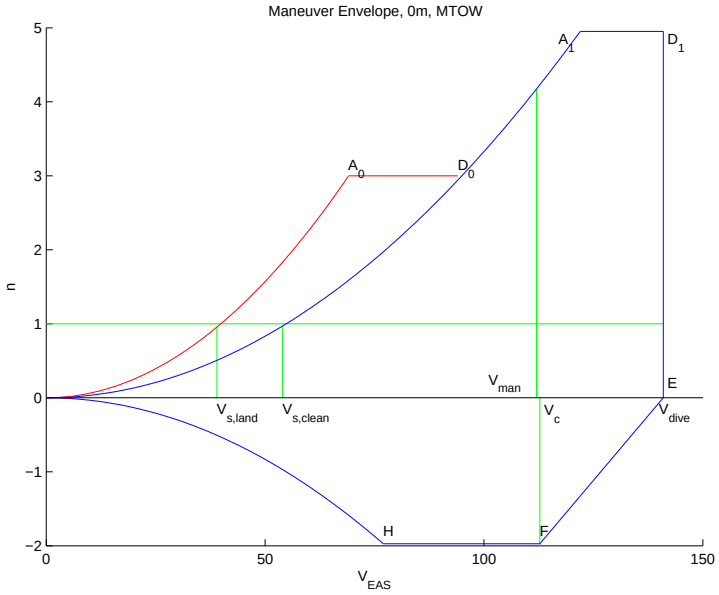

Figure 2-1: Maneuver Envelope of Proposed Design

The area inscribed by curves O-A_0-D_0 represents the envelope in landing configuration during which wing area is increased due to the extension of the slotted flaps. Furthermore, the lift coefficient C_L is increased to 2.6. The other inscribed area represents clean configuration flight.

$$n = \frac{1}{2}\frac{\rho_0 V^2 C_{L,\max}}{\left(W/S\right)} \tag{2-1}$$

Curves O-A_0 and O-A_1 are determined through Eq. 2-1, whereas curve O-H is constructed using Eq. 2-1 in a negative sense. Line A_1-D_1 is determined by the maximum load factor requirement, whilst line H-F is set by the minimum load factor requirement. The maximum load factor to which A_0-D_0 is sized depends on the force the actuators of the flap system can handle. For now, this limit has been set at 3g.

Line D_1-E is set by the maximum airspeed, the dive speed, which is a minimum of $0.8 \cdot V_c$ according to CS-25 regulations. The stall speeds $V_{s,land}$ and $V_{s,clean}$ are the speeds where the curves A-D intersect a load factor of 1, as indicated by the respective lines in Figure 2-1. CS-25 specifies a maneuver speed V_{man} equal to the location of A_1 or to the cruise speed V_c, whichever is less. In this design, $V_{man} = V_c$.

2.2 Payload-Range Diagram

The water bomber should only be able to fight fires within a certain radius of its base, but should also be able to perform transport or ferry flights over a specified distance. These range-related requirements are imposed by the customer. Furthermore, the customer specified a certain payload that should be hauled over these ranges. In order to relate payload to range, a Payload-Range diagram will be constructed.

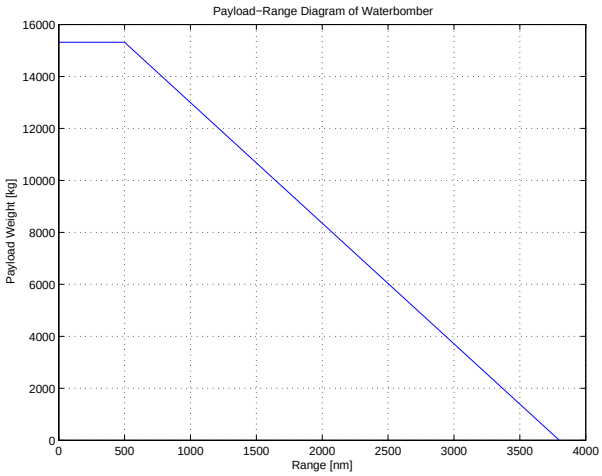

Figure 2-2: Payload-Range Diagram of Proposed Design

The water bomber should be able to fly 500 nautical miles with maximum payload and has been designed such that it meets this performance requirement, as can be seen in the Payload-Range Diagram depicted in Figure 2-2. Furthermore, the design features a large and relatively thick wing which yields a large fuel capacity. In case all payload is removed from the aircraft, the fuel tanks can be filled with 23,718 kilograms with fuel capacity to spare. In this configuration, a absolute maximum range or *ferry range* of 3,800 nautical miles can be reached which exceeds the requirement of 1,000 nautical miles of zero payload range as imposed by the client.

2.3 Climb Gradient

The climb gradient varies with several factors as described in Chapter 1. As the weight of the aircraft is set to its Maximum Take-Off Weight (MTOW), has a fixed wing area and installed power and its lift and drag coefficients do not vary, the attainable climb gradient only varies with air density. This in theory implies a different maximum climb gradient at different altitudes as shown in Figure 2-3. In this figure the attainable climb gradient has been plotted against the altitude, ranging from sea level to the determined cruise altitude of 4,000 meters. This data may be useful for operations in areas which vary in altitude and where the pilots require certain climb gradients to steer clear of any obstacles.

2.4 Stall Speed

The stall speed is determined using Eq. 2-2 which already has been introduced in Chapter 1. Again, as only the density varies, the aircraft exhibits a different stall speed at different altitudes.

$$L = \frac{1}{2} C_L \rho V^2 S \rightarrow V = \sqrt{\frac{2W}{C_L \rho S}} \tag{2-2}$$

These variances in stall speed have been plotted in Figure 2-4 for MTOW and Zero Payload Weight (ZPLW) respectively. This data is useful to pilots as it allows a check of whether a certain drop speed can be achieved.

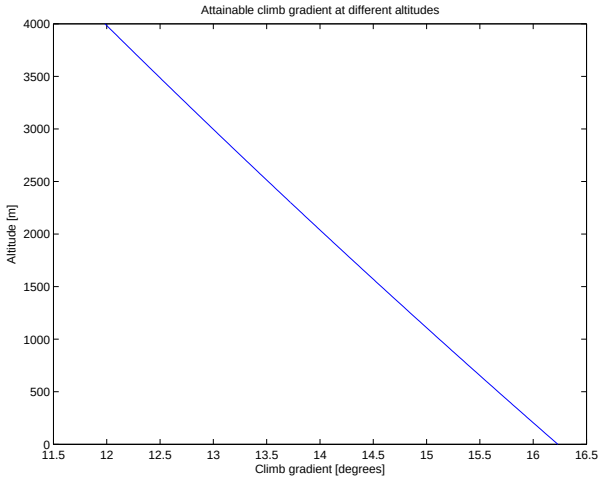

Figure 2-3: Attainable Climb Gradient at Different Altitudes

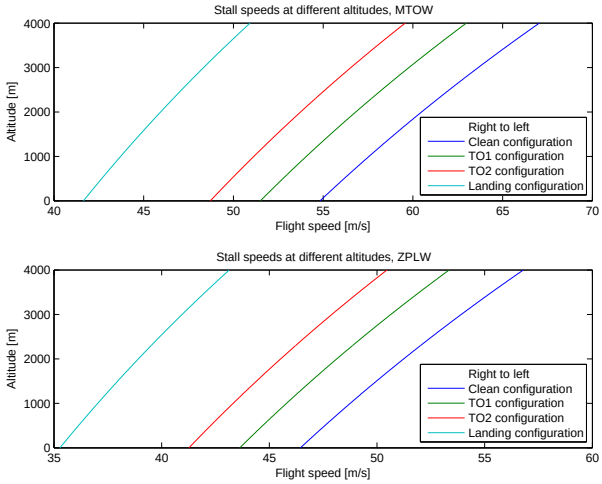

Figure 2-4: Stall Speeds at Different Altitudes for Different Weights

2.5 Cruise Speed

The allowable cruise speed depends on several factors. Available power sets an upper speed limit, whereas the required lift coefficient results in a lower limit. The upper limit can be determined through Eq. 2-3, where the available power has been determined in Chapter 2.

$$P_{req} = C_D \bar{q} S V \tag{2-3}$$

Through Eq. 2-2, a required C_L was calculated for given airspeeds. which was subsequently plotted, together with $C_{L,max}$, in Figure 2-5. As can be seen from this figure, the achievable steady flight cruise speed lies between a lower limit of 67 $\frac{\text{m}}{\text{s}}$ and an upper limit of 113 $\frac{\text{m}}{\text{s}}$.

2.6 Takeoff Performance

The aircraft was sized to climb gradient, taking into account the takeoff weight could be adjusted in order to require a maximum field length of 1,000 meters. In Figure 2-6, the actual required takeoff length is given for takeoff from both land as well as water by the solid and dashed lines respectively. Furthermore, as a distinction has been made between normal operation and One-Engine-Inoperative (OEI) scenarios, represented by the blue and red graphs respectively.

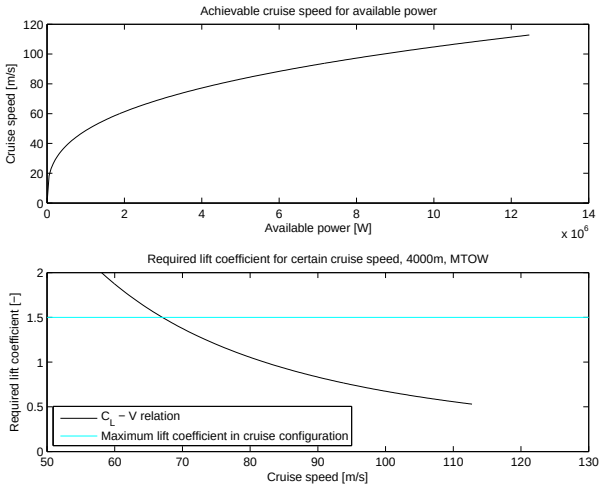

Figure 2-5: Achievable Cruise Speed at Different Altitudes

As the MTOW was reduced during the iterative Class II sizing, the design is overdesigned with respect to the takeoff field lengths. This causes the required OEI field length to actually lie beneath the set field length requirement of 1,000 meters. In fact, 4,400 kilograms of fuel, payload or a combination thereof, can still be carried along on takeoff. Mission-wise, this is very favorable as in case the aircraft lands at a small airfield and an engine happens to fail, with no quick replacement at site, it can actually fly out a little over 500 kilometers in order to land at a more accessible airfield.

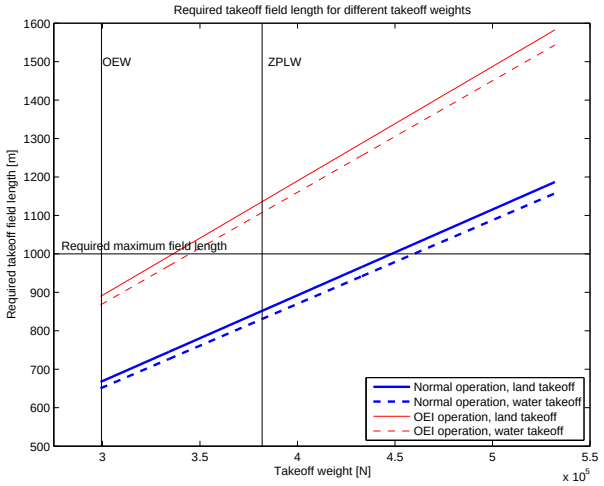

Figure 2-6: Required Take-Off Field Length for Different Take-Off Weights

Chapter 3

Risk Analysis

Risk management is done in order to identify and minimize the risks that may occur during the design, production and operational life of the product. The process of risk management consists of several steps. At first the risks are identified, followed by risk assessment in which the risks are classified based on their magnitude and likelihood. After these steps, the costs and benefits are determined for the risk mitigation strategies with a risk analysis. Eventually, the risk handling takes place where it is decided which mitigation options will be applied.

3.1 Risk Identification and Assessment

In the risk identification process, the risks that may occur during each process are classified in three main categories; Technical risks, schedule risks and cost risks. Most risks however, are interdependent and will affect more than one category. Then the technical risk assessment follows where possible risks are categorized according to their severity and likelihood. The risks are categorized to determine those that have the most severe consequences and are most likely to occur. The risks have been evaluated for four different time spans in which they might occur.

Risks during design and development phase

1. Aircraft is not developed within planned time
    - 1.1 Change in customer requirements
    - 1.2 Unconventional design choices that elongate the design process
2. Aircraft mass exceeds scheduled budget
3. Not enough funding to develop the aircraft
4. Development costs exceed the scheduled budget
    - 4.1 Unconventional materials are used/need to be developed
    - 4.2 Not enough reference vehicles for design choice to make proper budgets

Risks during manufacturing process

5. Aircraft is not produced on time
    - 5.1 Increased production time due to lack of experience
    - 5.2 Suppliers are unable to deliver on time
    - 5.3 Subcontractors are unable to deliver in time
    - 5.4 Design is altered
    - 5.5 Manufacturing/assembling of a part appears to be impractical and methods needs to be altered
6. Materials costs rise
7. Labour costs rise

Risks during Operations

8. Aircraft failure due to technical issues
9. Failure to Release fire retardant
10. Intake of fire retardant is not possible

10.1 Harsh landing environment

10.2 No retardant available

11. Aircraft failure due to mid-air collision
12. Large turnaround time

12.1 Intake of fire retardant takes long

13. Delay caused by transportation of vehicle to location of fire
14. Fuel prices rise
15. Retardant prices rise

Continuous Risks

16. Deviating currency exchange rate
17. Inaccurate dropping of retardant

3.2 Risks and Risk Map

A Risk Map is a visualization of the severity of all potential risks versus the likelihood of occurrence. On the x-axis, the risks are ranked from being very unlikely to an almost certain risk. On the y-axis, the scores are ranked starting at a negligible consequence of the risk up to catastrophic consequences. The lower left side portrays the risks that are not likely to occur and are of a small impact when they occur, the risks placed in the upper right corner are very likely to occur and their impact can be critical or even catastrophic. The risks that are placed in the upper right corner are risks which need to be minimized or preferably be removed first. This can be achieved through a risk mitigation strategy. The risks have been assessed and are shown in Figure 3-1.

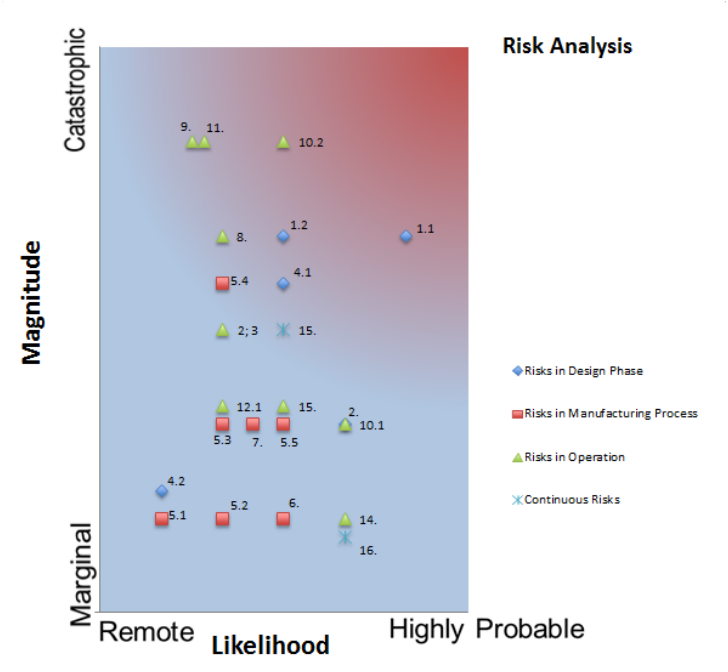

Figure 3-1: Risk Map

3.2.1 Top Risks

The risks which are most likely and are:

1. Aircraft cannot be developed with the planned time due to a change in customer requirements
2. Intake of fire retardant is not possible because no retardant is available

3.3 Risk Mitigation

Risk mitigation is performed to minimize or eliminate potential technical risks. To minimize the risks, the risk should become less likely and of a smaller impact. In the risk map, the risks should shift downward and to the left. Two types of measures are used for risk mitigation: pre-development measures and change in the design. The change in the design can be done by choosing a different technology, changing the way of operating or decreasing the probability of the risk by increasing the margins or redundancy.

The first risk which is appointed as a top risk is the event of delay in the development or production due to a change in the requirements of the customer. The likelihood of this risk is minimized by regular meetings with the client where the requirements and design options are discussed in detail. It fully depends on the change in the requirements of the customer how big the effects are on the design process, it can be tried to minimize the consequences by regularly consulting the client.

Top Risk number 2 is quite likely, yet difficult to mitigate as its magnitude can not be reduced. However, this risk can be made less likely by changing the design of the aircraft. As the aircraft can take in multiple types of retardant, for example liquids and solids, the likelihood of the risk will be reduced. However, the choice was made for using water with additives. If the design of the aircraft is adjusted such that it is able to take in fluids at harsh or very small locations the risk will be made less likely.

Chapter 4

Sensitivity Analysis

The final design is based on a large number of design parameters, many of which have been based on mathematical, numerical or statistical models. This chapter covers the sensitivity of these parameters with respect to the inputs of the models. These inputs may vary along with possible changes in the mission profile and requirements. Therefore, possible causes for changes in these mission characteristics are also identified.

4.1 Payload Weight

The payload weight is one of the main driving requirements for the design, and thus of major interest to analyze how the models for the sizing of the aircraft would react to a change in the payload weight. The weight estimation model is the model which is most influenced by this change. Reducing the capacity of 15,318 kilograms with 10% to 13,786 kilograms results in a reduction in Empty Weight of 495 kilograms to 30,030 kilograms. Therefore, the Take-off Weight is reduced to 52,216 kilograms. This Take-Off Weight serves as an input for many other system elements, such as the wing sizing, landing gear sizing and powerplant sizing. Changes in these parameters will, in turn, influence the Empty and Take-off Weight of the design. Concluding, a change in the payload weight parameter will require a full reiteration of the design process and will therefore significantly influence the resulting design.

4.2 Load Factor

The aircraft design has also been based on maneuvering envelope requirements of -2g to 5g. In order for the aircraft to sustain these load factors, the structural design of the wing must be optimized for these load factors. Skin thickness, stringer layout and rib layout all have to be adjusted in order to make the wing structure suitable for these maneuvers. Changes in these parameters will also influence the wing weight, but this wing weight is only relevant for the detailed design phase, and is therefore not of relevance to the used Class II models. Therefore, no major changes will occur in the outputs of the used models.

4.3 Range Requirements

Range is directly related to the amount of fuel that is carried on board. Since the fuel tanks have a volume of 28.3 m^3, it is possible to reach Maximum Take-Off Weight at zero payload by just filling the fuel tanks. In this case, 23,400 kilograms of fuel can be taken on board, which results in an achieved range of 3800 nautical miles. This range far exceeds the requirement of 1500 nautical miles at zero payload, and thus an increase in this requirement will not likely influence the design. However, the current full payload range requirement of 500 nautical miles is only achieved by a small margin at 8,400 kilograms of fuel. If this requirement were to increase, several redesign steps could be taken:

- The fuel weight could be increased, which would increase the Maximum Take-Off Weight, and thus would influence the wing and tail sizing as well as the engine sizing.
- The aerodynamic efficiency could be improved, which would reduce the cruise phase power requirement. This will however require significant redevelopment cost and time, with an indeterminate success rate.
- The cruise speed could be decreased. At lower speeds the power requirement is less, which will result in increased endurance and range.

4.4 Stall Speed

A change in the stall speed requirement can be handled in several ways. A reduction in stall speed will also decrease the wing loading. When the wing shape parameters are kept constant, this implies that a larger wing surface is required. The opposite is true for a stall speed increase. These changes in the wing will significantly influence the sizing of other systems through weight, control and stability and dimensional changes.

A lower stall speed can also be achieved by improving the performance of high lift devices, or by choosing a different airfoil. Both will influence the drag characteristics of the aircraft, which in turn could influence the fuel weight requirement and the powerplant design.

4.5 Climb Gradient

The climb gradient is the driving factor for the required power, as shown in Table 1-4. Therefore, a change in climb gradient could significantly influence the powerplant design. Changing the climb gradient requirement from 15 to 10 degrees will result in a power requirement change from 11.6 MW to 8.7 MW. Because of this large reduction, the climb gradient will not be the critical factor since the take-off power requirement is higher at 9.6 MW. For this requirement, it could be possible to use fewer engines or lighter engines, which will lower the Take-Off Weight. Subsequently, it might be worthwhile to redesign the remainder of the systems according to this new take-off weight.

On the other hand, when the climb gradient requirement is increased from 15 to 20 degrees the power requirement changes from 11.6 MW to 14.2 MW. To accommodate this, heavier, more powerful engines are needed or more engines need to be installed. This will also influence the take-off weight and therefore the design of other systems.

4.6 Take-Off Performance

The take-off distance requirement is one of the most critical mission requirements for the aircraft. With the current design, the aircraft can only take off within 1000 meters if the aircraft is not fully loaded with payload. If the requirement is changed that full payload must be taken on board during a take-off within 1000 meters, the power requirement increases to 12.8 MW, as shown in Table 1-4. This will affect the system sizing in the same way as with the climb gradient increase.

A change in the take-off distance itself, will also change the take-off power requirement. A significant decrease in take-off distance could make the take-off power requirement more critical than the climb gradient power requirement. When the take-off distance increases, the power required will still be determined by the climb gradient and thus will not be affected.

Chapter 5

Verification Process

Verification is an essential stap in the design process of an aircraft system, since it enables the designers to identify and rectify mistakes before they cause unoverseeable problems. This chapter describes the steps that have and will be taken in order to ensure that the aircraft design is both optimal and compliant to the requirements. First, the verification process of the models that have been created and used for the sizing of the aircraft is discussed, followed by a verification plan that is made to ensure whether the aircraft meets all the set requirements.

5.1 Verification of Numerical and Computational Models

In the design phase it is important to make sure that every model works correctly. One incorrect model can influence others models that otherwise would work correctly. Therefore, it is important that both the numerical as well as the computational models are verified. The verification described in this chapter is performed after the construction of the model and will, when possible, be checked with analytically obtained data.

5.1.1 Numerical Model for Hull Skin Thickness Calculations

This calculation consists of multiple parts. First the hull is shaped, after which the required thickness of all panels and stringers are calculated. Simultaneously, the required volume is calculated for the optimization of the aircraft. In all the parts the metric system has been consistently used and no mistakes were made during the process. However, a singularity was detected. The deadrise angle should not be 90 degrees, as a deadrise angle of 90 degrees is impossible since the fuselage would in this case be a thin line. Furthermore, there should be a minimum ratio between the draft and width of the fuselage, otherwise the pre-allocated shape cannot be defined and the program shows an error. However, this problem singularity will not occur as long as realistic values are selected, such that the program can still be used.

This numerical model has assumed two constants, being the gravitational acceleration and the density of water. The gravitational acceleration has been verified in Chapter 4 of Part I. The water density depends of the temperature, with a temperature between 0 and 30 degrees Celsius, the density varies between 999 $\frac{\text{kg}}{\text{m}^3}$ and 996 $\frac{\text{kg}}{\text{m}^3}$. The chosen constant is said to be 1000$\frac{kg}{m^3}$, inducing an error smaller than 1%, which is acceptable in the first steps of the design. Also, the numerical result of the volume has been compared with the analytically obtained results as shown in Table 5-1.

Table 5-1: Numerical and Analytical Results of the Hull Volume Below the Waterline

Calculated Volume below Water Surface	
Numerical Results [m^3]	64.52
Analytical Results [m^3]	66.19
Error [%]	2.52

A difference of 2.52% seems high, but the analytical method has an additional assumptions, being that the height of the wetted length at the nose decreases linearly. Therefore, the error of 2.5% is acceptable. The verification has shown that the model was legit and data can be used in further steps of the design process.

5.1.2 Model for Optimization of the Aircraft

This model is divided into a couple of sub-models. Since these are already analytical models, it is not possible to check with analytical results. The model itself iterates the different subsystems, during which some errors can occur if the dimensions of the fuselage exceed realistic values. Therefore the model can only be used in a particular range of values.

Model for Wing Dimensions
As a large number of equations for the wing part were defined in imperial units, most input data had to be converted to imperial data and converted back to metric units after the calculations had been performed. This is a potential bottleneck, as errors could be made during the conversions between the two unit systems. Therefore, the numerical model has been checked thoroughly for convesion errors, and fortunately no errors have been made. The conversion factors have been applied consistently and units have been covered. Only one constant is used, being the gravity constant which is set to 9.81 $\frac{\mathrm{m}}{\mathrm{s}^2}$. This is a reasonable assumption, since the aircraft flies at a low altitude and the reduction in gravity is negligible and gravity at sea level is generally assumed to be 9.81 $\frac{\mathrm{m}}{\mathrm{s}^2}$.

Model for Fuselage Dimensions
The model that calculates the dimensions of the fuselage was easily verified, since it contained no constants or singularities. Within this model a significant amount of data was combined. The units were clearly covered and the calculated values were realistic and therefore the model is valid.

Model for Longitudinal Stability & Control Calculation
The numerical model of control & stability has newly defined constants. There are some singularities, but only if the input values are unrealistic such as for example a wing sweep angle of 90 degrees and a fuselage width of 0 meters. However, a problem arises with respect to the angle ϕ, which is the angle between the zero lift line of the wing and the line connecting the aerodynamic center of the wing and horizontal tail. When ϕ exceeds 30 degrees, the model produces imaginary numbers. However, La Rocca stated that the downwash is zero if $\phi \geq 30 degrees$, therefore an if-statement is implemented to avoid the imaginary numbers [15]. Furthermore the equations used are valid for subsonic flow, aircraft flying at supersonic speed will have a different model. Finally, the units are covered and the model makes consistent use of the metric system. The model showed realistic values and is declared ready for further use.

Model forWeight and Center of Gravity Calculation
The weight and center of gravity calculations are based on other calculated data and assumptions of Roskam Part V [52]. Except the assumed constants from Roskam, which are assumed to be correct, no other constants have been assumed. No new constants have been established and the units are covered. During the calculations the imperial and metric system have been applied, but did not cause a problem as no conversions have been forgotten. Finally, the calculated data were realistic and therefore it has been declared safe for further usage.

Model of Tail Calculations
The method used to determine the tail size is based on the method described in Roskam [53]. The model uses data of reference aircraft and no new constants have been assumed. The units are all covered and only the metric system is used. Therefore, no errors could be made in conversion of data. Finally, as no singularities were found and the data was realistic, the model can be used.

5.1.3 Numerical model of Wing Structure

The numerical model of the wing structure calculates the stresses in the wingbox. In the MATLAB code, only metric units are used, avoiding confusing the units and introducing errors. No singularities were found in the program, however the program is not valid for every type of wingbox, as for example the code needs to be modified when a sweep angle is introduced. This numerical model is further verified using a analytical method. Table 5-2 presents the result of both methods.
The results show that the maximum difference between the analytical method and the numerical method is 5.44%. The Moment of Inertia and normal stress have the most significant error. The error between

Table 5-2: The Numerical and Analytical Results of the Wing Calculations

	Moment of Inertia at the Root [m^4]	Shear force at the Root [MN]	Bending Moment at the Root [$MN \cdot m$]	Maximum Normal Stress at the Root [MPa]
Numerical Results	0.0683	1.3116	11.086	78.82
Analytical Results	0.0712	1.3129	10.965	83.11
Error %	4.07	0.1	1.1	5.44

analytical and numerical normal stress is caused by the error in the Moment of Inertia which is the result of using a boom method. The boom method uses a simplification which states that the Moment of Inertia around around its own axis is equal to zero.

5.1.4 Model for Landing Gear Dimensions

This model is an analytical model that calculates the dimensions of the landing gear system, the type of tires and the structure load it has to bear. The model uses assumptions listed in Roskam [55]. These may differ from the actual value because they may be out of date, considering the age of the Roskam book. Unfortunately, as Roskam uses imperial units, the input data had to be converted to the metric units. Furthermore, the model has been checked at singularities. There are only singularities if the shock absorber does not absorb any energy and the fuselage has a length of zero, both very unrealistic, which implies that the system works fine within the required range.

5.1.5 Model for Sizing the Intake System and Fuel Tank

This model sizes the intake system, using the area of the probes and the corresponding scoop length. It also calculates the size of the fuel tanks and location with respect to the CG. The model is already analytical so the results cannot be checked with an analytical model. The density of water has now been assumed to be 1020 $\frac{kg}{m^3}$ since seawater is heavier and therefore the worst case scenario has been accounted for. Furthermore, two other constants have been assumed, being the constant for gravity and the density of air that already have been verified. The script uses only metric units and they are correctly covered, so no mistakes could be made during conversion. At last the model was checked for singularities. This check revealed that, in the operational range, no singularities have occurred.

5.1.6 Model for Propeller Sizing

This model calculates the size of the propeller by using the required power of the engine determined by the weight-to-power ratio. During the calculations, a imperial unit has been used once, which is immediately conversed to avoid complications. Thereafter, the model was checked on singularities and fortunately none were found.

5.1.7 Performance Calculation Model

Another model that was made is one that checks the different performance characteristics of the aircraft. No new constants have been added in the model and there are no singularities for realistic values. The units are all in the metric system and covered in the model. As the achieved data was realistic and complied with the requirements set at the start of the project, the model can be for further design phases.

5.2 Verification of Compliance to Design Requirements

Once a design or a concept has been established, it is essential that it is demonstrated that the design complies with the requirements that were defined when the design phase was initiated. This section

discusses several methodologies which can be used to verify the compliance of the next generation water bomber design to the initial requirements.

5.2.1 Testing

Testing the actual product under representative conditions provides direct proof of whether the design is capable of performing in the manner which was set by the requirements. In order to be able to perform tests, a prototype must be produced which will be used to demonstrate its operational capabilities. The prototype's operational capabilities should either meet or exceed the proposed requirements. The following criteria are to be evaluated during the prototype tests:

- **Demonstrated design dive speed** - It must be shown that the structural components of the aircraft design are strong enough to withstand the loads imposed by flying at the design dive speed of 270 knots. After this demonstration, the aircraft should be thoroughly inspected for cracks and other structural deteriorations. If no significant damage is found, the aircraft passes the test. For more reliability, this test should be repeated.
- **Range** - The aircraft must demonstrate that it can safely fly the ranges which were set in the requirements. The range requirements were defined to be at least 500 nautical miles at full payload and at least 1500 nautical miles without payload. Thus, these distances should be flown accordingly using the prototype, with a reserve margin of 10% added to the range requirements. If the aircraft design achieves this range at cruise altitude under unfavourable conditions, the requirement is met.
- **Take-off Performance** - The aircraft is designed and required to be able to take-off from land within 1000 meters while taking 4400 kilograms of payload. This capability should be demonstrated with the prototype. Secondly, the aircraft design is such that take-offs from water are also possible within 1000 meters, however in this scenario the aircraft is carrying slightly more payload at 4500 kilograms. This is also a proposed demonstration opportunity for the prototype. A second important test is to verify the take-off performance during a One-Engine-Inoperative (OEI) situation. The design is such that the 1000 meter limit is still achieved at a takeoff weight of 34,500 kilograms, which implies that around 4000 kilograms of fuel can still be taken on board. This scenario should also be tested using the prototype.
- **Climb Rate** - The prototype will demonstrate that it can achieve a climb rate steeper than 15 degrees at Maximum Take-Off Weight at 500 meters altitude.
- **Maneuvering Envelope** -It will be demonstrated that the aircraft is capable of performing maneuvers from -2g to 5g.
- **Scooping Performance** - The scooping operation should be performed with the prototype on several types of representative water bodies under different sea states.
- **Retardant Release Performance** - The effectiveness of the dropping method of the fire retardant is a crucial aspect of the design, and therefore it should be tested how the release system performs. This test is however not straightforward to perform, since it covers not only an analysis of the aircraft, but also requires the covered ground to be analyzed on how the retardant influences it. A method for testing the retardant dropping performance has been used by the USDA Forest service called the 'Cup-and-Grid Method', which involves installing a pre-determined grid of cups onto a testing area [60]. The aircraft releases the retardant over the test area, and after the drop the cups are weighed and analyzed to determine how the retardant has spreaded over the area. An example of such a test being performed is shown in Figure 5-1. This methodology will also be used when testing the retardant release performance of the next generation water bomber design.

5.2.2 Analysis

Not all requirements, especially for certification, need to be demonstrated on an actual part or full-scale test. A simple analysis can often form a much cheaper and quicker way to show compliance. This mainly goes for dimensions and part structural capabilities, which can be quickly evaluated using simple calculations and safety factors. Collecting data on the performance of the aircraft, and analyzing it, can provide a clear insight on the performance of aspects that vary significantly per flight. An important

Figure 5-1: The Dromader Spray Aircraft Dropping Water Over a Test Grid [60]

purpose for using analysis methods is for obtaining data on the performance of the retardant dropping operation.

5.2.3 Simulation

It is often impractical, unsafe or physically impossible to establish certain environments and situations in which the aircraft is to be tested. For these cases, proof that the aircraft complies to the requirements is obtained using simulation. For example, the aircraft's ability to sustain extreme weather during both flying and scooping operations is something that should be tested using simulation models. Also, simulating various aircraft failures and analyzing how the design and pilots cope with them is a major step in ensuring the airworthiness of the design.

5.2.4 Similarities

In the design of the aircraft, many design choices are based on available references. These references are vital for showing the feasibility of certain design options, and provide a good basis for the verification of the product.

5.2.5 Documentation Review

The documentation of the design contains many statements on every design parameter, which can be used to obtain whether a certain design requirement is met. The retardant capacity is one example of a parameter that can be verified by inspecting the design documentation.

Chapter 6

Compliance Matrix

The compliance matrix shows the imposed requirements by the customer and the values that are reached by the design. All requirements imposed by the customer have been met, the value at which the requirements have been met can be found in the compliance matrix and for a more detailed explanation it is recommended to consult the reference chapters given in the matrix.

Table 6-1: Compliance Matrix

Requirement	Value Imposed by Customer	Requirement Met?	Reached Value	Chapter
Volume Load Capacity	> 15 m^3	Yes	15.96 m^3	10 (Part III)
Take-off Runway Length	< 1000 m	Yes	At zero fuel weight and zero payload weight: 679 m. At filled fuel weight and zero payload: 860 m. At maximum fuel weight and 7.5 tons payload: 1000 m	2 (Part IV)
Climb Gradient	> 15 degrees at MTOW	Yes	At sea level and MTOW: 15.6 degrees	2 (Part IV)
Zero Payload Range	> 1500 nm	Yes	3800 nm	2 (Part IV)
Fill Payload Range	> 500 nm	Yes	500 nm	2 (Part IV)
Stall Speed	< 100 knots at MTOW	Yes	41.6 m/s (80.9 knots) at sea level in landing configuration at MTOW, 54.9 m/s (106.7 knots) at clean configuration at MTOW	2 (Part IV)
Manoeuvring Envelope	-2g to 5g	Yes	Structural Wing Integrity can handle: -2g to 5g & Flight Envelope: -2g to 5g	2 (Part IV), 4 (Part II)
Crew Members	2 pilots and 2 (other) crew members	Yes	2 pilots and 2 ground crew members	7 (Part II), 6 (Part I)
Water Reloading Possibilities	On land and on Water	Yes	On land and on Water	8 (Part I), 4 (Part III), 6 (Part II)
Ground Support Equipment	Must be carried on board	Yes	Is carried on board	5 (Part I) and 7 (Part II)
Cost Efficiency	More cost efficient than current aircraft	Yes	Despite high purchase costs the aircraft will be more cost efficient due to its long lifespan and high dropping accuracy compared with current aircraft	5 (Part V)
Multifunctionality	Aircraft must be multifunctional	Yes	Aircraft can perform fire fighting missions, cargo-, mail-, passenger transport flights	8 (Part I)
Flexibility	Carry other loads	Yes	Retardant tanks can be partially removed to transport other loads	8 (Part I) and 10 (Part III)

Part V

Recommendations for Future Design

Chapter 1

Project Design & Development Logic

In order to get from the results of this Design Synthesis Exercise project to an actual production line result, a large number of tasks are left to be completed. In this chapter, a roadmap of the tasks is given. The chronological planning for this path is presented in Chapter 2.

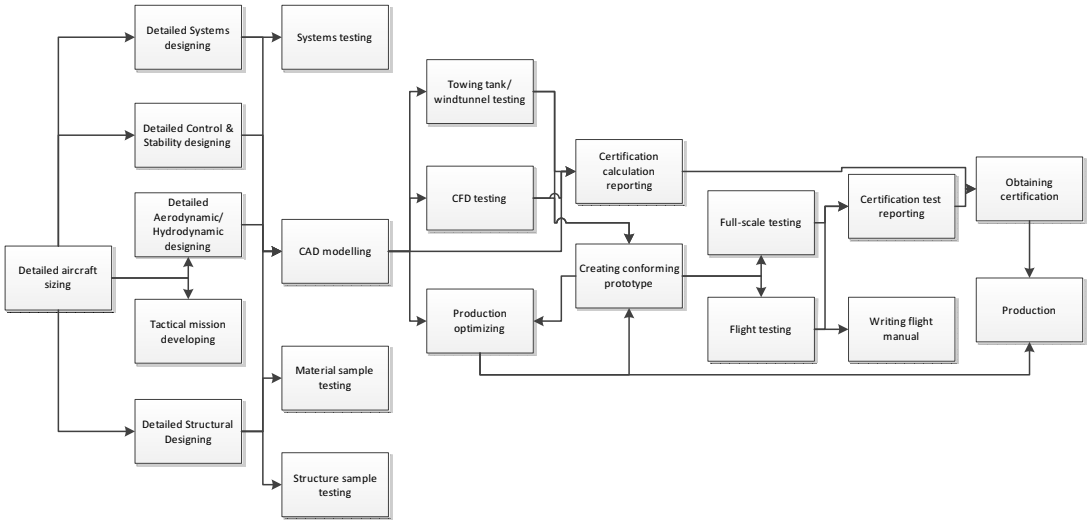

Figure 1-1: The Project Design & Development Flowchart

Figure 1-1 shows a flowchart containing most major steps in this process. This process can be divided into four major parts, being the detailed design, testing, production preparation and certification.

1.1 Design Phase

The design phase starts with a more detailed and thorough aircraft sizing, followed by the detailed design of the components structure, hydro- and aerodynamics, control & stability properties and detailed design of sub-systems. Also, the tactical mission development is initiated in this phase. As much as possible, the CAD modelling will be done during the design of the parts, which should ensure that all parts fit together.

1.2 Testing Phase

During the design phase, the first tests take place. This concerns sample material and structure tests, as well as system tests to aid their development. During and after the aero- and hydrodynamic design, tests should be carried out in a CFD environment, but also in windtunnels and towing tanks to check the stability and handling characteristics and to verify and validate the CFD calculations.

Also, as soon as the airplane handling characteristics can be estimated, simulator tests can be done with pilots to ensure the aircraft is flyable under the expected high-stress circumstances. After a conforming prototype has been created, full-scale testing can be done as well as flight testing. This should be planned such that destructive testing is done last, in order to get the most out of the prototype. During flight testing, the flight manual will also be written.

1.3 Production Preparation

Preparation for actual production should already start during the design phase. After the functional and structural design of each part, the parts should immediately be optimized for production in order to reduce production costs. Also, a production facility should be acquired and outfitted, and near design completion, parts and suppliers need to be sourced and contracted. For the supply chain, a logistics concept should have been made by this point. Also, the necessary tooling should be designed and built or otherwise acquired.

Another important step, though not shown in the diagram, is the start of sales and marketing. Although a launch customer, the Red Cross, is present, a significantly higher number of customers need to be found to make the production profitable. As aircraft are usually bought before they are produced, sales already need to be made before production is started.

1.4 Certification

During the design phase, preparation for the certification reports on the compliance with regulations may already commence. Compliance may be demonstrated through calculations. During case compliance has to be shown by means of testing, those certification reports are made whilst the tests are done. In all phases of certification, thorough contact should be maintained with the regulatory authorities. To ensure effective cooperation, this contact should take place between strong, dedicated and small delegations of both authorities and designer.

Chapter 2

Project Gantt Chart

In the Gantt chart, as shown in Figure 2-1 to 2-5, the logical order of the activities after the DSE project are shown on a time scale. As the design process is an iterative process and the design is constantly subjected to changes, the Gantt chart serves as an initial estimate for the remainder of the design process. When certain activities turn out to require more time than expected, the consequences on later stages of the project can be immediately identified. By means of this Gantt Chart the activities that are at risk of becoming bottlenecks are identified in an early phase, such that measures can be taken in order to to deliver the aircraft to the client in time. The design team may than decide about to reschedule certain activities, adjust the number of resources or decide on the number of people involved.

Figure 2-1: The Project Timeline

During the DSE project, many design choices are made and the design iterations were performed to optimize for the weight. The results of this iteration process are presented in Chapter 7. The main sizing is performed and a general layout is established. However, the design is far from finished and still many iterations have to be performed, parts and systems to be designed and detailed analyses are to be made. The post-DSE phase is divided in four phases. Right after the DSE project a start must will be made on the Detailed Design Phase, described in Figure 2-2. After approximately 10 months, the Testing Phase can commence which is estimated to take approximately 2.5 years. Due to the iterative nature of an aircraft design process, the different phases as indicated in Figure 2-1 are performed simultaneously. As a result, the end of the Detailed Design Phase is executed synchronously to the Testing Phase. As soon as most tests are completed, the Pre-Production Phase is initiated during which, among others, the tooling method and contact with suppliers should be established. Hereafter it is started with the certification procedures.

During the Detailed Design phase, as explained in Figure 2-2, the different components of the design are designed in more detail. This phase is initiated with a detailed analysis of the different mission phases using the current parameters and aircraft characteristics. This enables the design team to determine how the aircraft is currently designed with respect to all the different mission profiles. Using this information and the results obtained up to this point in the design process, a detailed design of the aircraft can be made. All components of the aircraft will be designed during this phase, ranging from a detailed design of the wing (line 5) to the design of the hydraulics (line 32). In total, the duration of this phase is estimated at 18 months. However, it is expected that the design team will be resizing and adjusting the design well after these 18 months. These activities are included within the the later design phases. For instance the windtunnel testing (line 40), will give results that are used during the design of the control surfaces and high lift devices (line 19). The redesign of the high lift devices due to the windtunnel test is therefore incorporated within the timespan for windtunnel testing.

During the Testing Phase, scale models of the aircraft are subjected to rigorous testing in order to validate whether the numerically obtained analysis and characteristics comply with the desired behavior of the aircraft. For instance, scale tests have to be performed to determine the consequences of the impact with water on the structure of the aircraft. Furthermore, using special high speed towing tank tests, the effect of the water on the structure and the behavior of the aircraft on the water can be analyzed. Since tests do not always present the results that are expected through the numerical analysis, it is expected that during this phase several design alterations have to be made. As these tests are the first encounter of the design with reality, delays and unsolvable design issues might be encountered.

ID	Task Name	Duration
1	**Detailed Design Phase**	**18 months**
2	*Mission developing*	*3 months*
3	Deep analysis of mission phases	3 months
4	*Detailed Aircraft sizing*	*8 months*
5	Wing sizing	4 months
6	Tail sizing	2 months
7	Power sizing	3 months
8	Fuselage sizing	4 months
9	Subsystem distribution	4 months
10	*Detailed Structural Design*	*12 months*
11	Hull structure	5 months
12	Fuselage structure	7 months
13	Wing structure	8 months
14	Tail structure	7 months
15	*Aerodynamics*	*12 months*
16	Panel method simulations	6 months
17	CFD simulation	8 months
18	Propellor-Wing Interaction	6 months
19	Control Surfaces & High lift Devices	6 months
20	Control and Stability	8 months
21	Flight Dynamical Behaviour	6 months
22	*Hydrodynamics*	*7 months*
23	Panel method simulations	4 months
24	CFD simulation	4 months
25	Hull design	4 months
26	Hydrofoil design	3 months
27	Control and Stability	6 months
28	*System Design*	*9 months*
29	Instrumentation selection	3 months
30	Equipment selection	3 months
31	Electrical system design	5 months
32	Hydraulic system design	5 months
33	Pleumatic system design	5 months
34	Fly-by-wire Design	6 months
35	Wiring	4 months
36	System Integration	9 months
37	CAD modelling	9 months

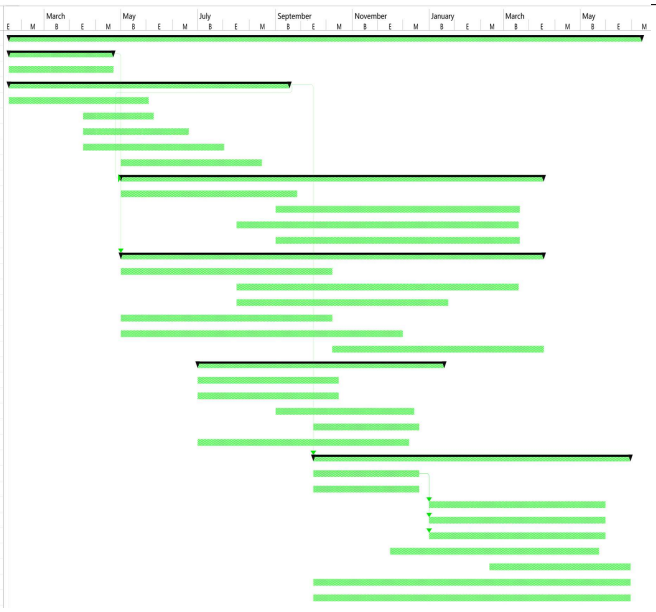

Figure 2-2: The Gantt Chart for Detailed Design Phase

ID	Task Name	Duration	Start
38	**Testing Phase**	**30 months**	**1 November 2014**
39	Material and structure testing	12 months	1 November 2014
40	Windtunnel testing	12 months	1 November 2014
41	Towing tank testing	6 months	1 November 2014
42	Water impact testing	6 months	1 November 2014
43	Extinguishing system Testing	4 months	1 April 2015
44	System Testing	18 months	1 April 2015
45	Prototype testing	18 months	1 October 2015
46	Pilot Simulator testing	12 months	1 March 2016

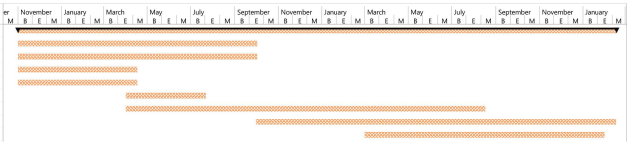

Figure 2-3: The Gantt Chart for Testing Phase

ID	Task Name	Duration	Start
47	**Production Preperation**	**36 months**	**1 June 2016**
48	Design optimization for production	24 months	1 June 2016
49	Tooling method decision	6 months	1 June 2016
50	Tooling equiment choice	6 months	1 November 2016
51	Supplier parts	12 months	1 June 2016
52	Contracting suppliers	18 months	1 November 2016
53	Location of production	12 months	1 May 2017
54	Supplier logistics	12 months	1 April 2018
55	Prototype production	18 months	1 October 2017

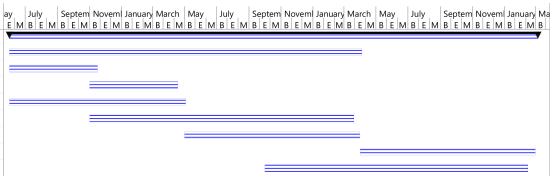

Figure 2-4: The Gantt Chart for Production Preparation

During the Pre-Production Phase, the design is optimized for production. Different production methods and different suppliers will be traded-off such that the design will be made producible. Almost simultaneously, half a year later, the certification process will be initiated. During this procedure the entire aircraft is certified with respect to the applicable certification standards, which for this design it is CS25. When all activities are performed according to this plan, the aircraft is certified by July 2021 and actual production for the launching customer can start.

ID	Task Name	Duration	Start
56	**Certification Process**	**60 months**	**1 December 2016**
57	Numerical Proofing	24 months	1 December 2016
58	Full Scale Testing	30 months	1 July 2018
59	Flight testing	36 months	1 September 2018

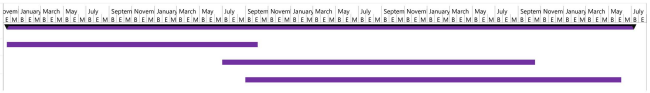

Figure 2-5: The Gantt Chart for Certification Process

Figure 2-6: The Gantt Chart Legend

Chapter 3

Manufacturing, Assembly & Integration Plan

The aircraft consists of many separate parts which should be assembled into sub-assemblies and finally the final aircraft. This chapter will discuss this process starting with a description of the sub-assemblies, while the last sections will cover the final assembly and a general factory layout suggestion.

No specific time is mentioned for each step, but it is intended that every part or assembly should be finished or delivered just before it is needed for further assembly, according to the Just-In-Time principle. Employing this principle saves storage space and therefore costs. However, this does imply that any late deliveries or unexpected delays affect the complete production process as these effects can be partially countered by implementing small buffers in the time plannings.

Where possible, rivetting was chosen over other bonding methods since, unlike bonding or welding, this allows for easier replacement of parts without advanced machinery in the field. Also, most non-load-bearing parts which can be made from thermoplastics should be (able to be) 3d-printed, again to increase field repairability. Another consideration was to use as many standard parts as possible, to cut costs. This also leads to computerized bending machines or rubber stamping as preferred forming methods, since these need no or only one mould, halving minimizing costs.

3.1 Fuselage Assembly

The fuselage assembly station work is shown schematically in Figure 3-1 which covers the entire fuselage, including all systems that should be installed within the fuselage, as well as the vertical tailplane.

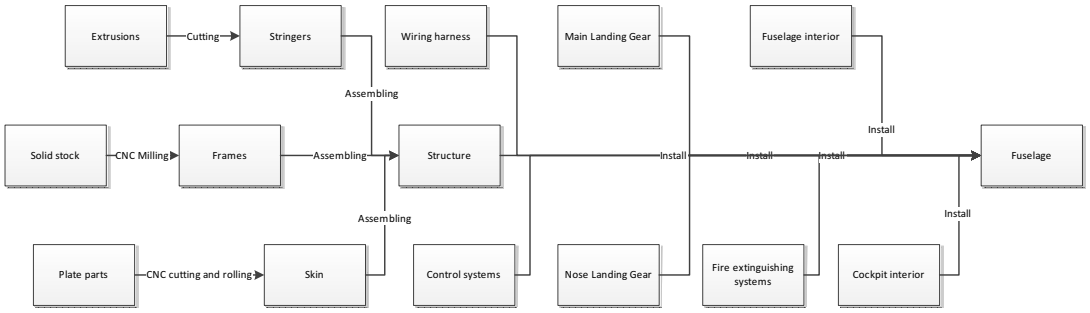

Figure 3-1: Fuselage Assembly Structure

Fuselage Structure Sub-assembly

The fuselage assembly starts with assembling the fuselage structure sub-assembly. The fuselage frames, the basis of the structure, is Computer Numerical Controlled (CNC) machined from a solid aluminium block. However, in case of large sales numbers, more focus can be put on using rough castings instead of solid slabs. However, the required moulds are expensive and should therefore only be considered if larger sales number can be achieved.

Next, the frames are put in a jig and fixed into a self-supporting skeleton by means of rivets. As the stringer-frame connections are a critical part of the load paths, they need reinforcements like shear clips. The stringers themselves are manufactured by cutting and forming bought extrusions into the required size and shape. At this point, also window and door frames and other reinforcements or hardpoints are installed. After the fuselage skeleton is completed, the skin panels, which are CNC cut and formed from plate stock, are fastened to the skeleton and sealed. This completes the fuselage structure sub-assembly.

Wiring Harness Sub-assembly
With a completed structure, the installation of all systems and interior can commence. After the structure has been covered internally with a layer of thermal and acoustic insulation, the fuselage wiring harness sub-assembly is installed. This is assembled of a large amount of electrical wires, cut to length, bundled on a jig and fitted with connectors in order to connect all electrical components within the aircraft.

Control Systems
After installing the wiring harness, the control system sub-assemblies are installed. These are all rods, cables, hinges, hydraulic lines and actuators used for operating moving parts such as the landing gear, control surfaces, scoops, extinguishant doors etc. For the actuated parts lying outside of the fuselage assembly, the lines are run up to the interface point and fitted with connectors there for easy installating during final systems integration. At this point, also the rudder and hyfrofoils are installed.

Landing Gear
After the control systems have been installed, the main and nose landing gears are installed, including their bay doors and furnishings. These are built as sub-assemblies of bought parts such as tires, rims, brakes and shock absorbers, and of forged or milled parts, such as the landing gear struts. From this point on, the aircraft frame can be lowered from its jacks and stand on its own.

Fire Extinguishing Systems
The next step is the installation of the retardant systems which includes the integration of the pre-fabricated retardant and additives tanks, mixing equipment and drop doors, but also the installation of the scoops as well as all electrical and hydraulic sensor and actuator systems involved. With the installation of these systems, all work on under-floor parts is completed.

Fuselage Interior
As the fuselage structure has been constructed and all required systems are installed, the interior can be finished. This includes installing watertight compartments, followed by the floors, covering the insides of the fuselage walls and roof and installing all interior lights, doors and windows. All custom non-loadbearing parts which can be made of thermoplastics will be 3D-printed.

Cockpit Interior
Parallel to the work on the rest of the fuselage interior, the cockpit can be finished. This installation includes completing the installation of all cockpit controls such as stick, throttles and pedals, integrating pre-assembled instruments and overhead control panels. Finally, the pilot seats are installed. With the installation of the interior, the fuselage assembly is completed and can be integrated with the other main assemblies.

3.2 Wing Assembly

Parallel to the assembly of the fuselage, the wing is assembled in another (part of the) plant. The simplified basic assembly is depicted in Figure 3-2 and explained upon below.

Wing Structure
First, the wing structure should be assembled which starts with the spars, which in turn consists of aluminum spars webs with spars caps jointed by means of welding of riveting to the top and bottom of the webs. Subsequently, the spars caps are sealed such that a fuel tank can be incorporated in the wing. Next, the wing ribs, CNC cut and formed from sheet metal, are mounted to the spars. Finally, adding the stringer extrusions and mounting hardpoints completes the wing structure skeleton.

Electrical System
After the wing skeleton is completed, the wing wiring harness, assembled in a similar manner as the fuselage wiring harness, is installed, as well as some electronic components, such lights, antenna's, sensors and actuators.

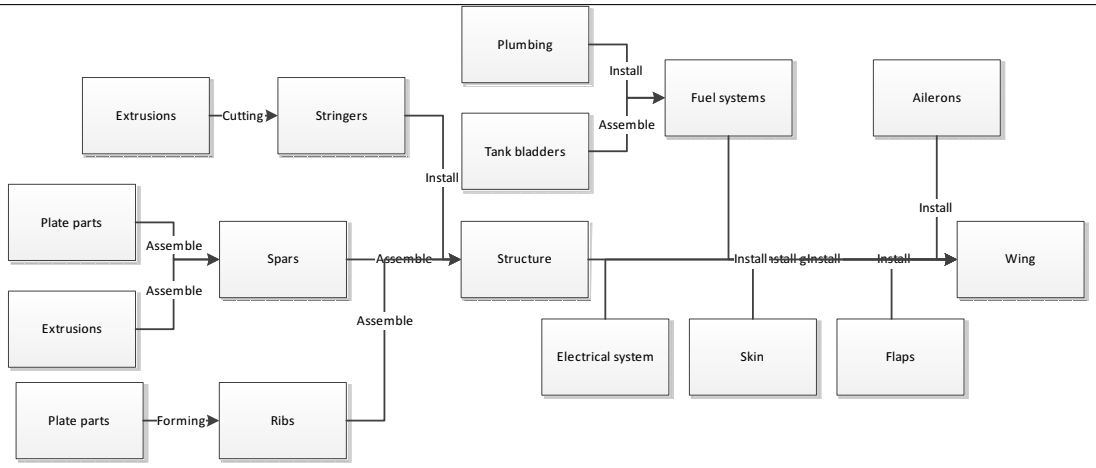

Figure 3-2: Wing Assembly Structure

Fuel System
Parallel to the installation of the electrical systems, the fuel systems are installed. This includes the bladder tanks, but also all required plumbing to transfer the fuel to the engines, and systems such as fuel level indicators, main and back-up fuel pumps, etc.

Finishing
Next, the control systems rods, hydraulics and actuators are installed in the wing, as well as their connections to the fuselage at the interface point. As all internal structure and systems are installed, the skin panel can be fastened to the skeleton. After completing the installtion of the skin panel, the pre-assembled flaps, floats and ailerons and their actuation mechanisms can be installed which completes the wing assembly.

3.3 Stabilizer Assembly

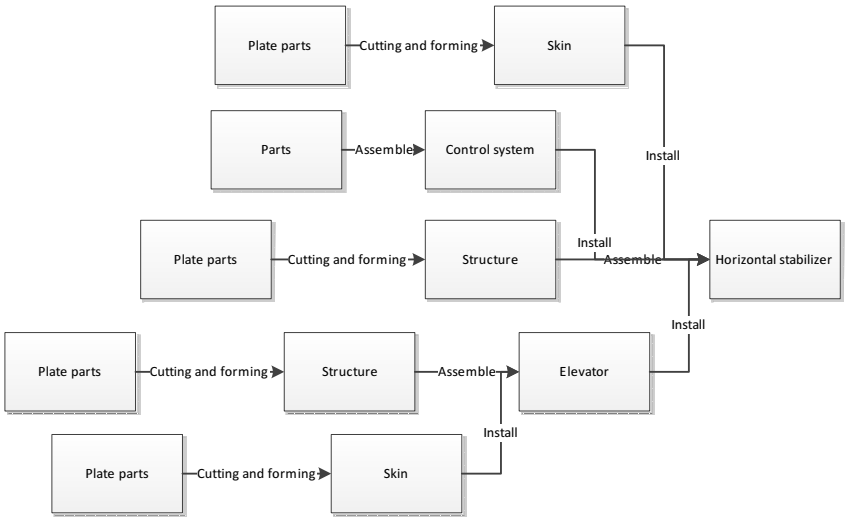

Figure 3-3: Stabilizer Assembly Structure

The stabilizer assembly, shown in Figure 3-3, consists of the horizontal stabilizer and all systems contained within it. Production of the stabilizer starts with the CNC cutting and forming of sheet metal parts, which are subsequently assembled into the skeleton of the stabilizer. Next, all parts of the control system passing through the stabilizer are installed. At this point, the electrical wiring, sensors,

actuators and lights are also installed. Finally, the skin is fixed to the internal structure, after which the parallel-assembled elevator is mounted to the stabilizer which concludes the stabilizer assembly.

3.4 Engine Assembly

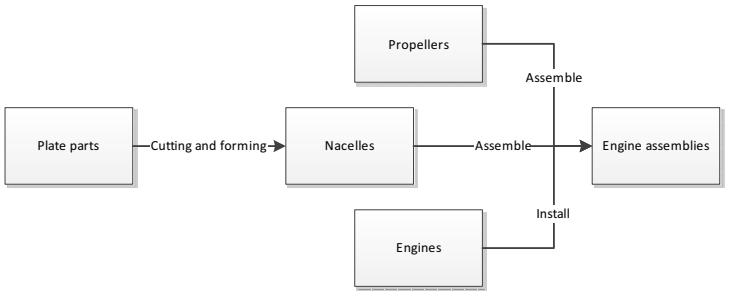

Figure 3-4: Engine Assembly Structure

The engine assembly, shown in Figure 3-4, consists of the engine, propeller and all other systems contained within the nacelle. Production starts with CNC cutting parts for the engine nacelles, which are subsequently formed into the nacelle. The engine is installed in the nacelle and connected to the required plumbing and wiring. Finally, the propeller is installed on the engine, concluding the engine assembly.

3.5 Final Assembly

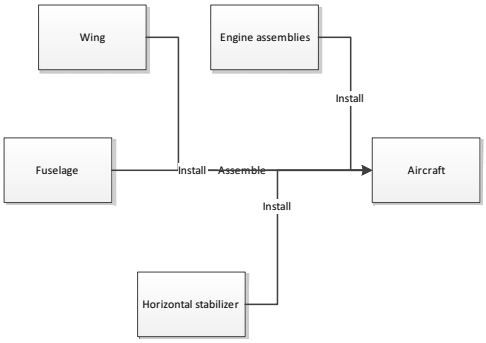

Figure 3-5: Final Assembly Structure

The final assembly station of the production line, as depicted in Figure 3-5, is the station where all main assemblies are joined to form the complete aircraft. Work centers on the completed fuselage assembly, to which the wing is joined. Next, hydraulic, electrical and mechanical connections between these assemblies are completed. After wing placement, the horizontal stabilizer assembly is connected to the fuselage assembly according to a similar procedure as the wing. Lastly, the four engine assemblies are installed on the wings.

After all assemblies have been mated, the aircraft can be filled with the required fluids and final systems integration checks can be performed. When passed, the aircraft is painted and given the go-ahead to perform the pre-delivery flight tests.

3.6 Production Facility Lay-out

For the production facility, a suggested floorplan is explained in Figure 3-6. In this floorplan all fabrication work is confined to the upper left corner of the workshop. This area has stations for cutting and

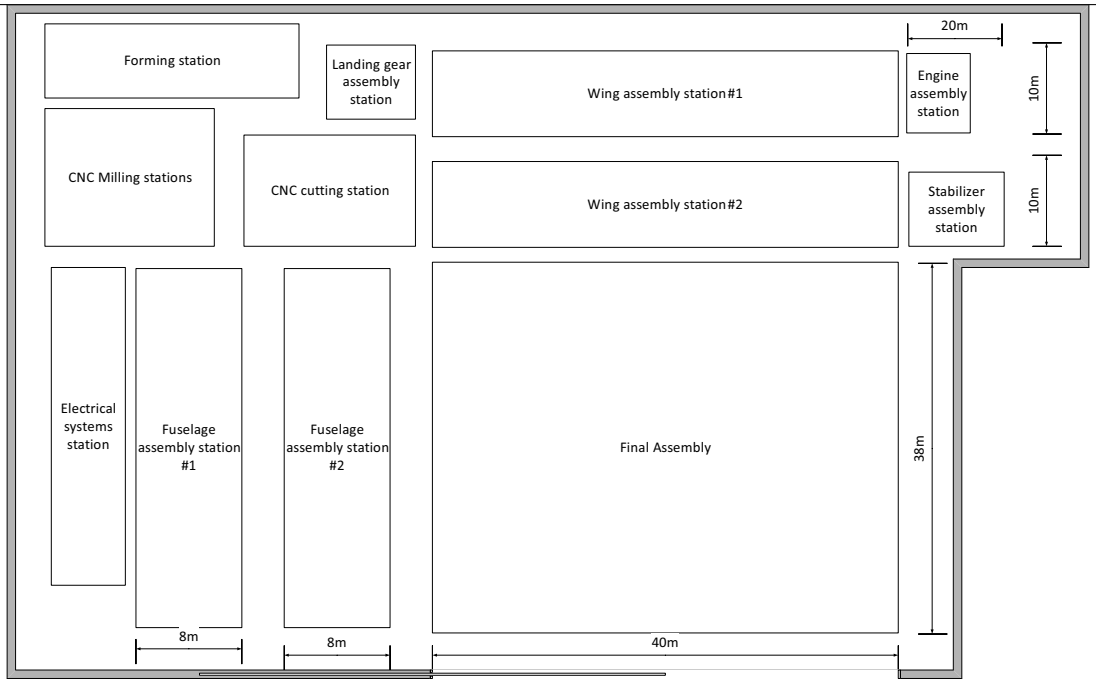

Figure 3-6: Concept for the Assembly Facility Floorplan

forming parts as well as for CNC machining. An electrical systems station is located to the left of the facility, with a large length because of the fabrication of wiring harnesses.

There are two fuselage and wing assembly stations, mainly because the most work is associated to these assemblies. The first station deals with the skeleton building and "dry" integration of components, while the second deals more with the integration of "wet", plumbing and sub-assembly installation, the installation of hydraulic lines or other assembly processes which involves the usage of fluids. For the fuselage, the assembly will change stations after the installation of the landing gear.

For transportation of parts throughout the facility, a bridge crane rated up to 30 metric tons is required over the entire length of the facility. Part warehousing, storage, engineering as well as the paint hangar should be housed in nearby buildings. Furthermore, it is important that especially the engineering department is close to the manufacturing facilities. In this way, a "Skunk Works"-like cooperation in which engineers and craftsmen are more able to communicate with each other, is facilitated. This should lead to a quicker and more accurate identification of problems, as well as to better and cheaper solutions.

Chapter 4

Sustainable Development

In 1987 the United Nations published the report "Our Common Future", which had a tremendous impact on the global awareness of the pressing need for sustainable development [8]. This report expressed the consequences of humanity's inability to fit its activities within the delicate balance of earth's precious ecosystem. Simultaneously, the report expressed the vision for a more prosperous, more sustainable and a more cooperative future. Within this vision for the future, the concept and fundamentals of sustainable development are defined as: "The development that meets the needs of the present without compromising the ability of future generations to meet their own needs" [8, p.37]. As a result, during the past decades governments have changed their laws and policies, multinationals reinvented their manufacturing methods and communities altered their behavior. Within this aircraft design project, the concept of sustainable development is discussed in this chapter regarding the effect of extinguishing wildfires, efficient manufacturing procedures and the end-of life process. However, in this report the operational sustainability is not elaborated upon as this has a relatively low impact on the total sustainability of the design. In the Mid-Term Report, concepts for sustainability during operation are discussed [67, p.51].

4.1 Effects of Extinguishing Wildfires

The composition of the earth's atmosphere is in a very delicate balance. The greenhouse gasses in the atmosphere absorb and emit the suns radiation making life, as we know it, possible. However, due to non-sustainable human activities, such as the burning of fossil fuels and deforestation, the concentration of these green house gasses has been increasing, causing global warming. One of these greenhouse gasses, carbon dioxide (CO_2) is stored in the cells of plants and trees during the photosynthesis process. Some carbon gets released back into the atmosphere through respiration, but the net effect is tremendous carbon storage. It is estimated that U.S. forests absorb between 1 billion and 3 billion kilogram of carbon dioxide each year [28]. When trees are burned, harvested, or otherwise die, they release their carbon back into the atmosphere causing the delicate balance to be disrupted.

It is estimated that losses of forest due to deforestation and wildfires contributes as much as 30 percent to annual global greenhouse gas emissions which is equivalent the entire global transportation sector [28]. While a relatively small portion of these emissions is caused by wildfires, the contribution of wildfires still resembles a substantial portion. Research has shown that the wildfires in the United States in 2007, accounted for approximately 4 to 6 percent of the North American greenhouse gas emissions for that year [13]. This implies that a severe fire season lasting only one or two months can release as much carbon into the atmosphere as the annual emissions of the entire transportation or energy sector of one individual state [13]. Hence, fighting wildfires in a more effective manner contributes to lower greenhouse gas emission rates.

With respect to sustainability, the need for more effective firefighting solutions is further increased by the fact that wildfires have increasingly become larger and more harmful. The six worst fire seasons since 1960 have occurred since 2000. This is caused by the current climate change that has led to stronger oscillations in temperatures and longer periods of drought in many parts of the world. Furthermore, past logging practices, which favored cutting the large pines and allowing less fire-tolerant plants to expand, caused the biomass to grow such that wildfires have become more frequent and severe [23].

The Water Bomber design's capability of carrying 15 m^3 of fire retardant increases the effectiveness of firefighting operations and therefore contributes to a more sustainable balance in the earth's atmosphere.

4.2 Materials and Manufacturing

The choice of materials for the aircraft can have a large influence on the sustainability of the design. Several considerations for sustainability with respect to the production of different materials should therefore be made. The two main material types that were evaluated for use were Aluminium alloys and CFRP (Carbon-Fiber-Reinforced Polymers). At first glance, the use of CFRP seems to be the more sustainable choice, as its weight is considerably lower compared to that of Aluminium which would therefore lead to fuel savings during the aircrafts operational life. However, as the production of CFRP requires considerably more energy than that of Aluminium, when the total lifetime of the aircraft is considered, the advantage of using CFRP instead of Aluminium will be negated by the high energy required during the production phase. This is mainly caused by the fact that the aircraft will accumulate less flying hours than regular commercial aircraft which is inherent to the aircrafts typical mission profile. Also, Aluminium can be recycled, while at present no method exists yet for the recycling of CFRP. Section 4.3 which elaborate in more detail on recycling of different materials. Therefore, the main material of choice will be aluminium.

Secondly, 3D printing technology is used for the manufacturing and design process of this aircraft. 3D printing technology offers a quick way of manufacturing compared to traditional casting or milling methods. This is attributed to the inkjet principle and to the fact the secondary tooling might not be required at the later stages of the development. As a consequence, 3D printed parts may be significantly cheaper compared to part manufactured though traditional methods for which cost of dies and other tooling is incorporated [22]. Furthermore, 3D printing enables the creation of designs that cannot be made using traditional techniques. According to General Electric, the finished parts using 3D techniques are stronger and lighter than those made on the assembly line and can withstand extreme temperatures up to 1600 degrees [10]. The design team recognizes the potential advantages of 3D printing techniques. However, at this point in the design process, additional research of the implications of these techniques on the design and manufacturing process is yet to be performed.

4.3 End-of-life

It is projected that after a service life of about thirty to forty years, the aircraft will be retired from service. One of the most important aspects with respect to sustainability in aircraft design is the end-of-life stage. Until recently, the end-of-life stage often got overlooked in the aerospace industry. However, new projects concerning the aircraft end-of-life stage have shown that proper considerations with respect to sustainability for this phase can have a large impact on the life-cycle sustainability of the aircraft. Current options for the end-of-life stage of manufactured products include reuse, re-manufacture, recycle, landfill, and incineration. Current guidelines stipulate that for metal products, recycling is the best end-of-life solution [34]. Therefore, for aircraft and most of their components, the common solutions are recycling and reuse through recycling. It should be reminded that there is a constant trade-off between minimizing environmental impact and minimizing deficit. The proposed methods however are deemed to be as cost-efficient as possible for disposal of the aircraft after its service life.

Before the aircraft will be parted out for recycling, all reusable parts will be removed. These include the engines, APU, avionics and landing gear. Due to the relative simplicity of the design, all of these parts can be reused in other aircraft or be used as spare parts which adds to the design's sustainability. After these items have been removed, the hull will be parted out. One of the solutions is to use PAMELA (Process for Advanced Management of End of-Life-Aircraft), developed by Airbus. As part of Airbus ACADEMY (Airbus Corporate Answer to Disseminate Environmental Management System), the PAMELA project was set up in 2005 in order to set new eco-efficient standards for the management of end-of-life aircraft [4]. The project has already demonstrated that over 85 percent of each aircrafts components could be safely removed and effectively recycled.

After decommission and removal of reusable parts, the PAMELA project will take care of parting out and recycling the remaining components. During the first phase of the project, the aircraft's hull will be cleaned and decontaminated after which the tanks will be drained when needed. In the next project phase, the hull will be parted out. During this phase, the best recovery options for different materials will be identified. The plane will be parted out, starting with the wing component, after which the tail will be decomposed and the fuselage will be cut up nose to back. All reusable materials that are extracted

from the components will be sorted and grouped. During the final phase, the reusable materials will be cast into ingots for further processing, after which they can be used again as secondary raw material for manufacturing purposes. Airbus has already demonstrated that the recovered materials, such as aluminium, can be successfully used for new aerospace production. This end-of-life program will be beneficial to both operators as well as the environment since the PAMELA program provides monetary returns while at the same time being a sustainable solution to disposal of the aircraft after decades of safe and reliable service.

Chapter 5

Cost Breakdown Structure

The Cost Breakdown Structure (CBS) in figure 5-1) gives an overview of all cost elements associated with the development and production of the aircraft. The CBS defines the costs related to the project in an hierarchical order and is structured as and "AND" tree. The total project costs are therefore shown as the sum of the total development and production costs. The development costs include all activities which will take place after the preliminary design of the water bomber, as defined in the PD&D Logic in Chapter 1.

5.1 Method & Results

The top level represents the total project cost while the lower levels give a detailed breakdown of the total cost. At this point in the design process, the development and production costs are estimated using a method provided by Raymer [47]. The Raymer method, which is largely based on statistics, gives an estimation of the total project cost and the associated development and production cost for a clean-sheet commercial aircraft. For this aircraft's estimation, all costs related to engines and avionics are based on manufacturing data (Rolls Royce Allison T56-A427 [44] unit price: USD 2.4 million, cost of avionics estimated at USD 150,000 per aircraft). One of the required inputs for the Raymer method is the expected production volume. For this aircraft, a sales volume of about 40 units is expected, as explained in Chapter 1 (Part I). The results as shown in Figure 5-1 are therefore for a project with a total production of 40 units.

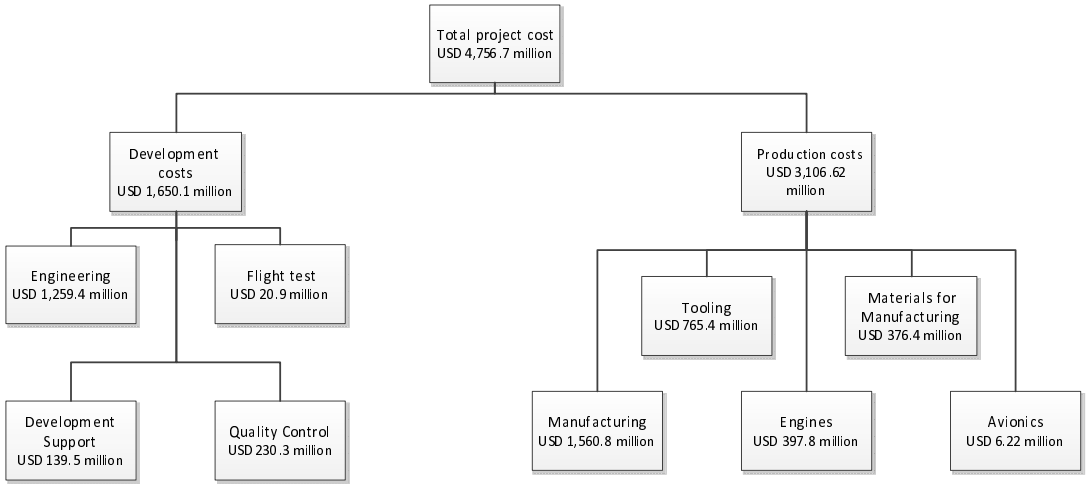

Figure 5-1: Cost Breakdown Structure for Proposed Design

5.2 Cost Price & Cost Efficiency

The cost price per unit is estimated at USD 118.9 million. This may seem high at first, however some considerations should be made. First, this price is based on a total production volume of 40 aircraft. As the Raymer method is largely influenced by the production volume, increased sales could lead to a significantly lower cost price. Therefore, this value is not set in stone. Also, one of the most important aspects that should be taken into account is the fact that the total development costs are included in the total price. Since the Raymer method is based on a clean sheet commercial design, development cost

are expected to be high. As this design will be less complex than regular commercial aircraft and as a significant part of the design will be based on existing designs, the development costs for this design are expected to be considerably lower than what is proposed by Raymer. Another possibility to reduce the development costs is to request subsidies from governments and international organizations to aid the development of the aircraft. Excluding the development costs the cost price of the aircraft is expected to be around USD 77.7 million. The main competition for this plane comes from retired commercial aircraft that are subsequently converted for use as aerial fire fighters. An example of an aircraft that can potentially be converted to a fire fighter with similar capacity is the McDonnell Douglas (Boeing) MD-11. A used MD-11 can be bought for about USD 30 million without engines, whereas the conversion cost for conversion from passenger to cargo aircraft is estimated at approximately USD 15 million [62]. Note that the conversion cost of USD 15 million is for conversion to a regular cargo aircraft, so conversion to a tanker aircraft is expected to cost more. Assuming three engines can be bought for about USD 5 million, a conservative estimate for the purchase cost of an alternative to the new aircraft is about USD 50 million. The main disadvantage of a converted, second hand MD-11 is the fact that it has already been used and therefore has been subject to wear and tear, which may lead to considerable maintenance cost during future use while spare parts are increasingly hard to come by. Also, assuming the purchased aircraft for conversion is 10 years old, it can serve for another 20 years at most, while the new aircraft will remain in service for 40 years. Secondly, a second hand aircraft has not been built specially for fire fighting purposes which can result in additional material wearing on places where it is not expected. This can lead to unexpected failures and if not monitored properly in the most catastrophic case to a crash. Thirdly, the MD-11 will be land-based only, which greatly reduces the usability for fire fighting and multipurpose opportunities compared to the amphibian aircraft. Also, through the use of new design features incorporated in the new aircraft design, the release of water will be more accurate, which results in smaller number aircraft required to fight a particular wildfire. Finally, the new design can be used for other purposes than aerial fire fighting, which will not be possible using an aircraft converted into a tanker. This design can perform passenger and cargo transport as easily as aerial fire fighting for at least the next 30 years to come, while still being able to operate from water. Concluding, the design of this amphibious aircraft is more expensive to purchase compared to a second hand aircraft with comparable water capacity, yet its longer lifespan, lower operating costs, efficient fire fighting characteristics and its multipurpose design will result in a much more cost efficient aircraft.

Chapter 6

Marketing Strategy

The firefighting aircraft is estimated to have a small production volume based on sales of other fire fighting aircraft. However, to make the design of the fire fighting aircraft as economically profitable as possible, it is advantageous to maximize the aircraft sales. To increase the sales, a marketing strategy has been selected, which is discussed in this chapter.

6.1 Types of Ownership

Customers that are interested in the services of the multifunctional fire fighting aircraft, besides the Red Cross, will most likely be governments, charity organizations or commercial investors. The budget that these potential clients are able to spend on fire fighting methods varies greatly. The main client, the Red Cross, is a charity organization which receives most of its income through donations and will not have a high annual fire fighting budget. The purchase of a firefighting aircraft would have a huge impact on its annual budget and for this reason different types of ownerships are considered to reduce the costs of fighting wildfires. To make the aircraft available for organizations with relatively low annual budgets, aircraft purchase and aircraft leasing are considered.

6.1.1 Leasing

When leasing an aircraft the lessor, the owner of the aircraft, leases the aircraft to the lessee. In this case the Red Cross could be a potential lessee. The lessee will lease the aircraft for a certain price per period but will not become the owner of the aircraft. Within the lease agreements there are several types of lease that can be agreed on, being wet lease and dry lease. The difference between these types of lease agreements are the items which are in- or excluded in the lease, such as a complete crew, maintenance- and insurance costs [57]. The advantage of a leasing agreement is that organizations who are in need of a fire fighting aircraft, such as governments and charities, do not have to purchase the aircraft but lease it whenever it is needed. The downsides of leasing for the lessee are the high costs over the long term use, excess costs for repairing and not being able to customize the aircraft.

6.1.2 Aircraft Purchase

The organization could purchase the aircraft and gain full ownership. The advantages of full ownership is that the multifunctionality of the aircraft can be utilized in the non fire season to perform passenger-, relief- or cargo transportation missions. Besides the alternate missions the aircraft could perform throughout the year, one of the advantages of ownership is that the aircraft can be located near high risk areas such that the time to reach the fire is decreased as much as possible. The disadvantages of the aircraft purchase could be the high purchase costs, risks that come with ownership and extra costs such as storage-, maintenance-, insurance- and liability costs.

6.2 Modular Aircraft

The aircraft will be built up from several modules, the modules will be relatively easy to replace in case of wear, failure or a desired upgrade. Certain modules are deemed necessary for the aircraft and others are optional. The price range of the aircraft will vary from the basic aircraft price to an enhanced version which comes at a higher price. Examples of necessary modular items are: wings, tip floats, engines and the control canard. Examples of the optional modular items are: CADAS, air conditioning and the retardant tanks. With a modular aircraft the client has more freedom to design, repair and update its aircraft.

Chapter 7

List of Innovations

The design of the "Next Generation" water bomber has a wide set of capabilities and functionalities that enable aircraft to effectively fight wildfires. This set of capabilities is what sets this aircraft apart from previous generations of aerial firefighters. A list of innovations that make this aircraft set apart from other aerial firefighting vehicles is presented below:

- **Amphibious platform** The RAFT has the largest retardant capacity of any amphibious aircraft in the world. Its amphibious platform enables it tho scoop water which reduces turnaround times.
- **CADAS** The Computer Augmented Detection and Aiming System (CADAS) provides the pilot with environmental information and automatic aiming. This system, in combination with current detection and aiming techniques, significantly improves the efficiency of aerial firefighting operations.
- **Water cannons** The RAFT has the option of two computer controlled water cannons which allows the release of a concentrated jet at specific targets. Although several helicopters are already equipped with a water cannon, the high cruise speed of the RAFT yields a significantly smaller response times.
- **Multiple retardant tanks** The ability to use four separate retardant tanks and the installation of adjustable release doors, allows the water bomber to drop retardant into various drop patterns.
- **Different types of retardant** The aircraft is able to drop water, foams and long-term retardants which is a significant advantage over current aerial firefighting vehicles which are, in general, only able to drop two types of retardant.
- **3D printing** As non-load bearing parts of the RAFT can be 3D printed, less moulds are required and less waste is produced during the manufacturing of the aircraft. Furthermore, some of these parts can be 3D printed on location which increases the maintainability of the aircraft.
- **Hydrofoils** The implementation of hydrofoils to the design decreases the take-off length of the amphibious aircraft which increases the deployment area of the water bomber.
- **Control canards** Control canards enable the aircraft to quickly recover from a stall and guarantee controllability should other control surfaces fail.
- **Electric actuation of control surfaces** The use of electrical actuators over hydraulic actuators is a lighter, more efficient solution which requires significantly less maintenance.
- **Inflatable or retractable wing tip floats** Wing tip floats are installed to enhance the lateral stability of the aircraft during on-water operations. However, as these components result in significant drag penalties during flight, inflatable floats are installed, which decreases drag during flight.

Chapter 8

Conclusions and Recommendations

The Red Cross expressed the need for the development of an aerial vehicle that can extinguish wildfires in a more cost-efficient and time-efficient manner. As the scale and impact of wildfires are increasing, a new interest in a third generation of firefighting aircraft emerges, based on an expanding market for flexible deployment and additional missions. To meet this need, the design team has been given the task to design the next generation water bomber. During the first design phases of the design process, a trade-off is performed between three different concepts, a fixed-wing design, a rotorcraft concept and a tilt-rotor design. Based on the given requirements, the technical analysis and performed trade-off the fixed-wing amphibious design concept was chosen. This entire process is described in the Mid-Term Report [67]. The aim of the later design process stage, described in this report, is to further develop the chosen concept up to the point that the main dimensions of the aircraft are known and the first design iterations are performed, which involves the design and integration of main subsystems.

8.1 Mission Analysis

In the beginning of this design stage, all aspects related to the market possibilities of the design, the different mission scenario's and all other prerequisites for designing the aircraft are investigated. Using sales figures from reference aircraft it is estimated that 40 aircraft over the next 30 years will be sold. As the next generation water bomber will be a revolutionary aerial firefighting aircraft with a significantly larger payload capacity compared to current aerial firefighters, it has the potential to succeed the aging CL-215 and CL-415 fleet and therefore has the potential for similar sales figures as these aircraft, up to 80 aircraft.

From the imposed requirements, the mission parameter have been identified that are critical in the sizing of the aircraft. For take-off and landing, a maximum runway field length up to 1,000 meters may be used and the aircraft must be able to perform repeated loading and dropping procedures before it needs to be refueled. Furthermore, the design must be able to perform a climb of at least 15 degrees and fly at a minimum stall speed of 51.5 $\frac{\text{m}}{\text{s}}$ at Maximum Take-Off Weight. Due to these challenging operating conditions, low altitudes in combination with low velocity, an extra dimension of redundancy in safety is added to the final design. This extra redundancy is provided by the use of control canards, enabling the aircraft to quickly recover from stall. Furthermore, to reduce the risk of the startle effect, the cockpit controls will be kept as simple and intuitive as possible and a specific pilot training program will be initiated. Furthermore, a Computer Augmented Detection and Aiming System (CADAS) is proposed for offering crucial real-time information about the development of the fire.

Also other mission types are considered as the wildfire season is only part of the year. Therefore other missions for which the design can be used, are human relief missions, transport missions and reconnaissance.

8.2 Main Sizing

Based on the conditions and parameters obtained in the mission analysis, the main components of the aircraft such as the wing, hull and tail dimensions are determined resulting in a general layout for the design. Designing a complex aircraft is heavily interdependent multiple design iterations which have been performed before obtaining the results as described in this section.

The power requirement is set to be 11.6 MW. As such, the required power loading will be set at 0.0462 $\frac{\text{N}}{\text{W}}$ and the 0.0462 $\frac{\text{N}}{\text{m}^2}$. Given these loadings, a wing surface area of 192.6 m^2 with a span of 39.25 meters and a taper ratio of 0.4 is obtained. Based upon the C_L range required for the different mission phases and the desired stall characteristics, a NACA4317 wing profile has been selected. Within

the wing, a wing box is located that is sized for loads from -2 to 5g, both for filled- and empty fuel tanks. For which the most critical loading case has proven to be at zero fuel weight and maximum lift generation of 5g. This induces the highest yield stress at the top corners, closest to the leading edge at the root of the wings. The thickness of the skin will thus be largest at the root.

Thereafter, using reference aircraft and control and stability requirements the dimensions for the T-tail have been determined. This results in a horizontal tail surface area of 43.22 m^2 with a span of 15.06 meters and a taper ratio of 0.4 is obtained. In addition a vertical tail surface area of 36.08 m^2 with a span of 6.01 meters and a taper ratio of 0.4 is achieved.

As the aircraft is a flying boat that is able to scoop on water, the bottom of the fuselage is designed to have a V-shaped hull. The part of the hull that will be submerged at zero velocity at zero payload is 25 meters long, with a maximum width of 3.3 meters. A two step hull configuration is chosen as it is steadier and provides enhanced controllability of the aircraft during maneuvering on the water. An exact overview of all the parameters reference isgiven in Chapter 7.

8.3 System Sizing

Concurrently to the main sizing, the dimensions and the characteristics of the systems have been designed. It has been decided to equip the wing with slats and flaperons. The flaperons are critical for lateral controllability as controllability issues may arise during water operations such as landing, scooping and take-off. From the power requirement, it has been decided to equip the aircraft with four turboprop Rolls Royce Allison T56-A-10WA engines with a propeller diameter of 4.1 meters. The four engines are located on top of the wing, as close as possible to the center line of the aircraft such that they have sufficient clearance with respect to the water and do not create a large moment in the case of a one-engine-out scenario. Furthermore, the landing gear consists of a main gear of two struts each with four tires with a diameter of 0.76 meters and the nose gear positioned 12.70 meters from the main landing gear.

For versatility reasons it was decided that the aircraft can make use of two different retardant types. Class A foam suppressants are mixed with water, increasing the penetration to the fire such that the fire is directly extinguished. Secondly, long-term retardants can be used that remain effective long after losing its moisture, such that they are used for reducing the flammability of vegetation surrounding the fire. For the filling of the tanks during scooping, inlet probes are used with a cross-sectional area of 250 cm^2 yielding a total scooping distance of 600 meters. The water is subsequently distributed over four subtanks with anti-slosh baffles preventing longitudinal sloshing. Each subtank can be opened independently enabling different drop patterns for more efficient firefighting. Furthermore, there is an option for two computer controlled water cannons which allow the release of a concentrated jet at specific targets. For the lateral stability during on the water operations wing tip floats will be located 18 meters from the center line. These floats will be retractable and inflatable such that during flight the floats will be deflated and retracted within the wing reducing the overall drag of the aircraft.

8.4 Recommendations for Future Design

At the end of this design process, the planning for the later design processes up to the actual production has been made. As the design is far from finished at this point in time, many iterations have to be performed, parts and systems to be designed and detailed analysis are to be made. A draft is made for the manufacturing, assembly procedure and the general factory layout is introduced. It has been chosen to opt for the Just-In-Time principle and a "Skunk Works" cooperation between engineers and craftsmen such that time and costs are saved where possible. Furthermore, riveting is the most favored bonding method since this allows fore easier replacement of the parts.

As wildfires contribute to the imbalance in annual global greenhouse gas emissions, the development of an more effective aerial firefighting aircraft contributes to a more sustainable balance in the Earth's atmosphere. Moreover, efficient manufacturing procedures such as 3D-printing technologies, the use of aluminium and end-of-life procedures, the needs of today are met without compromising the needs of tomorrow.

The remainder of the design process is roughly divided in four phases. First the different components of the design are designed in more detail during the Detailed Design Phase. Subsequently, during the

Testing Phase, scale models of the aircraft are being subjected to rigorous testing in order to validate the numerically obtained analysis. Also, during this phase, sample material and structure tests are performed to aid their development. Thereafter, during the Pre-Production Phase, the design is optimized for production with respect to production methods and cooperation's are started made with suppliers. Almost simultaneously, the aircraft is certified with respect to the applicable certification standards, which for this design is CS25. When all activities are performed according to this plan, the aircraft is certified by July 2021 and actual production for the launching customer can start. At an expected demand of 40 aircraft, the aircraft is priced at USD 118.9 million In addition, it has been decided that the aircraft may also be leased using a lease construction.

Bibliography

[1] *Hydrodynamica 1*. TU Delft, 2008.

[2] IFEX 3000. Ifex 3000 impulse technology. `http://www.ifex3000.nl/eframe.htm`. Retrieved on 7-1-2014.

[3] IFEX 3000. Ifex nederland bv: Exstinguishing system. `http://www.ifex3000.nl/efireh.htm`. Retrieved on 7-1-2014.

[4] Airbus. Process for advanced management of end of life aircraft. `http://www.airbus.com/innovation/eco-efficiency/aircraft-end-of-life/pamela/`, 2014. Retrieved on 12-01-2014.

[5] American Helicopter Services & Aerial Firefighting Association. Aerial firefighting tutorial. `http://www.ahsafa.org/?page_id=52`. Retrieved on 06-12-2013.

[6] Federal Aviation Authority. *FAR PART 25, Airworthiness Standards: Transport Category Airplanes*. January 2014.

[7] Dowty Propellers General Electric Aviation. C-130j advanced propeller system. `http://www.geaviation.com/systems/products-and-services/pdf/Dowty-c-130J.pdf`. Retrieved on 14-01-2014.

[8] Gro Harlem Brundtland. *Report of the World Commission on Environment and Development: Our Common Future*. United Nations, March 1987.

[9] Susan Bushell, David Willis, and Paul Jackson. *Jane's All the World's Aircraft*. Janes Information Group, 104 edition, April 2013.

[10] Tim Catts. Ge turns to 3d printers for plane parts. `http://www.businessweek.com/articles/2013-11-27/general-electric-turns-to-3d-printers-for-plane-parts`. Retrieved on 17-01-2014.

[11] NASA Druden Flight Research Center. Flight tests of electric actuators at nasa dryden promise improved safety reliability for future aircraft. `http://www.nasa.gov/centers/dryden/news/NewsReleases/1998/98-84.html`. Retrieved on 16-01-2014.

[12] National Interagency Coordination Center. `http://www.nifc.gov/nicc/`. retrieved on 09-12-2013.

[13] Chris Geronc Angie Belotea Don McKenzied Xiaoyang Zhange Susan ONeillf Christine Wiedinmyera, Brad Quayleb and Kristina Klos Wynne. Estimating emissions from fires in north america for air quality modeling. February 2006.

[14] Kern County. Jobdescription, air tactical group supervisor. `http://www.co.kern.ca.us/person/Webjobs/JS4591.pdf`, June 2002.

[15] R. Curran and W. Verhagen. *Risk Management and Reliability*. TU Delft, 2011.

[16] Jan Luis de Kroes. Subsonic plane or flight simulator thereof, adjustable fuselage control surface, computer program product and method, July 2013.

[17] Bureau d'Enquêtes et d'Analyses pour la Sécurité de l'Aviation Civile. Final report on the accident on 1st june 2009 to the airbus a330-203 registered f-gzcp operated by air france flight af 447 rio de janeiro - paris. July 2012.

[18] E. Dimitrova, F. Heddes, T. Heil, N. van Hoorn, and R. Heuijermans. Wing box simulation model, February 2013.

[19] Edward G. Keating et al. *Air Attack Against Wildfires: Understanding U.S. Forest Service Requirements for Large Aircraft*. RAND Homeland Security and Defense Center, 2012.

[20] Inc. Evergreen International Aviation. Protecting valuable resources with an advanced multi-mission aircraft. `http://www.evergreenaviation.com/supertanker/index.html`. Retrieved on 12-11-2013.

[21] Jr. Fred W. S. Locke. A correlation of the dimensions, proportions, and loadings of existing seaplane floats and flying boat-hulls. *NACA Wartime Reports*, March 1943.

[22] Simranpreet Singh Gill and Munish Kapla. *Comparative Study of 3D Printing Technologies for Rapid Casting of Aluminium Alloy*. Taylor & Francis Group, 2009.

[23] Ross Gorte. *The Rising Cost of Wildfire Protection*. Headwaters Economics, June 2013.

[24] FEC Heliports. *Foam Mixing Fire Suppression Package*. February 2003.

[25] Martin Hepperle. Javafoil - analysis of airfoils. `http://www.mh-aerotools.de/airfoils/javafoil.htm`, 2006. Retrieved on 26-12-2013.

[26] Forecast International. The market for aviation apu engines. `http://www.forecastinternational.com/samples/F644_CompleteSample.pdf`. Retrieved on 16-01-2014.

[27] Irkut, EADS, and Rolls-Royce Deutschland. Irkut, eads and rolls-royce deutschland have finalised feasibility study on amphibious aircraft be-200: viable business case with good market prospective. `http://www.eads.com/eads/int/en/news/press.en_20030618_be200.html`, June 2003. Retrieved on 12-11-2013.

[28] Toni Johnson. Deforestation and greenhouse-gas emissions. `http://www.cfr.org/forests-and-land-management/deforestation-greenhouse-gas-emissions/p14919#p5`. Retrieved on 19-01-2014.

[29] Ilan Kroo and Juan Alonso. Aircraft design: Synthesis and analysis,tails,tail design and sizing,. http://adg.stanford.edu/aa241/stability/taildesign.html.

[30] Jean-Marc Moschetta Kwanchai Chinwicharnam, David Gomez Ariza and Chinnapat Thipyopas. Aerodynamic characteristics of a low aspect ratio wing and propeller interaction for a tilt-body mav. September 2013.

[31] A.K. Kim L. Liu. A review of water mist fire suppression systems - fundamental studies. *Journal of Fire Protection Engineering*, 10, 2000.

[32] B.SC. L. P. Coombes and B.Sc R.H. Read. The effect of various types of lateral stabilisers on the take-off of a flying-boat. *Air Ministry R. & M. No. 1411*, October 1930.

[33] M. Langley. *Seaplane float and hull design*. Sir Isaac Pitman & Sons, LTD, 1935.

[34] S. G. Lee, S. W. Lye, and M. K. Khoo. *A Multi-Objective Methodology for Evaluating Product End-of-Life Options and Disassembly*. Division of Manufacturing Engineering, School of Mechanical and Production Engineering, Nanyang Technological University, Republic of Singapore, 2001.

[35] Fire Program Solutions LLC. *WIldland Fire Management Aerial Application Study: Final Report*. USDA Forest Service, National Interagency Fire Center, October 2005.

[36] P.M. Heyma L.L.M. Veldhuis. Aerodynamic optimisation of wings in multi-engined tractor propeller arrangements. 1995.

[37] Sandra McCulloch. Martin mars water bomber grounded after 53 years in b.c. `http://www.timescolonist.com/news/local/martin-mars-water-bomber-grounded-after-53-years-in-b-c-1.624458`. Retrieved on 12-11-2013.

[38] T.H.G. Megson. *Aircraft Structures for Engineering Students*. Elsevier, 4th edition, 2007.

[39] ASM Aerospace Specification Metals. Aluminium alloy 2024. *ASM Metals*. Consulted on Thursday January 16 2014.

[40] Airbus Military. The versatile airlifter for the 21st century. `http://www.airbusmilitary.com/aircraft/a400m/a400mabout.aspx`. Retrieved on 09-01-2014.

[41] Nicole Montesano. State filing confirms evergreen shutdown. `http://newsregister.com/article?articleTitle=state-filing-confirms-evergreen-shutdown--1383965975--10248--breaking-home`, November 2013. Retrieved on 13-11-2013.

[42] W. M. Munro. *Marine Aircraft Design*. Sir Isaac Pitman & Sons, LTD, 1933.

[43] William Munro. *Marine Aircraft Design*. 1933.

[44] Joakim Kasper Oestergaard. Rolls royce t56 turboprop. `http://www.bga-aeroweb.com/Engines/Rolls-Royce-T56.html`. Retrieved on 17-01-2014.

[45] California Department of Forestry and Fire Protection (CAL FIRE). *Firefighting Aircraft Recognition Guide*. CAL FIRE, 104 edition, April 2013.

[46] John B. Parkinson. The design of the optimum hull for a large long-range flying boat. *NACA Wartime Reports*, September 1944.

[47] Daniel P. Raymer. *Aircraft Design: A Conceptual Approach*. AIAA Education Series. American Institute for Aeronautics and Astronautics, third edition edition, 1999.

[48] Tom Robinson, Jose Musse, and John Anderson. Global emergency response the ilyushin solution. `http://www.fire.uni-freiburg.de/emergency/ger.htm`. Retrieved on 12-11-2013.

[49] Dr.ir. Gianfranco La Rocca. Aerospace design and systems engineering elements ii,wing design part 4. `https://blackboard.tudelft.nl`, 2013.

[50] Dr.ir. Gianfranco La Rocca. Systems engineering and aerospace design, requirement analysis and design principles for ac stability and control (part 1). `https://blackboard.tudelft.nl`, 2013.

[51] Gianfranco La Rocca. Requirement analysis and design principles for a/c stability & control. `https://blackboard.tudelft.nl/webapps/portal/frameset.jsp?tab_tab_group_id=_10_1&url=%2Fwebapps%2Fblackboard%2Fexecute%2Flauncher%3Ftype%3DCourse%26id%3D_40996_1%26url%3D`. Retrieved on 25-11-2013.

[52] Jan Roskam. *Airplan Design Part V: Component Weight Estimation*. Roskam Aviation and Engineering Corporation, 1985.

[53] Jan Roskam. *Airplan Design Part II: Preliminary Configuration Design and Integration of the Propulsion System*. Roskam Aviation and Engineering Corporation, 1989.

[54] Jan Roskam. *Airplane Design Part I: Preliminary Sizing of Airplanes*. Roskam Aviation and Engineering Corporation, 1989.

[55] Jan Roskam. *Airplane Design Part IV: Layout of Landing Gear and Systems*. Roskam Aviation and Engineering Corporation, 2000.

[56] Mohammad H. Sadraey. *Aircraft Design: A Systems Engineering Approach*. Wiley, October 2012.

[57] Global Plane Search. Aircraft lease definition. `http://www.globalplanesearch.com/aircraft_leasing/definition.htm`. Retrieved on 10-01-2014.

[58] US Forest Service. *Seeing Red: A Short History of Fire Retardant and the Forest Service*. US Forest Service, 2007.

[59] Dylan Stableford. Watch a water bomber extinguish a truck fire on a remote canadian highway. `http://news.yahoo.com/water-plane-called-in-to-extinguish-truck-fire-on-remote-canadian-highway-152641387.html`, August 2013. Retrieved on 16-01-2014.

[60] Ann Suter. Drop testing airtankers: A discussion of the cup-and-grid method. December 2000.

[61] TU Solar Boat Team. `http://www.solarboatteam.nl`, January 2014. Retrieved on 21-01-2014.

[62] Aviation Today. Md11 prcing enjoys reversal of fortunes. `http://www.aviationtoday.com/regions/usa/MD11-Pricing-Enjoys-Reversal-of-Fortunes_3429.html.UtkvFdKwbrd`. Retrieved on 17-01-2014.

[63] Prof. E.G. Tulapurkara. Airplane design(aerodynamic),fuselage and tail sizing - 4. http://nptel.ac.in/courses/101106035/35. Retrieved on 08-01-2014.

[64] UnifireAB. Unifire primary monitor specifications. `http://www.unifire.com/sites/default/files/pliki/unifire_monitor_specifications.pdfl`. Retrieved on 7-1-2014.

[65] UnifireAB. Unifire primary monitor specifications. `http://www.unifire.com/sites/default/files/pliki/FORCE80_MANUAL_2013.pdf`. Retrieved on 7-1-2014.

[66] E.V.M. van Baaren, S.A.W. van den Broek, D.A. Eisses, L.H. Geijselaers, F. Heddes, W.F.S. van Lingen, H.A. Mulder, L.A. van der Schaft, G. Stolwijk, and M.C.G. van der Werf. *Baseline Report, , Towards a new generation of water bombers*. October 2013.

[67] E.V.M. van Baaren, S.A.W. van den Broek, D.A. Eisses, L.H. Geijselaers, F. Heddes, W.F.S. van Lingen, H.A. Mulder, L.A. van der Schaft, G. Stolwijk, and M.C.G. van der Werf. *Mid-Term Report, Towards a new generation of water bombers*. December 2013.

[68] L.L.M. Veldhuis. Propeller wing aerodynamic interference. June 2005.

[69] Graham Warwick. Report: Greece orders beriev be-200 firefighting amphibians. `http://www.flightglobal.com/news/articles/report-greece-orders-beriev-be-200-firefighting-amphibians-220539/`. Retrieved on 12-11-2013.

Appendix A

Work Contributions

Table A-1: Overview of Individual Contributions to Final Report

Deliverable Item		Contributors
	Title Page	-
	Preface	M.C.G. van der Werf, L.H. Geijselaers
	Executive Summary	M.C.G. van der Werf
	Abstract	F. Heddes
	Introduction	E.V.M. van Baaren
Mission Analysis		
5.	Functional Flow Diagram	L.H. Geijselaers
6.	Functional Breakdown Structure	F. Heddes
12.	Market Analyis	M.C.G. van der Werf, G. Stolwijk
18.	Operations & Logistics Concept Description	M.C.G. van der Werf, H.A. Mulder
28.	Communication Flow Diagram	S.A.W. van den Broek
	Safety Aspects	W.F.S. van Lingen, H.A. Mulder
	Multifunctionality	W.F.S. van Lingen
Main Sizing		
37 & 38	Wing- and Power Loading Diagrams	L.A. van der Schaft
	Airfoil Selection	F. Heddes
	Weight Estimations and Iterations	G. Stolwijk, W.F.S. van Lingen, F. Heddes
	Fuselage	D.A. Eisses, H.A. Mulder, F. Heddes
	Wing Sizing	M.C.G. van der Werf
	Structural Wing Design	D.A. Eisses, F. Heddes
	Tail Sizing	F. Heddes
	Fuel System	L.H. Geijselaers, S.A.W. van den Broek
	Retardant Tank	E.V.M. van Baaren
System Sizing		
	Intake System	M.C.G. van der Werf
	Release System	E.V.M. van Baaren
37.	Controls and High-Lift Devices	M.C.G. van der Werf
	Effectiveness	E.V.M. van Baaren
	Hydrofoils	L.A. van der Schaft
	Landing Gear	L.H. Geijselaers, G. Stolwijk
	Retardant Types	M.C.G. van der Werf
	Safety	W.F.S. van Lingen, H.A. Mulder
	Engine Selection	L.A. van der Schaft
	Engine Positioning	S.A.W. van den Broek
	Water Stability Devices	L.H. Geijselaers
	Electrical Block Diagram	L.H. Geijselaers
Design Performance Analysis		
	Control & Stability Analysis	M.C.G. van der Werf, F. Heddes
	Flight Performance	L.A. van der Schaft
9.	Technical Risk Assessment and Risk Map	D.A. Eisses
27.	Sensitivity Analysis	G. Stolwijk, D.A. Eisses
	Verification & Validation	G. Stolwijk, F. Heddes
	Compliance Matrix	D.A. Eisses
Recommendation for Future Design		
19.	Project Design & Development Logic	S.A.W. van den Broek, H.A. Mulder
20.	Project Gantt Chart	S.A.W. van den Broek
25.	Sustainable Development Strategy	W.F.S. van Lingen, S.A.W. van den Broek
30.	Manufacturing, Assembly Integration Plan	H.A. Mulder
21.	Cost Breakdown Structure	M.C.G. van der Werf, W.F.S. van Lingen, L.H. Geijselaers
	List of Innovations	E.V.M. van Baaren
	Conclusion & Recommendations	S.A.W. van den Broek
	Contributions	M.C.G. van der Werf
	References	M.C.G. van der Werf
	Appendices	M.C.G. van der Werf